

ALMA MATER STUDIORUM · UNIVERSITY OF BOLOGNA

---

School of Science  
Department of Physics and Astronomy  
Master Degree in Physics

# Fermion masses, leptogenesis and gravitational waves in $SO(10)$

Supervisor:

Prof. Silvia Pascoli

Submitted by:

Luca Marsili

Co-supervisor:

Prof. Jessica Turner

Academic Year 2021/2022



## Abstract

Grand Unification Theories (GUTs) predict the unification of three of the fundamental forces and are a possible extension of the Standard Model, some of them predict neutrino mass and baryon asymmetry. We consider a minimal non-supersymmetric  $SO(10)$  GUT model that can reproduce the observed fermionic masses and mixing parameters of the Standard Model. We calculate the scales of spontaneous symmetry breaking from the GUT to the Standard Model gauge group using two-loop renormalisation group equations. This procedure determines the proton decay rate and the scale of  $U(1)_{B-L}$  breaking, which generates cosmic strings, and the right-handed neutrino mass scales. Consequently, the regions of parameter space where thermal leptogenesis is viable are identified and correlated with the fermion masses and mixing, the neutrinoless double beta decay rate, the proton decay rate, and the gravitational wave signal resulting from the network of cosmic strings. We demonstrate that this framework, which can explain the Standard Model fermion masses and mixing and the observed baryon asymmetry, will be highly constrained by the next generation of gravitational wave detectors and neutrino oscillation experiments which will also constrain the proton lifetime.



## Sommario

Le teorie della grande unificazione, note anche come GUTs, predicono l'unificazione di tre delle quattro forze fondamentali: debole, forte ed elettromagnetica. Le GUTs sono una possibile estensione del modello Standard e predicono le masse dei neutrini e l'asimmetria materia-antimateria. Nel nostro lavoro abbiamo considerato una particolare GUT,  $SO(10)$ . In particolare abbiamo considerato un modello di  $SO(10)$  non-supersimmetrico che può riprodurre correttamente le masse e gli angoli di mescolamento dei fermioni. Abbiamo calcolato le scale di energia in cui avvengono i meccanismi di rottura spontanea della simmetria che rompono  $SO(10)$  nel gruppo di gauge del modello Standard usando le equazioni del gruppo di rinormalizzazione a due loop. Questa procedura determina il tasso di decadimento del protone e la scala di rottura del gruppo  $U(1)_{B-L}$ , che genera un network di stringhe cosmiche e che genera la massa dei neutrini sterili. Successivamente abbiamo identificato le regioni dello spazio dei parametri liberi del modello in cui è possibile predire correttamente la simmetria materia-antimateria tramite leptogenesi, le abbiamo confrontate con le masse e gli angoli di mescolamento dei fermioni, e abbiamo studiato come possono essere testate con il doppio decadimento beta senza neutrini, con il decadimento del protone e con un segnale di onde gravitazionali prodotto dal network di stringhe cosmiche. Abbiamo dimostrato che questo framework che restituisce correttamente le masse e gli angoli dei fermioni e l'asimmetria materia-antimateria può essere ampiamente testato dai futuri esperimenti sui neutrini e sulle onde gravitazionali e che ci daranno più informazioni sulla vita media del protone.



# Contents

<b>1</b>	<b>Introduction</b>	<b>4</b>
<b>2</b>	<b>Standard Model, CP Violation and Neutrino Oscillations</b>	<b>7</b>
2.1	The Standard Model group . . . . .	7
2.2	Charged and neutral current interactions . . . . .	9
2.3	Higgs mechanism . . . . .	11
2.4	Fermion masses and mixing . . . . .	13
2.5	Mixing and CP violation in the lepton sector . . . . .	16
<b>3</b>	<b>Neutrino masses, See-Saw Model and Left-Right Symmetry</b>	<b>19</b>
3.1	Adding Neutrino Masses into the Standard Model . . . . .	19
3.2	Weinberg Operator . . . . .	20
3.3	See-Saw Model . . . . .	21
3.4	Left-Right symmetry . . . . .	24
3.5	$SU(4)_C \times SU(2)_L \times SU(2)_R$ : the Pati-Salam model . . . . .	28
<b>4</b>	<b><math>SO(10)</math>: The general framework</b>	<b>30</b>
4.1	Spinorial representation of $SO(10)$ . . . . .	30
4.2	$SO(10)$ breaking . . . . .	35
4.3	Gauge coupling unifications . . . . .	42
4.4	Proton decay . . . . .	53
4.5	Yukawa sector . . . . .	56
4.6	Scan of the parameter space . . . . .	58
4.7	Benchmark point: BP1 . . . . .	65
<b>5</b>	<b>Leptogenesis</b>	<b>68</b>
5.1	Sakharov conditions . . . . .	68

5.2	Lepton asymmetry . . . . .	70
5.3	Boltzmann equation and $N_1$ -leptogenesis . . . . .	71
5.4	Sphalerons . . . . .	77
5.5	Realistic models of leptogenesis . . . . .	81
5.6	Application to our model . . . . .	86
5.6.1	Spontaneous CP violation in SO(10) . . . . .	87
5.6.2	3DME equations . . . . .	88
5.6.3	Results . . . . .	89
<b>6</b>	<b>Cosmic strings</b>	<b>92</b>
6.1	Topological defects and string solutions . . . . .	92
6.2	String dynamics . . . . .	95
6.3	String network evolution . . . . .	101
6.3.1	Network evolution: VOS model . . . . .	103
6.3.2	Cosmic network simulation . . . . .	106
<b>7</b>	<b>Testing SO(10) with a Stochastic Gravitational Waves Background</b>	<b>108</b>
7.1	Gravitational Waves . . . . .	108
7.2	Stochastic Gravitational Waves Background . . . . .	109
7.3	SGWB spectrum from a cosmic string network . . . . .	110
7.4	Prediction of our model . . . . .	112
7.5	SO(10) with Pulsar Time Arrays . . . . .	115
<b>8</b>	<b>Conclusions</b>	<b>121</b>
	<b>Bibliography</b>	<b>124</b>
<b>A</b>	<b>A brief introduction to cosmology</b>	<b>136</b>





# Introduction

The Standard Model describes three of the fundamental forces: strong, weak, and electromagnetic. It is a gauge theory and its gauge group is  $SU(3)_c \times SU(2)_L \times U(1)_Y$ . It matches experimental results extremely well although it does not take into account some phenomena such as neutrino masses, baryogenesis, and dark matter. Neutrinos were first theorized by Wolfgang Pauli in 1930 and discovered around 20 years later, in 1956, by Cowan and Reynes. In the beginning, neutrinos were assumed to be massless, this was the situation in the '60s when the foundations of the Standard Model were established. Neutrino oscillations have been discovered by Super-Kamiokande [1] and SNO [2] in the late '90s: this implies that neutrinos have mass, even if it is very tiny.

The Standard Model does not account also for the baryon asymmetry.

All the astrophysical objects are made of matter and it has not been found any objects made of antimatter. The Universe is therefore asymmetric and the origin of this asymmetry has not an established explanation yet. It is possible to produce such an asymmetry also within the Standard Model even though it fails to predict a sufficient amount of such an asymmetry to agree with experimental observation. One elegant possible mechanism which explains such an asymmetry is leptogenesis [3]: the origin of such an asymmetry is the decay of a heavy particle: a sterile neutrino. Another more abstract problem of the Standard Model is represented by its theoretic foundations and its apparent arbitrariness: there is no physical principle that motivates why the gauge group  $SU(3) \times SU(2)_L \times U(1)_Y$  is what it is. Moreover, quarks and leptons are embedded separately and this implies that there are many free parameters and we cannot predict the values of the fermion masses. There is a need to address those fundamental questions that make the Standard Model incomplete and find a more general theory of the fundamental interactions.

One possibility is represented by Grand Unified Theories, usually called GUT.

The main motivation behind those models is the assumption of gauge coupling uni-

fication [4]. One of the main predictions of quantum field theory is the running of the coupling. If we study the running of the couplings of the Standard Model we can see that they seem to run toward the same value. Therefore it makes sense to assume that there has to be an extended gauge group with only one coupling which spontaneously breaks down to the Standard Model at lower energies. A model with this feature is called GUT and we are focusing on the model that has  $SO(10)$  as a gauge group.

It embeds many theories which are interesting on their own such as  $SU(5)$  [5], another GUT theory, flipped  $SU(5) \times U(1)$  [6, 7, 8, 9] and left-right symmetric models such as the Pati-Salam model  $SU(4)_c \times SU(2)_R \times SU(2)_L$  [10]. Such models embed the Standard Model gauge group which becomes just an intermediate step towards a more general theory based on the physical principle of the gauge couplings unification. The particular path between  $SO(10)$  and the Standard Model group can happen in an arbitrary number of intermediate steps in which one usually passes through one of the subgroups we have stated above.  $SO(10)$  predicts also the existence of a new particle that does not interact via Standard Model interactions with the other particles that we identify with the sterile neutrino. The presence of this particle in the model allows for an explanation both of light neutrino masses via the seesaw mechanism [11, 12, 13] and leptogenesis [14, 15, 16, 17]. The seesaw mechanism is a model which explains naturally why the neutrino mass is so small requiring the existence of a heavy right-handed neutrino: the heavier the right handed neutrino, the smaller the mass of light neutrinos. One of the most striking features of  $SO(10)$  is that at energies greater than the unification scale all particles cannot be distinguished by any type of interaction and the difference between leptons and quarks emerges only after a spontaneous symmetry breaking of the Pati-Salam model. This fact is particularly important because it allows us to predict also the values of the fermion masses [18].

The main prediction of GUT theories and the only way in which it was possible to verify them experimentally, until the discovery of gravitational waves, is proton decay. The  $SO(10)$  heavy gauge bosons are the origin of baryon number violating interactions which are the cause of the decaying of the proton. The order of magnitude of the proton lifetime predicted by GUT is from  $10^{30}$  yr to  $10^{36}$  yr. The current bound is from Super-K experiment [19] and it rules out some models but not  $SO(10)$ . The next-generation experiment Hyper-Kamiokande [20] will push this bound up to  $10^{35}$  yr in case of a non-observation. The discovery of gravitational waves provided a new tool to test  $SO(10)$  and leptogenesis [21, 22]. In general when  $SO(10)$  is spontaneously broken down to the Standard Model a variety of topological defects is produced during a phase transition

between two intermediate states, when there is a  $U(1)$  cosmic strings are generated [23]. Unlike other kinds of topological defects cosmic strings evolve following a scaling solution and their energy remains a constant fraction of the total energy of the universe. Such a cosmic string network generates a Stochastic Gravitational Wave Background (SGWB) which could be detected by next-generation gravitational wave experiments.

In Ref. [24] and in Ref. [25] it has been studied the possibility of testing  $SO(10)$  using gravitational waves with a general discussion for all the breaking chains. This work follows a companion article [26] in which we examine more carefully a particular breaking chain consistent with the current Super-K bound on proton decay and we scan over the parameter space of the theory to determine if it predicts correctly fermion masses. Subsequently, we study the points in the parameter space we have found with such a scan to determine if some of these points predict the correct amount of baryon asymmetry via leptogenesis. In the end, we focus on how we can test such a model both with proton decay from the observation of Hyper-K and with next-generation gravitational wave experiments such as LISA [27]. In particular we concentrate on Pulsar Time Array experiments such as NANOGrav [28], EPTA [29], IPTA [30] and PPTA[31] that may have found a signal that could be interpreted as a SGWB and we study its consistence with our model. An important point of our work is the link between the leptogenesis scale and cosmic strings production that correspond to the  $U(1)_{B-L}$  breaking scale, that we call  $M_1$  and that can also be constrained by proton decay experiments. We explore this interplay between different tests and predictions of our model, study its consistency with present data, especially from PTA experiments, and discuss the possibility of next-generation experiments to test this model.

The work is organized as follows: in Chapter 2 we give an introduction to Standard Model and neutrino physics, in Chapter 3 we study some of the extensions of the Standard Model in particular seesaw mechanism and left-right symmetric models, in Chapter 4 we introduce  $SO(10)$  and present the results of the scan of the parameter space. In Chapter 5 we discuss leptogenesis and see how we can compute baryon asymmetry of the successful points of the parameter space, in Chapter 6 we introduce cosmic strings, in Chapter 7 we discuss how to test  $SO(10)$  with gravitational waves and we demonstrate that the regions of the model parameter space that yield successful leptogenesis and fermionic masses and mixing will be associated to a GW signal. Finally, in 8 we summarize and discuss our results.

# Standard Model, CP Violation and Neutrino Oscillations

The gauge theory group of the Standard Model is  $SU(3)_c \times SU(2)_L \times U(1)_Y$ . At low energy the symmetry is spontaneously broken via the Higgs mechanism [32] down to  $SU(3)_c \times U(1)_{\text{em}}$ . The Higgs mechanism gives mass to gauge bosons and to fermions which otherwise could not have mass due to the impossibility of finding a gauge invariant mass term [33, 34, 35]. It is a chiral theory and therefore its matter content is organized in left and right handed spinors. In order for a species to have a mass it has to have both right handed and left handed spinors in the Standard Model matter content. We first introduce the basic features of the Standard Model group and its matter content, then we are going to describe the charged and neutral interaction. After this we can study the Higgs mechanism and see how gauge bosons and fermions can acquire mass. At the end we are going to study neutrino oscillations that require an extension of the Standard Model.

## 2.1 The Standard Model group

$SU(3)$  describes strong interactions and it the gauge group of Quantum Chromodynamics. It is a non-abelian gauge theory and its Lie-Algebra is:

$$[T_i, T_j] = \epsilon_{ijk} T_k. \quad (2.1)$$

The bosons are embedded in the adjoint representation which for  $SU(N)$  has  $N^2 - 1$  elements. There are 8 QCD bosons which are called gluons. The covariant derivative is:

$$D_\mu = \partial_\mu + ig_3 A_\mu^a T^a. \quad (2.2)$$

For a simple  $SU(2)$  model, instead, one can study the gauge bosons of the theory and find that there are three bosons:  $A_\mu^1, A_\mu^2, A_\mu^3$ . We can organize them in two charged bosons:

$$A_\mu^1 + iA_\mu^2 = W_\mu^+, \quad (2.3)$$

$$A_\mu^1 - iA_\mu^2 = W_\mu^-, \quad (2.4)$$

$$(2.5)$$

and  $A_\mu^3$  which is neutral and may be a photon candidate. Therefore the candidate for being the charge operator in this model is  $Q \equiv T_3$ . This is not what we observe experimentally. We need to add an hypercharge operator associated to the  $U(1)_Y$  group. In this case the charge operator becomes:

$$Q = T_{3L} + \frac{Y}{2}. \quad (2.6)$$

With adding an abelian group we obtain four gauge bosons:  $A_1, A_2, A_3$  and  $B$ . The covariant derivative can be written as

$$D_\mu = \partial_\mu + igA_\mu^a T^a + ig' B_\mu Y. \quad (2.7)$$

Those does not correspond to the physical bosons: indeed the physical bosons are obtained after a rotation \*:

$$\frac{A_\mu^1 - iA_\mu^2}{\sqrt{2}} = W_\mu, \quad (2.8)$$

$$A_\mu = \sin \theta_w A_\mu^3 + \cos \theta_w B_\mu, \quad (2.9)$$

$$Z_\mu = \cos \theta_w A_\mu^3 - \sin \theta_w B_\mu, \quad (2.10)$$

where  $\theta_w$  is the Weinberg mixing angle.

The Standard Model is a chiral theory and the matter content is organized in left and right handed spinors. The matter content is:

$$L_L \equiv \begin{pmatrix} e_L \\ \nu_L \end{pmatrix}, Q_L \equiv \begin{pmatrix} u_{rL}^i \\ d_{rL}^i \end{pmatrix}, \quad (2.11)$$

$$e_R, u_R^i, d_R^i, \quad i = 1, 2, 3, \quad (2.12)$$

---

\*Differently than strong interaction that can be studied by itself, weak and electromagnetic interaction cannot because of this mixing.

	$SU(3)_c$	$SU(2)_L$	$U(1)_Y$
$L_L$	<b>1</b>	<b>2</b>	-1
$Q_L$	<b>3</b>	<b>1</b>	$\frac{1}{3}$
$e_R$	<b>1</b>	<b>1</b>	-2
$u_R$	<b>3</b>	<b>1</b>	$-\frac{2}{3}$
$d_R$	<b>3</b>	<b>1</b>	$\frac{1}{3}$

Table 2.1: Quantum number for the Standard Model spinors.

where right handed spinors are singlets of  $SU(2)_L$ , being in a trivial representation the action of the generators is the following:  $T^a\psi_R = 0$ . Left handed spinors are, instead, doublets of  $SU(2)_L$ . For what regards strong interactions leptons are singlets of  $SU(3)_c$  while quarks are embedded in a  $SU(3)_c$  triplet.

In Table 2.1 we can see the quantum numbers for all the three gauge groups of each spinors.

## 2.2 Charged and neutral current interactions

We have described the matter content and the gauge structure of the Standard Model. let us start writing the interaction lagrangian of the electroweak sector. We proceed considering only the leptonic term since the procedure for quarks would be equivalent. From the expression of the covariant derivative of Eq. 2.7 we find that the interaction term can be written as

$$\mathcal{L} = -\frac{1}{2}\overline{L}_L \begin{pmatrix} gA_\mu^3 - g'B & A_\mu^1 + iA_\mu^2 \\ A_\mu^1 - iA_\mu^2 & gA_\mu^3 - g'B & A_\mu^1 \end{pmatrix} \gamma^\mu L_L + g'\overline{e}_R B_\mu \gamma^\mu e_R. \quad (2.13)$$

We can rewrite the equation above using the physical gauge bosons. We find that  $A$  carries the electromagnetic interactions,  $W$  the charged current interactions and  $Z$  the neutral current interactions. The charged current lagrangian is

$$\mathcal{L}_{CC} = -\frac{g}{\sqrt{2}}\overline{\nu}_L W_\mu \gamma^\mu e_L + \text{h.c.}, \quad (2.14)$$

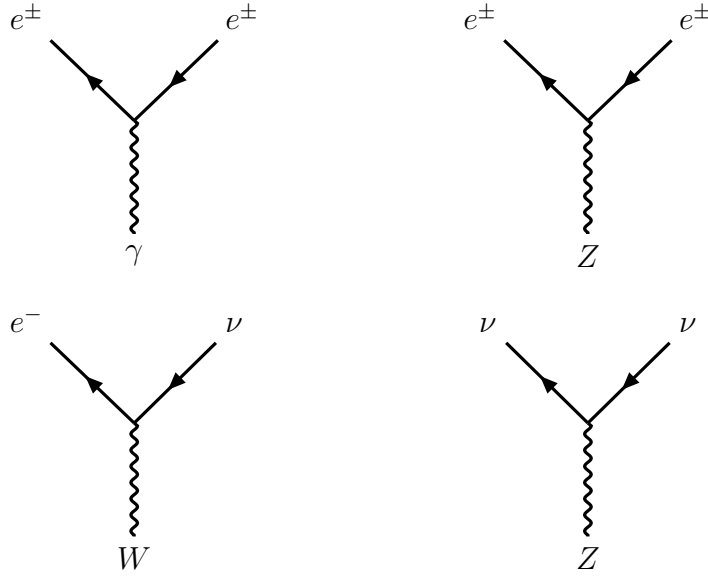


Figure 2.1: Feynman diagrams of the electroweak interactions of the lepton sector. In the upper part of the figure on the left we have the vertex for the electromagnetic interaction and on the right the vertex for the neutral current interaction. In the lower part of the figure we have the vertices of the charged current interaction.

and we can notice how only left handed spinors interact through such interaction. The neutral current interaction is instead

$$\begin{aligned}
 \mathcal{L}_{\text{NC}} = & -\frac{1}{2} \{ \bar{\nu}_L [(g \cos \vartheta_W + g' \sin \vartheta_W) Z_\mu + (g \sin \vartheta_W - g' \cos \vartheta_W) A_\mu] \nu_L \\
 & - \bar{e}_L [(g \cos \vartheta_W - g' \sin \vartheta_W) Z_\mu + (g \sin \vartheta_W + g' \cos \vartheta_W) A_\mu] \gamma^\mu e_L \\
 & - 2g' \bar{e}_R [-\sin \vartheta_W Z + \cos \vartheta_W A] e_R \} \quad (2.15)
 \end{aligned}$$

The charged and the neutral interactions are short range interactions while the electromagnetic are long range interactions. Therefore, the only gauge boson that can be massless is the photon while  $W$  and  $Z$  have to be massive. We cannot add a mass term directly to the lagrangian since it wouldn't preserve the gauge invariance but we need another way to do that. The solution is the Higgs mechanism which we are going to study in the next section.

## 2.3 Higgs mechanism

The concept of symmetry breaking is particularly important in the Standard Model. A symmetry can be broken simply by adding to the lagrangian a term which violates such a symmetry. This is what would happen if we simply add a mass term for the gauge bosons. It is possible to break a symmetry also in another way, with the spontaneous symmetry breaking. In general when one says that a theory has a symmetry one assumes implicitly that also the vacuum state of the theory is invariant under that symmetry. If the vacuum is not invariant we have the so-called spontaneous symmetry breaking: at low energies the system is in the vacuum state and the symmetry seems broken but at higher energies the symmetry is reestablished. A symmetry with such properties can be called also hidden symmetry. The spontaneous symmetry breaking of a gauge theory is called Higgs mechanism and in this way we can give a mass to the vector bosons preserving gauge invariance. In this way we obtain the following breaking:

$$SU(3)_c \times SU(2)_L \times U(1)_Y \rightarrow SU(3)_c \times U(1)_{em} \quad (2.16)$$

In the next chapters we are going to extend the Standard Model gauge group using a GUT model and then recovering it at low energies via the spontaneous symmetry breaking. This happen in the same way as it will describe it in this section, although, due to the complexity of dealing with bigger groups, there will be more possibilities in how to break the symmetries and choosing the right Higgs will not be so trivial as for the electroweak breaking.

$\mathcal{L} \rightarrow \mathcal{L}' = \mathcal{L}$	$ 0\rangle \rightarrow  0'\rangle =  0\rangle$	Exact symmetry
$\mathcal{L} \rightarrow \mathcal{L}' = \mathcal{L}$	$ 0\rangle \rightarrow  0'\rangle \neq  0\rangle$	Hidden symmetry (SSB)
$\mathcal{L} \rightarrow \mathcal{L}' \neq \mathcal{L}$	$ 0\rangle \rightarrow  0'\rangle \neq  0\rangle$	Broken symmetry

### $SU(2)_L \times U(1)_Y \rightarrow U(1)_{em}$ breaking

let us add to the matter content a scalar doublet of  $SU(2)$ ,

$$\Phi = \begin{pmatrix} \Phi^+ \\ \Phi^0 \end{pmatrix}. \quad (2.17)$$

We need always to consider the most general langrangian consistent with the matter content and the gauge group, therefore the Standard Model lagrangian becomes

$$\mathcal{L}_{SM} = \mathcal{L}_{gauge} + \mathcal{L}_{Higgs} + \mathcal{L}_Y, \quad (2.18)$$

where the first one contains the kinetic and the interaction terms of fermions and gauge bosons,  $\mathcal{L}_Y$  contains the Yukawa coupling between the Higgs and the fermions and

$$\mathcal{L}_{\text{Higgs}} = -(D_\mu \Phi)^\dagger (D_\mu \Phi) - \mathcal{V}(\Phi) \quad (2.19)$$

with

$$\mathcal{V}(\Phi) = -\frac{\mu^2}{2} \Phi^\dagger \Phi + \frac{\lambda}{4} (\Phi^\dagger \Phi)^2. \quad (2.20)$$

The minimum of the potential now is not zero but

$$\Phi_0^\dagger \Phi_0 \equiv \frac{v^2}{2} = \sqrt{\frac{-\mu^2}{\lambda}} \quad (2.21)$$

We choose as a vacuum configuration that correspond to a minimum of the potential

$$\Phi_0 = \begin{pmatrix} 0 \\ v \end{pmatrix}. \quad (2.22)$$

In this case one says that the Higgs takes a Vacuum Expectation Value (VEV). Indeed this breaks  $SU(2)_L \times U(1)_Y$  symmetry:

$$\begin{aligned} T_1 \Phi_0 &\neq 0, & T_2 \Phi_0 &\neq 0, \\ T_3 \Phi_0 &\neq 0, & Y \Phi_0 &\neq 0, \end{aligned} \quad (2.23)$$

leaving unbroken the following generator:

$$T_3 + \frac{Y}{2} \Phi_0 = 0. \quad (2.24)$$

This assures the existence of the massless photon at low energies. This is indeed the charge operator which is conserved by the vacuum. Therefore the vacuum is invariant under

$$e^{i\alpha(x)Q} \Phi_0 = \Phi_0, \quad (2.25)$$

thus the only gauge group that remains is  $U(1)_{\text{em}}$  as we wanted.

## Gauge bosons masses

We can develop  $\Phi$  around its VEV, in the unitary gauge we have:

$$\Phi(x) = \begin{pmatrix} 0 \\ v + H(x) \end{pmatrix}. \quad (2.26)$$

The action of the covariant derivative on the Higgs doublet is [36]

$$D_\mu \Phi(x) = \frac{1}{\sqrt{2}} \begin{pmatrix} 0 \\ \partial_\mu H \end{pmatrix} - \frac{i}{2\sqrt{2}} \begin{pmatrix} gA_\mu^3 + g'B_\mu & gA_\mu^1 - igA_\mu^2 \\ gA_\mu^1 + igA_\mu^2 & -gA_\mu^3 + g'B_\mu \end{pmatrix} \begin{pmatrix} 0 \\ v + H \end{pmatrix} \quad (2.27)$$

By plugging it in the kinetic term in  $\mathcal{L}_{\text{Higgs}}$  and rewriting everything in terms of the physical gauge bosons we obtain

$$\begin{aligned} -(D_\mu \Phi)^\dagger (D^\mu \Phi) &= -\frac{1}{2} \partial_\mu H \partial^\mu H - \frac{1}{8} (v + H)^2 g^2 W_\mu^\dagger W^\mu \\ &\quad - \frac{1}{8} (v + H)^2 (g^2 + g'^2) Z_\mu Z^\mu. \end{aligned} \quad (2.28)$$

Therefore when the Higgs gets a VEV different than zero  $W$  and  $Z$  bosons acquire a mass while the photon remain massless just as we wanted. The mass of the gauge bosons are proportional to the VEV and to the coupling of the bosons with the Higgs:

$$m_W = \frac{gv}{2}, \quad m_Z = \frac{\sqrt{g^2 + g'^2}}{2} v. \quad (2.29)$$

let us plug Eq. 2.26 in the potential  $V$ , we get

$$V = \lambda v^2 H^2 + \lambda v H^3 + \frac{\lambda}{4} H^4 \quad (2.30)$$

The Higgs then obtain a mass proportional to the self-interaction coupling:

$$m_H = \sqrt{\lambda} v. \quad (2.31)$$

In the next section we are studying the Yukawa part of the Standard Model lagrangian.

## 2.4 Fermion masses and mixing

let us consider the Yukawa lagrangian

$$\mathcal{L}_Y = Y_u \bar{Q} \tilde{\Phi} u_R + Y_d \bar{Q} \Phi d_R + Y_e \bar{L} \Phi e_R + \text{h.c.}, \quad (2.32)$$

where  $\tilde{\Phi} = i\sigma_2 \Phi^*$  has been used in order to make up quark term gauge invariant. Developing  $\Phi$  around its VEV as we have done in the last section we obtain the fermion Dirac mass terms:

$$\mathcal{L}_Y = v Y_u \bar{u}_L u_R + v Y_d \bar{d}_R d_L + v Y_e \bar{e}_R e_L + \text{h.c.}. \quad (2.33)$$

The masses are proportional to the Yukawa couplings which are free parameters in the Standard Model.

## Flavour mixing

So far we have explored the basic features of Standard Model considering only one flavour generation. let us extend the discussion to all of the three flavours. In this case the Yukawa coupling are  $3 \times 3$  matrices  $Y_{\alpha\beta}$ . In general those matrices are not diagonal and the fermions states we have considered so far have not definite mass. We are still using the notation of the last section, but for  $u$  and  $d$  we mean  $u = (u, c, t)$  and  $d = (d, s, b)$ .

We can start from a basis in which  $Y_e$  is diagonal while  $Y_u$  and  $Y_d$  are not. In this case we can rewrite Eq. 2.32 as:

$$\mathcal{L}_Y = Y'_{\alpha\beta} \overline{Q}'_L \tilde{\Phi} u'_R + Y'_{d\alpha\beta} \overline{Q}'_L \Phi d'_R + Y_e \bar{L} \Phi e_R + \text{h.c.}, \quad (2.34)$$

where we have called the flavour quark basis as  $\{Q'_L, u'_R, u'_L\}$ .

let us diagonalize the Yukawa matrices:

$$Y_u = Y_{u\alpha} \delta_{\alpha\beta} = V_L^{U\dagger} Y'_u V_R^U, \quad (2.35)$$

$$Y_d = Y_{d\alpha} \delta_{\alpha\beta} = V_L^{D\dagger} Y'_d V_R^D. \quad (2.36)$$

We can now switch to the mass basis:

$$u_L = V_L^{U\dagger} u'_L, \quad d_L = V_L^{D\dagger} d'_L, \quad (2.37)$$

$$u_R = V_R^{U\dagger} u'_R, \quad d_R = V_R^{D\dagger} d'_R. \quad (2.38)$$

The main physical consequence of the fact that flavour and mass basis are different is that quarks interactions mix flavour. let us write the charged current Lagrangian in the flavour basis and then rotate in the physical basis:

$$\mathcal{L}_{CC} = \frac{g}{\sqrt{2}} \overline{u}'_L \gamma^\mu d'_L W_\mu + \text{h.c.} \quad (2.39)$$

$$= \frac{g}{\sqrt{2}} \overline{u}_L V_L^{U\dagger} V_L^D \gamma^\mu W_\mu + \text{h.c.} \quad (2.40)$$

The matrix  $V_L^{U\dagger} V_L^D \equiv V_{\text{CKM}}$  is the Cabibbo-Kobayashi-Maskawa (CKM) matrix [37] and it is the mixing matrix for the quark sector.

$$V_{\text{CKM}} = \begin{pmatrix} V_{ud} & V_{us} & V_{ub} \\ V_{cd} & V_{cs} & V_{cb} \\ V_{td} & V_{ts} & V_{tb} \end{pmatrix} \quad (2.41)$$

In general a  $N \times N$  unitary matrix can be parameterized with  $N(N-1)/2$  mixing angles and  $N(N+1)/2$  phases. Not all the phases are physical though, since they can be removed with a global  $U(1)$  transformation:

$$u_L \rightarrow e^{i\alpha_U} u_L, \quad u_R \rightarrow e^{i\alpha_D} d_L. \quad (2.42)$$

One can reparameterize Eq. 2.40 for each color and each flavour, expliciting all the phases and find that there remains only one physical phase. We can understand that also noticing that reparameterizing all six spinors present in the charged current with the same phase does not change Eq. 2.40 and then only 5 of the 6 phases can be removed. Therefore  $V_{\text{CKM}}$  can be parameterized using three mixing angles  $\{\theta_{12}, \theta_{13}, \theta_{23}\}$  and one phase  $\delta_q$ .

$$V_{\text{CKM}} = \begin{pmatrix} \tilde{c}_{12}\tilde{c}_{13} & \tilde{s}_{12}\tilde{c}_{13} & \tilde{s}_{13}e^{-i\delta_q} \\ -\tilde{s}_{12}\tilde{c}_{23} - \tilde{c}_{12}\tilde{s}_{13}\tilde{s}_{23}e^{i\delta_q} & \tilde{c}_{12}\tilde{c}_{23} - \tilde{s}_{12}\tilde{s}_{13}\tilde{s}_{23}e^{i\delta_q} & \tilde{c}_{13}\tilde{s}_{23} \\ \tilde{s}_{12}\tilde{s}_{23} - \tilde{c}_{12}\tilde{s}_{13}\tilde{c}_{23}e^{i\delta_q} & -\tilde{c}_{12}\tilde{s}_{23} - \tilde{s}_{12}\tilde{s}_{13}\tilde{c}_{23}e^{i\delta_q} & \tilde{c}_{13}\tilde{c}_{23} \end{pmatrix}, \quad (2.43)$$

where  $\tilde{s}_{ij} = \sin \theta_{ij}^q$ ,  $\tilde{c}_{ij} = \cos \theta_{ij}^q$ .

## CP Violation

In the next chapters the presence of CP violation will be crucial to try to explain matter-antimatter asymmetry. let us derive the conditions that determine whether  $V_{\text{CKM}}$  violates CP or not. We are following Ref. [38]. let us start from noticing that  $u_L$  and  $d_L$  transform under CP transformation as:

$$\overline{u}_L \xrightarrow{\text{CP}} -u_L^T \mathcal{C}^{-1} \gamma^0 D^\dagger \left( \vec{\xi}_U \right), \quad d_L \xrightarrow{\text{CP}} D \left( \vec{\xi}_D \right) \gamma^0 \mathcal{C} \overline{d}_L^T, \quad (2.44)$$

where  $D^\dagger \left( \vec{\xi}_U \right) = \text{diag} (e^{i\xi_u}, e^{i\xi_c}, e^{i\xi_t})$  and  $D \left( \vec{\xi}_D \right) = \text{diag} (e^{i\xi_d}, e^{i\xi_s}, e^{i\xi_b})$  are unspecified CP phases.

The charged current  $j_{W,Q}^\mu = 2\overline{u}_L V_{\text{CKM}} \gamma^\mu d_L$  transforms then as:

$$j_{W,Q}^\mu \xrightarrow{\text{CP}} -2\overline{d}_L D \left( \vec{\xi}_D \right) V_{\text{CKM}}^T D^\dagger \left( \vec{\xi}_U \right) \gamma_\mu u_L. \quad (2.45)$$

The gauge boson  $W$  transforms instead as:

$$W_\mu \xrightarrow{\text{CP}} e^{i\xi_W} W^{\mu\dagger}. \quad (2.46)$$

Then the transformed charged current lagrangian  $j_{W,Q}^\mu W_\mu$  takes the same form of its hermitean conjugate. Then we do not have CP Violation if:

$$j_{W,Q}^\mu W_\mu \xrightarrow{\text{CP}} (j_{W,Q}^\mu W_\mu)^\dagger. \quad (2.47)$$

This implies:

$$V_{\text{CKM}} = V_{\text{CKM}}^*. \quad (2.48)$$

Therefore if the CP phase  $\delta_q$  is different from  $0, 2\pi, \dots$  then we have CP violation. Such violation has indeed been measured for B and K decays [39, 40]. We can proceed in a similar way for finding the CP-invariance condition on the Yukawa interactions. After some algebra one still find that Yukawa interaction are CP-invariant if  $V_{\text{CKM}} = V_{\text{CKM}}^*$ .

## 2.5 Mixing and CP violation in the lepton sector

In the lepton sector being the neutrino massless there is no need to adding a mixing matrix and we can simply assume  $Y_e$  to be diagonal. This changes if we add to the particle content of the Standard Model  $\nu_R$  and therefore adding an extra Yukawa term in the lagrangian that becomes

$$\mathcal{L}_Y = Y_u \bar{Q} \tilde{\Phi} u_R + Y_d \bar{Q} \Phi d_R + Y_e \bar{L} \Phi e_R + \text{h.c.} + Y_D \bar{L}_L \tilde{\Phi} \nu_R. \quad (2.49)$$

This implies adding a mass term for the neutrino. In such a case we have again two different basis the flavour basis  $\{e', \nu'\}$  and the mass basis  $\{e, \nu\}$ . We can consider again the charged current interaction between massive eigenstates and we find:

$$\mathcal{L}_{CC} = -\frac{g}{\sqrt{2}} U_{PMNS}^* \bar{\nu}_L \gamma^\mu L_L W_\mu. \quad (2.50)$$

The Pontecorvo-Maki-Nakagawa-Sakata matrix [41] has the same structure and therefore it has the same free parameters, 3 mixing angles and 1 phases. In some model we are going to see that  $\nu_R$  is a majorana neutrino and therefore is not invariant under global transformations. In such a case there will be three physical phases.

### Neutrino Flavour Oscillation

The main physical consequence of the existence of  $\nu_R$  is that there is mixing also in the lepton sector and neutrinos, when propagating in vacuum or trough matter, may change flavor. As we have seen, neutrinos interact with other particles through charge current and neutral current interactions and when they are produced, for example with cosmic rays, supernovae, or in the Sun, they are in a flavour eigenstate. If the neutrino are massive, the mass eigenstates basis can be different from the flavour basis and therefore we can write:

$$|\nu_\mu\rangle = \sum_i U_{\mu i}^* |\nu_i\rangle. \quad (2.51)$$

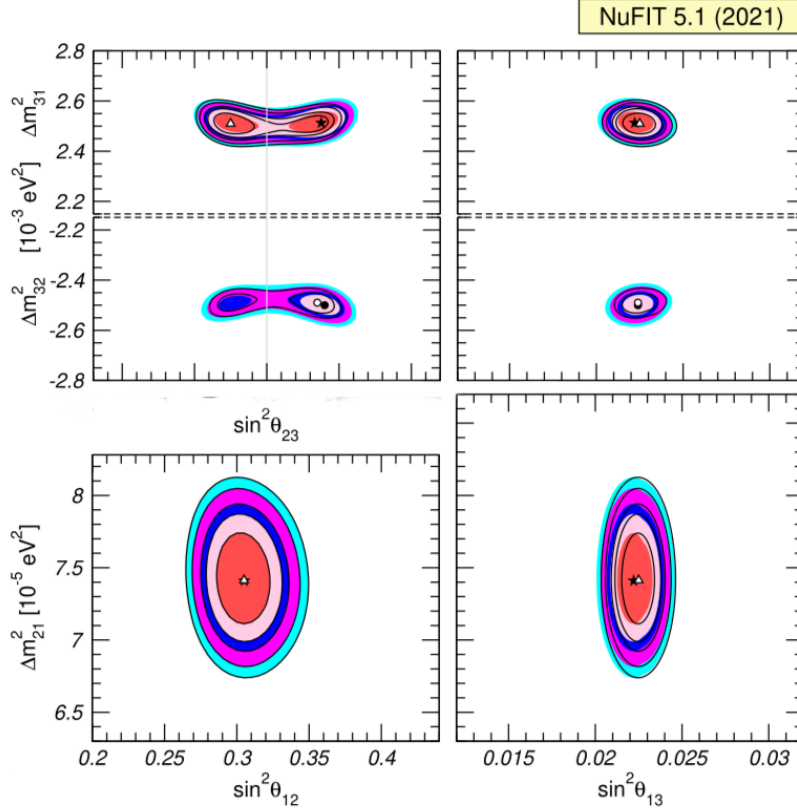


Figure 2.2: Results from the global fit for neutrino oscillations on the values of  $\theta_{12}$ ,  $\theta_{13}$ ,  $\Delta m_{21}^2$  and  $\Delta m_{32}^2$ . Pictures taken from [42].

Neutrino travels from the source to the detector as massive eigenstates and therefore in general one can expect that at the detector neutrinos may have changed flavour, in this case we say that there has been an oscillation. The oscillation probability is:

$$P(\nu_\alpha \rightarrow \nu_\beta) = \left| \sum_i U_{\alpha i}^* U_{\beta i} e^{-i \frac{\Delta m_{i1}^2}{2E} L} \right|. \quad (2.52)$$

In Eq. 2.52,  $U_{\alpha i}$  is the PMNS mixing matrix and  $\Delta m_{ij}^2$  is the square of the mass difference between the  $i$ -th massive eigenstate and the lightest neutrino. Indeed these oscillations has been observed by Super-K [43], SNO [44], MINOS[45], T2K [46], KamLAND [47], NoVA [48] and other experiments: neutrinos have a mass.

We still do not know the absolute value of the masses which is being searched for by experiments such as KATRIN [49]. Since we only know the squared difference between masses from we can say that there are at least three massive neutrinos but we still do

not have determine the mass ordering. There are two possibilities:

- In the normal ordering (NO) it is assumed  $m_1 < m_2 < m_3$  and therefore we have

$$m_2 = \sqrt{m_1^2 + \Delta m_{21}^2}, \quad m_3 = \sqrt{m_1^2 + \Delta m_{13}^2}. \quad (2.53)$$

In such case the current results with a  $1\sigma$  range in the neutrino sector are, considering the atmospheric data of Super-K [42]:

$$\theta_{12}^\circ = 33.44_{-0.74}^{+0.77}, \quad \theta_{13}^\circ = 8.57_{-0.12}^{+0.13}, \quad (2.54)$$

$$\frac{\Delta m_{21}^2}{10 - 5} \text{eV}^2 = 7.42_{-0.20}^{+0.21}, \quad \frac{\Delta m_{23}^2}{10^{-3}} \text{eV}^2 = 2.515_{-0.028}^{+0.02}, \quad (2.55)$$

in this region  $\theta_{23}$  is constrained to be in the second octant  $45^\circ < \theta_{23}^\circ < 90^\circ$ . Without considering Super-K data we have:

$$\theta_{12}^\circ = 33.45_{-0.75}^{+0.77}, \quad \theta_{13}^\circ = 8.62_{-0.12}^{+0.12}, \quad (2.56)$$

$$\frac{\Delta m_{21}^2}{10^{-5}} \text{eV}^2 = 7.42_{-0.20}^{+0.21}, \quad \frac{\Delta m_{23}^2}{10^{-3}} \text{eV}^2 = 2.510_{-0.027}^{+0.027}, \quad (2.57)$$

in this region  $\theta_{23}$  is constrained to be in the first octant  $0^\circ < \theta_{23}^\circ < 45^\circ$ .

- In the inverse ordering (IO) instead it is assumed  $m_3 < m_1 < m_2$ .

The current values of  $\theta_{23}$  and  $\delta$  have still big uncertainties and it makes more sense to give only the  $3\sigma$  interval. The difference between considering or not Super-K atmospheric data is particularly significant. In the first case we have

$$\theta_{23} = (39.7, 50.9), \quad \delta = (144, 350), \quad (2.58)$$

while in the second case

$$\theta_{23} = (39.5, 52.0), \quad \delta = (105, 405). \quad (2.59)$$

In the scan of the next chapter due to such big uncertainties we are going to treat this observables as predictions of our model and we will not use them in the fit.

# Neutrino masses, See-Saw Model and Left-Right Symmetry

Neutrino masses are one of main problems in particle physics: how to extend Standard Model in order to explain neutrino masses? One of the main candidates is the seesaw model: one needs to add to the Standard Model an heavy right handed neutrino and it explain naturally the tiny mass of the left handed neutrino. In this chapter we are going to introduce the seesaw model and see how it can be embedded in some left-right symmetric extension of the Standard Model.

## 3.1 Adding Neutrino Masses into the Standard Model

One of the problems of the Standard Model is that it is incomplete: it does not explain neutrino masses. We are going to see some of the extensions of the Standard Model which explain neutrino masses, in particular we are going to introduce the See-Saw mechanism and left-right symmetric model.

### Dirac and majorana Mass

The simplest possibility is to add a right-handed neutrino  $\nu_R$  and a Dirac mass term in the same way as one does for electrons. Considering only one flavour one has:

$$\mathcal{L}_{\text{leptons}} = Y_e \bar{e}_L e_R + Y_\nu \bar{\nu}_L \nu_R + \text{h.c.} \quad (3.1)$$

The main drawback of this procedure is the enormous amount of fine tuning required to be consistent with the upper bound on neutrino masses:  $\sum m_\nu \lesssim 0.26 \text{ eV}$  (95%CL) [50].

Assuming that the mass of the lightest neutrino is around  $10^{-2}\text{eV}$  this implies

$$\frac{Y_\nu}{Y_e} \sim 10^{-8}. \quad (3.2)$$

Instead of adding a right-handed neutrino we could generate a majorana mass for the left-handed neutrino. In this case the Lagrangian is

$$\mathcal{L}_{\text{leptons}} = Y_e \bar{e}_L e_R + m_L \nu_L^T C^{-1} \nu_L^* + \text{h.c.}. \quad (3.3)$$

The main problem of this approach is that a majorana mass term is not gauge invariant and cannot be embedded in the Standard Model. In order to do that we need to introduce the Weinberg operator.

## 3.2 Weinberg Operator

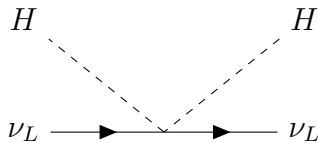


Figure 3.1: Feynman diagram for the Weinberg operator.

Since we are interested in a chiral gauge invariant mass term, let us study the combinations of the lepton and Higgs doublet which are singlet of  $SU(2)$ . We have

$$l_L = \begin{pmatrix} \nu_L \\ e_L \end{pmatrix}, \quad \Phi = \begin{pmatrix} 0 \\ H \end{pmatrix}. \quad (3.4)$$

We are interested in terms that contains  $\nu_L$  and so we use  $\tilde{\Phi} = i\sigma_2\Phi$ .

An invariant term is  $l_L^T \tilde{\Phi}$ . With this element we can build a 5 dimensional operator which allow us to embed the neutrino Majorana mass once the Higgs gets a VEV. This operator is the Weinberg operator [51] :

$$\mathcal{L}_W = \frac{(l_L^T i\sigma_2 \Phi) C (\Phi^T i\sigma_2 l_L)}{\Lambda_W} \quad (3.5)$$

In this case the theory is not renormalizable anymore and we have what is called an effective field theory. The presence of such an operator implies that this theory works

properly only at low energies and it is a hint of a new physics at the scale  $\Lambda_W$ . If one wants to study the system at higher scale one has to find an UV completion, that is a new model with more degrees of freedom which is renormalizable. At low energy one can integrate out this degrees of freedom and come back to the original effective theory. In general working using effective field theories is very powerful because one can obtain results which hold for every possible model chosen as UV completion. We shall return later to the concept of effective theories in when we will discuss the proton decay. Other than simply embed into the Standard Model a gauge invariant neutrino mass term, the most important feature of the Weinberg operator is that it explains naturally the tiny mass of the neutrino mass. Indeed when the Higgs gets a VEV one has

$$m_\nu = \frac{m_L v^2}{\Lambda_W}, \quad (3.6)$$

and considering  $m_L \sim \mathcal{O}(1)$  we obtain approximately  $\Lambda \sim 10^{14}$  GeV, this is the scale of a possible UV completion.

### 3.3 See-Saw Model

One of the possible UV completion is the See-Saw model: it is natural to embed it in GUT theories and gives a natural explanation of why neutrino mass is so small. As we have seen, in order to find an UV completion we need to introduce new degrees of freedom at the Weinberg scale. The simplest possibility is to introduce a fermion that does not interact with other particles via Standard Model Interaction, it is called heavy right-handed neutrino (RHN). In this case we have the so-called See-Saw Type I. Another possibility is to add a Higgs triplet that led to the so-called See-Saw Type II. We are going to give a brief summary of this two mechanism that later will be embedded in an SO(10) model.

#### See-Saw Type I

As we have seen in the earlier sections one needs to introduce a right-handed neutrino  $\nu_R$  in order to explain neutrino mass. let us start from the Majorana+Dirac mass model for neutrinos in which we insert in the Lagrangian a Dirac mass term and a Majorana mass term for the right handed neutrino:

$$\mathcal{L} = m_D \bar{\nu}_L n \nu_R + M_R \nu_R^T \mathcal{C} \nu_R + \text{h.c.} \quad (3.7)$$

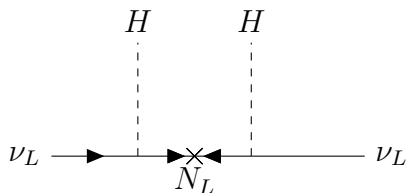


Figure 3.2: Feynman diagram for the type I See-Saw Model. We can see how integrating out  $N$  one can recover the Weinberg operator

The new degrees of freedom of our model is the majorana fermion  $N = N_L^c + N_L$  defined as

$$N_L^c \equiv \nu_R. \quad (3.8)$$

let us rewrite Eq. 3.7 in terms of this new particle. First, we have to notice that

$$N_L^T \mathcal{C} N_L = (\mathcal{C} \bar{\nu}_R^T)^T \mathcal{C} (\mathcal{C} \bar{\nu}_R^T) = \nu_R^\dagger \mathcal{C} \nu_R^*, \quad (3.9)$$

$$\bar{N}_L \mathcal{C} \nu_L = (\mathcal{C} \bar{\nu}_R^T) \mathcal{C} \nu_L = \bar{\nu}_R \nu_L. \quad (3.10)$$

With the help of equation Eq. 3.10 we obtain:

$$\mathcal{L} = m_D N_L^T \mathcal{C} \nu_L + \frac{1}{2} N_L^T \mathcal{C} N_L + \text{h.c.}, \quad (3.11)$$

where we have  $M_R^* \equiv M_N$ .

Then, plugging  $\nu_L$  in the  $SU(2)$  doublet, inserting the Higgs we obtain and considering all flavours we obtain

$$\mathcal{L}_{\text{seesaw I}} = i \bar{N}_i \not{\partial} N_i - Y_{\alpha i} \bar{l}_\alpha \tilde{\Phi} N_i - \frac{1}{2} M_i \bar{N}_i^c N_i. \quad (3.12)$$

Looking at Fig. 3.2, we can notice how integrating out  $N$  we reobtain the Weinberg operator at low energy. If we consider the second term in the right hand side we can see how  $N$  interact with leptons and the Higgs boson.

\* In particular from this term is easy to notice the link between leptogenesis and neutrino masses. Indeed succesfull leptogenesis put some constraints on heavy and light neutrino masses. let us now compute the light neutrino mass. let us now call the light neutrinos  $\nu$  and the heavy neutrino  $N$ , we can rewriting the lagrangian using a non diagonal mass matrix:

$$M_{\nu N} = \begin{pmatrix} 0 & m_D^T \\ m_D & M_N \end{pmatrix}, \quad (3.13)$$

---

\*The process  $N \rightarrow \Phi l$  is of fundamental important for leptogenesis, as we shall see in the next section.

We can rotate the system to the mass eigenstate basis with the matrix  $U$  that diagonalize  $M_{\nu N}$  and in doing so we find the diagonal neutrino mass matrix

$$m_{diag} = U^T M_{\nu N} U = \begin{pmatrix} m_\nu & 0 \\ 0 & M_N \end{pmatrix}. \quad (3.14)$$

Since  $N$  is at the Weinberg scale it is reasonable to assume:  $m_D \ll M_N$ . With this assumption an ansatz for  $U$  is the following:

$$U = \begin{pmatrix} 1 & \theta^\dagger \\ -\theta & 1 \end{pmatrix}, \quad (3.15)$$

$$UU^\dagger \sim 1 + \mathcal{O}(\theta^\dagger\theta). \quad (3.16)$$

With imposing  $m_{diag}$  to be diagonal we find the following condition for  $\theta$ :

$$m_D^T - \theta^T M_N = 0. \quad (3.17)$$

This implies:

$$m_\nu = -\theta^T m_D = -m_D^T M_N^{-1} m_D. \quad (3.18)$$

This is the celebrated neutrino mass formula predicted by the See-Saw mechanism. It is clear how the existence of an heavy neutrino automatically implies the fact that left-handed neutrino should be light.

## See-Saw Type II

Another possibility for adding new degrees of freedom to the Weinberg theory that also appears in some breaking chain of  $SO(10)$  is an Higgs triplet  $\Delta_L$  that couples with  $\nu_L$  [52, 53]. In this case the lagrangian is

$$\mathcal{L}_{ssII} = (Y_\Delta)_{\alpha\beta} \bar{l}_\alpha^c \Delta_L l_\beta + \text{h.c.} \quad (3.19)$$

As we shall see later this type of see-saw emerges in left-right symmetric models and the VEV for the Higgs is

$$\nu_L \sim \frac{\mu v^2}{M_\Delta^2}. \quad (3.20)$$

Again, it is natural to assume  $v \ll M_\Delta$  and then this explain the bounds on neutrino mass. In general one uses a See-Saw I+ II in which we take account for both the contributions and in this case we find the light neutrino mass to be

$$m_\nu = Y_\Delta \nu_L - m_D^T M_N^{-1} m_D. \quad (3.21)$$

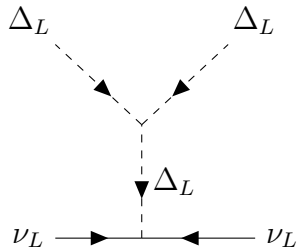


Figure 3.3: Feynman diagram for the type II See-Saw Model.

### 3.4 Left-Right symmetry

The minimal model that is able to predict the see-saw model is a model with left-right symmetry [54]. Today is well known that parity is violated and for this reason we need to distinguish between left and right spinors: only left handed spinors interacts with  $W$  and  $Z$  bosons. In this model one assume that this symmetry is broken only at lower energies while at higher energies left-right symmetry is reestablished. This implies automatically the existence of the right handed neutrino and it explain light neutrino masses trough the see-saw mechanism. This model is a good introduction for some of the basic concepts of  $SO(10)$ , since some of the intermediate steps in its breaking down to the Standard Model are left-right symmetric. One crucial feature that we will start studying in this section is the  $U(1)_{B-L}$  breaking, fundamental for neutrino masses and gravitational waves production.

#### Matter Content

In the extension of the electroweak sector the gauge group is

$$SU(2)_L \times SU(2)_R \times U(1)_X \times Z_2^C. \quad (3.22)$$

The matter content of this group for one flavour is

$$\begin{pmatrix} e_L \\ \nu_L \end{pmatrix}, \begin{pmatrix} u_{iL} \\ d_{iL} \end{pmatrix} \leftrightarrow \begin{pmatrix} e_R \\ \nu_R \end{pmatrix}, \begin{pmatrix} u_{iR} \\ d_{iR} \end{pmatrix}, \quad i = 1, 2, 3. \quad (3.23)$$

The symmetry between left and right spinors is induced by charge conjugation:

$$l_L^c = l_R. \quad (3.24)$$

The existence of the right-handed neutrino now is automatically implied by the assumption of the symmetry between left and right handed spinors.

## Electric charge and hypercharge

Similarly to what we did for the Standard Model  $SU(2)_L \times U(1)_Y$  group the ansatz for the charge operator in  $SU(2)_L \times SU(2)_R \times U(1)_X \times Z_2^C$  is [55]

$$Q = T_{3L} + T_{3R} + \frac{X}{2} \quad (3.25)$$

Now imposing the known charges of the particle content of the theory one can find the hypercharge  $X$  of each particle. For example:

$$Qu_R = \frac{2}{3}u_R = 1/2u_R + \frac{X}{2} \quad \Rightarrow Xu_R = \frac{1}{3}u_R, \quad (3.26)$$

$$Qd_L = \frac{-1}{3}d_L = -1/2d_L + \frac{X}{2} \quad \Rightarrow Xd_L = \frac{1}{3}d_L, \quad (3.27)$$

$$Qe_R = -e_R = -1/2e_R + \frac{X}{2} \quad \Rightarrow Xe_R = -e_R, \quad (3.28)$$

$$Q\nu_R = 0 = 1/2\nu_R + \frac{X}{2} \quad \Rightarrow X\nu_R = -\nu_R. \quad (3.29)$$

From Eq. 3.29 we can see how in fact  $X = B - L$  in this model [56]. At this point we can already see an hint of how this model is linked to the generation of neutrino mass. Indeed, generating a majorana term for neutrinos implies breaking lepton number and therefore  $B - L$ , so we expect that the scale of the heavy majorana mass correspond to the  $B - L$  breaking. <sup>†</sup>

This happens in the same way of  $SO(10)$ , being this model just an intermediate step of the breaking of  $SO(10)$  down to  $G_{SM}$ .

We could have done the inverse process instead: in the extended Standard Model,  $B$  and  $L$  are accidental global symmetry. Assuming left-right symmetry we can verify how  $B - L$  is free from anomalies and then we can gauge this group building the model we are currently studying.

## L-R breaking

Let us show how we can break a left-right symmetric model down to the Standard Model and let us see how the seesaw type mechanism emerges.

Let us first study the  $SU(2)_L \times SU(2)_R \times U(1)_{B-L} \rightarrow G_{SM}$  process. We need to introduce

---

<sup>†</sup>The breaking of this  $U(1)$  gauge group predicts the existence of cosmic strings as we shall see later and thus the string tension scale is linked to the mass of the heavy neutrinos.

two Higgses which are generic multiplets of  $SU(2)$  that we will call  $\chi_L$  and  $\chi_R$ . The Higgs potential is:

$$\mathcal{V} = -\frac{\mu^2}{2} (\chi_L^2 + \chi_R^2) + \frac{\lambda}{4} (\chi_L^2 + \chi_R^2)^2 + \frac{\lambda' - \lambda}{2} \chi_L^2 \chi_R^2. \quad (3.30)$$

If we minimize the potential we see that there can be different situation depending on the sign of  $\lambda' - \lambda$ . The physically allowed case is  $\lambda' > \lambda$ . This implies:

$$\langle \chi_L^2 \rangle \langle \chi_R^2 \rangle = 0 \Rightarrow \langle \chi_L^2 \rangle = 0, \quad \langle \chi_R^2 \rangle = v_R \neq 0. \quad (3.31)$$

If we look at the Yukawa terms in this Lagrangian we do not want standard particles to acquire a further mass term proportional to  $v_r$  while we expect that new particles predicted by this model have mass proportional to the breaking scale. The best candidates for left and right  $\chi$  are then  $SU(2)$  triplets that we call  $\Delta_L = (1, 3, 2)$  and  $\Delta_R = (3, 1, 2)$  [57]. The decomposition under charge eigenstates of the triplets is

$$\Delta_R = \begin{pmatrix} \frac{\Delta^+}{2} & \Delta^{++} \\ \Delta^0 & -\frac{\Delta^+}{2} \end{pmatrix}, \quad (3.32)$$

and one can prove that [54]

$$\langle \Delta_R \rangle = \begin{pmatrix} 0 & 0 \\ v_R & 0 \end{pmatrix}. \quad (3.33)$$

The Yukawa part of the Lagrangian before of the SSB that is responsible for the fermion masses is:

$$\mathcal{L}_Y = Y_\Delta (l_R^T C i \sigma_2 \Delta_R l_R) + (L \leftrightarrow R). \quad (3.34)$$

We can see how when  $\Delta_R$  gets a vev  $\nu_R$  acquire a Majorana mass.

## Accidental VEV and Type I+II See-Saw

Until now we have supposed that  $\langle \Delta_L \rangle = 0$ .

Instead, we are going to prove that it is different than zero, even if remains very small and can be neglected at the parity breaking scale. Before  $G_{SM}$  breaking the most general

potential for the Higgs triplets is [54]

$$\begin{aligned}
V(\Delta_L, \Delta_R) = & -\mu^2 \text{Tr} \left( \Delta_L^\dagger \Delta_L + \Delta_R^\dagger \Delta_R \right) \\
& + \rho_1 \left[ \left( \text{Tr} \left( \Delta_L^\dagger \Delta_L \right) \right)^2 + \left( \text{Tr} \left( \Delta_R^\dagger \Delta_R \right) \right)^2 \right] \\
& + \rho_2 \left[ \text{Tr} \left( \Delta_L^\dagger \Delta_L \Delta_L^\dagger \Delta_L \right) + \text{Tr} \left( \Delta_R^\dagger \Delta_R \Delta_R^\dagger \Delta_R \right) \right] \\
& + \rho_3 \left[ \text{Tr} \left( \Delta_L^\dagger \Delta_L \right) \text{Tr} \left( \Delta_R^\dagger \Delta_R \right) \right] \\
& + \rho_4 \left[ \text{Tr} \left( \Delta_L^\dagger \Delta_L^\dagger \right) \text{Tr} \left( \Delta_L \Delta_L \right) + \text{Tr} \left( \Delta_R^\dagger \Delta_R^\dagger \right) \text{Tr} \left( \Delta_R \Delta_R \right) \right],
\end{aligned} \tag{3.35}$$

and when the Higgs gets a VEV it can be reconduced to Eq. 3.30. Now we need a further Higgs to break  $G_S M$ :  $\Phi = (2, 2, 0)$ . In the Yukawa part of the Lagrangian there are going to be terms such as:

$$\mathcal{L}_Y = Y_\Phi \bar{l}_R \Phi l_L + \text{h.c.}, \tag{3.36}$$

and this implies that  $\Phi$  has to be a bi-doublet, so that it transforms as:

$$\Phi \rightarrow \Phi' = \mathcal{U}_L \Phi \mathcal{U}_R^\dagger. \tag{3.37}$$

The decomposition of  $\Phi$  is:

$$\Phi = \begin{pmatrix} \phi_1^0 & \phi_2^+ \\ \phi_1^- & -\phi_2^0 \end{pmatrix}. \tag{3.38}$$

One can prove that when  $\Phi$  gets a VEV it becomes:

$$\Phi = \begin{pmatrix} v_1 & 0 \\ 0 & v_2 \end{pmatrix} \quad \text{s.t.} \quad v_1^2 + v_2^2 = v^2, \tag{3.39}$$

and that it breaks  $G_{\text{SM}}$  down to  $U(1)_{\text{em}}$ .

Coming back to the fact that  $\langle \Delta_L \rangle \neq 0$  we need to consider the interaction potential between  $\Phi$  and  $\Delta$ .

We simply have to consider one term of this potential:

$$\mathcal{V}(\Phi, \Delta_L, \Delta_R) = \alpha \text{Tr} \left( \Delta_L^\dagger \Phi \Delta_R \Phi^\dagger \right). \tag{3.40}$$

let us call  $\langle \Delta_L \rangle \equiv v_L$  and let us point out that until now we have assumed  $v_L = 0$ .

We can see tough, that if we add to Eq. 3.35 the interaction term above and if we then derive with respect to  $v_L$  imposing the minimum condition, that  $v_L$  cannot be equal to

zero.

Instead we obtain:

$$v_L \sim \frac{\alpha v_W^2 v_R}{m_{\Delta_L}^2} \sim \frac{\alpha M_W^2}{M_R}. \quad (3.41)$$

Now we can write the final Yukawa terms of the Lagrangian and find

$$\mathcal{L}_Y = Y_\Phi \bar{l}_R \Phi l_L + Y_\Delta (l_R^T \mathcal{C} i \sigma_2 \Delta_R l_R + l_L^T \mathcal{C} i \sigma_2 \Delta_L l_L) + \text{h.c.} \quad (3.42)$$

When all the Higgs bosons get a vev one can show repeating the steps of the earlier section we can see how the Type I+II seesaw is embedded in a left-right symmetric model.

### 3.5 $SU(4)_C \times SU(2)_L \times SU(2)_R$ : the Pati-Salam model

So far we have studied the gauge structure of the electroweak sector: since we were interested in finding a model for neutrino masses we were interested only in leptons,  $SU(3)$  singlets, and we didn't worry about QCD. Now we will start building a model for Grand Unification<sup>‡</sup> and therefore we need to take account also for  $SU(3)$  and add it to our left-right gauge group.

We can start with the following model:  $SU(3)_C \times SU(2)_R \times SU(2)_R \times U(1)_{B-L}$ . A further step forward to unification was made by Pati and Salam [10]: they treated leptons, singlet of  $SU(3)$ , as a fourth colour and used  $SU(4)$  to describe together leptons and quarks. Adding the electroweak sector we obtain the Pati-Salam model (PS):  $SU(4) \times SU(2)_R \times SU(2)_L$ .

We organize the right-handed spinors in this way:

$$\left( \begin{pmatrix} e_R \\ \nu_R \end{pmatrix}, \begin{pmatrix} u_{1R} \\ d_{1R} \end{pmatrix}, \begin{pmatrix} u_{2R} \\ d_{2R} \end{pmatrix}, \begin{pmatrix} u_{3R} \\ d_{3R} \end{pmatrix} \right), \quad (3.43)$$

and the same hold for left spinors.

The breaking of PS model down to Standard Model happen in two steps, first  $SU(4) \rightarrow SU(3) \times U(1)_{B-L}$  and then left-right symmetry breaking.

---

<sup>‡</sup>To be precise this is not a proper example of GUT theories since the gauge group is not simple and therefore there are different couplings for different interactions and we do not reach gauge coupling unification

## Fermion masses

The main feature of this model is that it embeds in the same representation quarks and leptons, allowing for the possibility of predicting fermion masses. This is the main feature of PS model which we shall find also in  $SO(10)$ . Here we start studying the prediction of the ratio between lepton and quarks masses for two Higgs bosons:  $(1, 2, 2)$  and  $(15, 2, 2)$ . As we shall see in the next section this bosons appear in the breaking of some  $SO(10)$  Higgs responsible for the fermion masses. It is convenient to study already the predictions of this Higgs, in this way later we can concentrate more on the group structure of the Higgs without worrying about the details of the computation. let us first study the following term:

$$\mathcal{L} = Y_1 \bar{l}_R \Phi_1 l_L \quad (3.44)$$

in which  $\Phi_1$  is a bi-doublet and an adjoint representation of  $SU(4)$ :  $\mathbf{15}$ . Being a linear combination of  $SU(4)$  generators,  $\mathbf{15}$  has to be traceless. Upon a normalization constant it can be written as

$$\mathbf{15} = \begin{pmatrix} \frac{1}{3} & 0 & 0 & 0 \\ 0 & \frac{1}{3} & 0 & 0 \\ 0 & 0 & \frac{1}{3} & 0 \\ 0 & 0 & 0 & -1 \end{pmatrix}. \quad (3.45)$$

Let us embed  $\mathbf{15}$  in the bidoublet structure and let  $\Phi_1$  take a VEV, we obtain

$$\Phi_1 = \begin{pmatrix} V & 0 \\ 0 & V^\dagger \end{pmatrix} \quad (3.46)$$

where:

$$V = \begin{pmatrix} \frac{1}{3} & 0 & 0 & 0 & 0 & 0 & 0 & 0 \\ 0 & \frac{1}{3} & 0 & 0 & 0 & 0 & 0 & 0 \\ 0 & 0 & \frac{1}{3} & 0 & 0 & 0 & 0 & 0 \\ 0 & 0 & 0 & \frac{1}{3} & 0 & 0 & 0 & 0 \\ 0 & 0 & 0 & 0 & \frac{1}{3} & 0 & 0 & 0 \\ 0 & 0 & 0 & 0 & 0 & \frac{1}{3} & 0 & 0 \\ 0 & 0 & 0 & 0 & 0 & 0 & -1 & 0 \\ 0 & 0 & 0 & 0 & 0 & 0 & 0 & -1 \end{pmatrix}. \quad (3.47)$$

If we plug this expression in the Lagrangian it is easy to prove that  $m_{\text{quarks}} = \frac{1}{3} m_{\text{leptons}}$ . Another possibility that we will see in the next section is using  $\Phi_2 = (1, 2, 2)$ . Since this is a singlet of  $SU(4)$  it does not distinguish between quarks and leptons so we obtain simply:  $m_{\text{quarks}} = m_{\text{leptons}}$ .

# $SO(10)$ : The general framework

The framework of our model is  $SO(10)$ .  $SO(10)$  is one of the promising models that aim to extend the Standard Model and in particular embeds left-right symmetric models and the seesaw mechanism. There are different possibilities for breaking  $SO(10)$  down to the Standard Model, each one of these is called a breaking chain. We will discuss in this chapter the group theory of  $SO(10)$ , how we can achieve gauge couplings unification and then we will focus on a particular breaking chain. Finally we will study the Yukawa sector of such a breaking chain and scan the parameter space in order to predict fermion masses.

## 4.1 Spinorial representation of $SO(10)$

The representations of  $SO(10)$  can be single valued, the usual vector representation, or double valued, the so-called spinorial representation. In this section we are going to build the spinors structure of  $SO(10)$  proceedings in a similar way as one do for the Lorentz group.  $SO(10)$  with a spinorial structure is called  $Spin(10)$  but we will keep mentioning it as  $SO(10)$ . Let us start more generally with  $SO(2n)$ . It can be proved that states that there exists  $2^n \times 2^n$  matrices  $\Gamma_i$  with  $i = 1, 2, \dots, 2n$  that satisfies the so-called Clifford algebra:

$$\{\Gamma_i, \Gamma_j\} = \frac{1}{2i} \delta_{ij}. \quad (4.1)$$

Starting with  $n = 1$  we see that we just need to have

$$\Gamma_1^{(1)} = \sigma_1, \quad \Gamma_2^{(1)} = \sigma_2. \quad (4.2)$$

Proceeding by induction following Ref. [?] we obtain the matrices at  $n + 1$  from the matrices at  $n$  following the rule below:

$$\Gamma_i^{(n+1)} = \begin{pmatrix} \Gamma_i^{(n)} & 0 \\ 0 & -\Gamma_i^{(n)} \end{pmatrix}, \quad (4.3)$$

$$\Gamma_{2n+1}^{(n+1)} = \begin{pmatrix} 0 & \mathbf{1}_{n \times n} \\ \mathbf{1}_{n \times n} & 0 \end{pmatrix}, \quad (4.4)$$

$$\Gamma_{2n+2}^{(n+1)} = \begin{pmatrix} 0 & -\mathbf{i}_{n \times n} \\ \mathbf{i}_{n \times n} & 0 \end{pmatrix}. \quad (4.5)$$

Let us now introduce a new set of matrices  $\Sigma_{ij} = \frac{1}{2}i[\Gamma_i, \Gamma_j]$  which are generators of the  $2n$ -dimensional representation of  $SO(2n)$ . Calling  $R(\omega)$  the fundamental single valued representation, i.e. a  $2n$ -dimensional rotation, and  $U(\omega) = e^{i\omega_{ij}\Sigma_{ij}}$  the unitary representation one can prove that  $\Gamma_i$  transforms respectively as:

$$\Gamma_i \rightarrow \Gamma'_j = R_{ji}\Gamma_i, \quad (4.6)$$

$$\Gamma_i \rightarrow \Gamma'_i = U^\dagger \Gamma_i U. \quad (4.7)$$

let us now introduce  $\psi$ : a  $2^n$ -dimensional vector that transform as

$$\psi \rightarrow \psi' = U\psi. \quad (4.8)$$

This object is called spinor. The unitary representation  $U$  we have seen so far is not irreducible. Indeed we can find a matrix that commutes with all the  $\Gamma_i$  and therefore with all the generators  $\Sigma_{ij}$ . This matrix is defined as

$$\Gamma_{\text{FIVE}}^{(n)} = (-i)^n \Gamma_1 \Gamma_2 \dots \Gamma_{2n}. \quad (4.9)$$

Therefore we can split the spinor in chiral components that transform according to the unitary irreducible representation

$$\psi = \begin{pmatrix} \psi_+ \\ \psi_- \end{pmatrix}. \quad (4.10)$$

Starting from the original spinor we obtain this chiral components using the so-called projectors, which are built from  $\Gamma_{\text{FIVE}}$  \*.

$$\mathcal{P}_+\psi = (\mathbf{1} + \Gamma_{\text{FIVE}})\psi = \psi_+, \quad (4.11)$$

---

\*This is why we are considering  $SO(2n)$  and not  $SO(2n + 1)$ . Indeed, in such types of models we would not have any  $\Gamma_{\text{FIVE}}$  and therefore no chirality.

$$\mathcal{P}_-\psi = (\mathbf{1} - \Gamma_{FIVE})\psi = \psi_- \quad (4.12)$$

Continuing the analogy with the Lorentz group let us introduce the charge conjugation operator. In the last section we have seen that a chiral mass term is of the type  $\psi^T \mathcal{C} \psi$  and  $\mathcal{C} = i\sigma_2$  makes the term Lorentz invariant. The charge operator  $B$  in  $SO(2n)$  has the same role. From simple computations one sees that it need to satisfies:

$$B^{-1} \Sigma_{ij}^T B = -\Sigma_{ij}. \quad (4.13)$$

After introducing this operator we can notice that there is a big difference between models with odd  $n$  and models with even  $n$ . In the former models  $B$  maps  $\psi_+$  into  $\psi_+$  and  $\psi_-$  into  $\psi_-$  and therefore one can build a model using only  $\psi_+$ . In theories with even  $n$  instead, this type of terms mix  $\psi_+$  with  $\psi_-$  and therefore one cannot build chiral models. <sup>†</sup>

## Ket Notation and $SO(10) \rightarrow SO(6) \times SO(4)$

We can rewrite in a more compact way Eq. 4.5 using cross product, for example we have

$$\Gamma_i^{(n+1)} = \Gamma_i^{(n)} \times \sigma_3, \quad (4.14)$$

and then we can look at  $\gamma$  matrices for a certain  $n$  as an iterate cross product of  $\sigma$  matrices. Similarly we can also express the conjugation operator  $B$  in this notation. Starting from  $SU(2)$  invariance where  $\mathcal{C} = i\sigma_2$  we obtain for  $SO(2n)$

$$B = i\sigma_2 \times \dots \times i\sigma_2. \quad (4.15)$$

This cross product allow us to introduce a compact notation for labeling spinors and understand better how we can embed smaller gauge group in  $SO(10)$  with the ultimate wish of embedding the Standard Model group in this GUT theory. let us start noticing that we can also express  $\Gamma_{FIVE}$  as

$$\Gamma_{FIVE} = i\sigma_3 \times \dots \times i\sigma_3. \quad (4.16)$$

It is possible now label a spinor with the eigenstates of each  $\sigma_3$  matrix that can be either  $+$  or  $-$ . In this way

$$\psi_+ = |\epsilon_1 \epsilon_2 \epsilon_3 \epsilon_4 \epsilon_5\rangle, \quad (4.17)$$

---

<sup>†</sup>This is a motivation of why  $SO(10)$  may be a good candidate. The fact that  $n = 5$  allow for using only  $\psi_+$  in the model which does not allow for direct mass terms, property required by gauge invariance.

where  $\epsilon = \pm 1$  and the product of the eigenvalues should be positive because

$$\Gamma_{\text{FIVE}} = \psi_{\pm} = \pm \psi_{\pm}. \quad (4.18)$$

We can express  $\psi_{-}$  in the same way but with the product of the eigenvalues equal to  $-1$ . let us apply this notation to see how we can embed  $SO(6) \times SO(4)$  in  $SO(10)$ .

First, let us show how  $SO(6) \times SO(4)$  is equivalent to the Pati-Salam group of the previous section. There can be 4 left-handed spinors in  $SO(6)$ : a singlet  $|+++ \rangle$  and a triplet  $|+- \rangle, |-+ \rangle, |-- \rangle$ . Indeed if we identify the generators of  $SU(4)$  with a combination of the generators of  $SO(6)$  we discover that the spinors of  $SO(6)$  transform as the fundamental representation of  $SU(4)$ , which further decompose as

$$\mathbf{4} = \mathbf{1} + \mathbf{3} \quad (4.19)$$

under  $SU(3)$ . From what we have said earlier we see that since in  $SO(4)$   $n$  is even we need to consider both  $\psi_{+} = |++ \rangle, |-- \rangle$  and  $\psi_{-} = |+- \rangle, |-+ \rangle$ . If we call  $\sigma_k$  the generators of  $SU(2)$  and assume

$$\sigma_k = \epsilon_{kij} \Sigma_{ij}, \quad (4.20)$$

we have that both  $\psi_{+}$  and  $\psi_{-}$  are doublets of  $SU(2)$  which are also left-right symmetric because of the presence of both the chiral component. At this point we can understand how  $SO(10)$  breaks into Pati-Salam Group:

$$|\epsilon_1 \epsilon_2 \epsilon_3 \epsilon_4 \epsilon_5 \rangle \rightarrow |\epsilon_1 \epsilon_2 \epsilon_3 \rangle \times |\epsilon_1 \epsilon_2 \rangle. \quad (4.21)$$

This is not the only possibility of breaking  $SO(10)$ , for example we could make a similar example with  $SO(10) \rightarrow SU(5) \times U(1)$ .

## D-Parity

let us notice that  $\psi_{+}$  for  $SO(10)$  is 16-dimensional. As we have seen in the earlier chapter 16 is also the number of chiral fermions in the Standard Model plus a right-handed neutrino. Therefore we can embed all fermions of one flavour family in one representation, thus allowing for the prediction of fermion masses and explaining the origin of neutrino masses:

$$\psi_{+} = \left( u \quad d \quad \nu \quad e \quad u^c \quad d^c \quad \nu^c \quad e^c \right)_L. \quad (4.22)$$

From 4.22 we can see that within  $SO(10)$  transformation there is also the transformation  $D$ :

$$\psi \xrightarrow{D} \psi^c. \quad (4.23)$$

Let us study carefully the possible breaking of this parity with two important examples [58, 59]: **210** and **54**. This shall be useful in the next section. Let us first introduce  $\mathbf{210} = [\mathbf{10} \times \mathbf{10} \times \mathbf{10} \times \mathbf{10}]_{AS}$ . This is a completely antisymmetric 4-rank tensor and it is responsible of the breaking  $SO(10) \rightarrow SO(6) \times SO(4)$ . Indeed, it can be decomposed under  $SU(4)_c \times SU(2)_L \times SU(2)_R$  as:

$$\mathbf{210} = (\mathbf{1}, \mathbf{1}, \mathbf{1}) + (\mathbf{15}, \mathbf{1}, \mathbf{1}) + (\mathbf{6}, \mathbf{2}, \mathbf{2}) + (\mathbf{15}, \mathbf{3}, \mathbf{1}) + (\mathbf{15}, \mathbf{1}, \mathbf{3}) + (\mathbf{10}, \mathbf{2}, \mathbf{2}) + (\overline{\mathbf{10}}, \mathbf{2}, \mathbf{2}). \quad (4.24)$$

When the first term gets a VEV we have the desired breaking. Following Ref. [?] we are going to prove that this singlet of Pati-Salam group breaks D-parity. Being a 4-rank tensor we can rewrite **210** as

$$\Phi_{\mu_1 \mu_2 \mu_3 \mu_4} \equiv \psi | \Gamma_{\mu_1} \Gamma_{\mu_2} \Gamma_{\mu_3} \Gamma_{\mu_4} | \psi \rangle \quad \mu : 1, \dots, 10. \quad (4.25)$$

In our notation [54] we can express  $D$  in terms of the generators of  $SO(10)$

$$D = \Sigma_{23} \Sigma_{67}. \quad (4.26)$$

Let us first write the singlet in the notation of 4.25. Decomposing the fundamental representation under Pati-Salam group:

$$\mathbf{10} = (\mathbf{6}, \mathbf{1}, \mathbf{1}) + (\mathbf{1}, \mathbf{2}, \mathbf{2}). \quad (4.27)$$

In the tensorial notation we can express:

$$(\mathbf{6}, \mathbf{1}, \mathbf{1}) = \Phi_{\mu} \quad \mu = 1, \dots, 6, \quad (4.28)$$

$$(\mathbf{1}, \mathbf{2}, \mathbf{2}) = \Phi_{\mu} \quad \mu = 7, \dots, 10. \quad (4.29)$$

$$(4.30)$$

From this notation we see that:

$$(\mathbf{1}, \mathbf{1}, \mathbf{1})_{210} = (\mathbf{1}, \mathbf{2}, \mathbf{2}) \times (\mathbf{1}, \mathbf{2}, \mathbf{2}) \times [(\mathbf{1}, \mathbf{2}, \mathbf{2}) \times (\mathbf{1}, \mathbf{2}, \mathbf{2})]_{AS} \equiv \Phi_{i_1 i_2 i_3 i_4}, \quad (4.31)$$

where  $(i_1, i_2, i_3, i_4)$  is a permutation of  $(1, 2, 3, 4)$ . let us now act with the  $D$  operator to this singlet. A simple application of the commutation relation of gamma matrices leads to

$$D \Phi_{i_1 i_2 i_3 i_4} D^\dagger = -\Phi_{i_1 i_2 i_3 i_4}. \quad (4.32)$$

This singlet is parity odd and then breaks D-parity when gets a VEV. With a similar procedure let us show that instead **54** preserves D-parity allowing for left-right symmetric breaking chains of  $SO(10)$ . **54** decomposes under Pati Salam group as [60]

$$\mathbf{54} = (\mathbf{1}, \mathbf{1}, \mathbf{1}) + (\mathbf{20}, \mathbf{1}, \mathbf{1}) + (\mathbf{6}, \mathbf{2}, \mathbf{2}) + (\mathbf{1}, \mathbf{3}, \mathbf{3}). \quad (4.33)$$

Considering only  $SO(6)$  we have that the rank-2 symmetric tensor is  $\mathbf{6} \times \mathbf{7} = \mathbf{20} + \mathbf{1}$  where  $\mathbf{1}$  can be seen as a diagonal matrix. The singlet of  $\mathbf{54}$  can thus be seen as a traceless diagonal matrix belonging to the Cartan algebra of  $SO(10)$  and therefore preserving the rank of the group and commuting with all the generators. This implies, calling  $(\mathbf{1}, \mathbf{1}, \mathbf{1}) \equiv \sigma_{54}$ ,

$$[\sigma_{54}, D] = 0. \quad (4.34)$$

We have proved that  $\mathbf{54}$  preserves parity and it is responsible for the breaking

$$SO(10) \rightarrow SU(4) \times SU(2)_L \times SU(2)_R \times Z_2^C. \quad (4.35)$$

## 4.2 $SO(10)$ breaking

In this section we are going to study how we can break  $SO(10)$  down to the Standard Model. There are many ways of doing that and this led to a broad realm of subgroups depending on the Higgs representation used. The largest subgroups of  $SO(10)$  are [61]:

$$G_{51} = SU(5) \times U(1), \quad (4.36)$$

$$G_{422} = SU(4) \times SU(2)_L \times SU(2)_R. \quad (4.37)$$

The other principal subgroups that one encounters <sup>‡</sup> are:

$$G_{3221} = SU(3) \times SU(2) \times SU(2) \times U(1)_X, \quad (4.38)$$

$$G_{3211} = SU(3) \times SU(2)_L \times U(1)_R \times U(1)_X, \quad (4.39)$$

$$G_{421} = SU(4) \times SU(2)_L \times U(1)_X. \quad (4.40)$$

$$(4.41)$$

In general one breaks  $SO(10)$  in more steps and there can be one (I), two(II), three (III) or four(IV) intermediate symmetries. We can organize all the breaking chains in four categories [24] [25]

- Breaking chains via standard  $SU(5)$  and  $U(1)$  intermediate symmetry.
- Breaking chains via  $SU(5)^{flip} \times U(1)$
- Breaking chains in which  $SU(5)$  is at the lowest intermediate scale before  $G_{SM}$

---

<sup>‡</sup>When in the subgroups is present  $Z_2$  symmetry we label these groups as  $G^c \equiv G \times Z_2^c$

- Breaking chains via  $G_{422}$  or its subgroups

let us first talk briefly about the first three categories which involves  $SU(5)$  as a subgroup.  $SU(5)$  is by itself a model of grand unification and its main difference with  $SO(10)$  is that it does not embed all fermion in one representation but instead we need both the fundamental  $\mathbf{5}$  and the rank two antisymmetric  $\mathbf{10}$ . Moreover it keeps account only of Standard Model matter content and one cannot embed naturally a right handed neutrino in this model that therefore does not predicts neutrino mass at least in its minimal version. The embedding of  $SU(5)$  in  $SO(10)$  is one of the most studied [62]. The decomposition of the basic representations of  $SO(10)$  in  $SU(5)$  are

$$\mathbf{10} = \mathbf{5} + \bar{\mathbf{5}}, \quad (4.42)$$

$$\mathbf{16} = \mathbf{10} + \bar{\mathbf{5}} + \mathbf{1}. \quad (4.43)$$

$$(4.44)$$

From Eq. 4.44 we can see already how  $\mathbf{16}$  is a good candidate for breaking  $SO(10)$  down to  $SU(5)$ . In this case actually one can prove that with this breaking one gets  $SU(5) \times U(1)$  therefore falling on the first category taken into exam. One can build the other representations of  $SO(10)$  via tensor product of 10 and 16, for example:

$$[\mathbf{10} \times \mathbf{10}]_{\text{S}} = \mathbf{54}, \quad (4.45)$$

$$[\mathbf{10} \times \mathbf{10}]_{\text{AS}} = \mathbf{45}, \quad (4.46)$$

$$\mathbf{16} \times \mathbf{16} = \mathbf{10} + \mathbf{120} + \mathbf{126}, \quad (4.47)$$

$$\mathbf{16} \times \bar{\mathbf{16}} = \mathbf{1} + \mathbf{45} + \mathbf{210}, \quad (4.48)$$

$$[\mathbf{10} \times \mathbf{10} \times \mathbf{10} \times \mathbf{10}]_{\text{AS}} = \mathbf{210}. \quad (4.49)$$

Then using Eq. 4.44 one can decompose all the representation down the subgroup taken into consideration.

The main drawback of  $SU(5)$  group is that it requires SUSY to achieve gauge coupling unification. [63, 64, ?] This affect also the breaking chain of the first three categories. Since we are using non supersymmetric  $SO(10)$  model we are going to focus on the last case. Since some of the possible subgroups are left-right symmetric, in the following discussion we will focus particularly in D-parity breaking and the embedding of left-right symmetry breaking in  $SO(10)$ , for this reasons we have already introduced carefully this concepts.

In this work we focus in the breaking chain IIIc <sup>§</sup>

$$\begin{aligned}
& SO(10) \\
& \mathbf{54} \downarrow \text{broken at } M_X \\
& G_3^c \equiv SU(4) \times SU(2)_L \times SU(2)_R \times Z_2^C \\
& \mathbf{210} \downarrow \text{broken at } M_3 \\
& G_2^c \equiv SU(3)_c \times SU(2)_L \times SU(2)_R \times U(1)_X \times Z_2^C \\
& \mathbf{45} \downarrow \text{broken at } M_2 \\
& G_1 \equiv SU(3)_c \times SU(2)_L \times SU(2)_R \times U(1)_X \\
& \overline{\mathbf{126}} \downarrow \text{broken at } M_1 \\
& G_{SM} \equiv SU(3)_c \times SU(2)_L \times U(1)_Y.
\end{aligned} \tag{4.50}$$

In this section we are going to examine carefully each step of the symmetry breaking and then we will conclude with a general summary of all the principal breaking chain.

## SO(10) $\rightarrow$ $\mathbf{G}_{422}$

In the earlier section we have noticed how  $G_{422} \sim SO(6) \times SO(4)$ . Moreover the two groups have the same rank so we need a traceless representation that commutes with all the generators of the Cartan invariant under  $SO(6) \times SO(4)$  representation. A reasonable guess is: [65, 66]

$$\langle \mathbf{54} \rangle = v_\Phi \text{diag}(2, 2, 2, 2, 2, 2, -3, -3, -3, -3). \tag{4.51}$$

Let us verify that  $\Phi \equiv \mathbf{54}$  can indeed take this form and that it is an actual minimum of the potential. The most general potential for this representation is

$$\mathcal{V} \Phi = -\frac{1}{2}\mu^2 \Phi_{ij} \Phi_{ij} + \frac{1}{4}\lambda_1 (\Phi_{ij} \Phi_{ij})^2 + \frac{1}{4}\lambda_2 \Phi_{ij} \Phi_{jk} \Phi_{kl} \Phi_{li}, \tag{4.52}$$

with:

$$\sum_i \Phi_{ii} = 0. \tag{4.53}$$

Using a more general version of Eq. 4.51 we can write  $\langle \mathbf{54} \rangle = \delta_{ij} \Phi_i$  and, treating the traceless condition as a Lagrange multiplier following Ref. [67], we can rewrite the

---

<sup>§</sup>We are following the convention of [24],[25] and [26]

potential as

$$\mathcal{V}(\Phi) = -\frac{1}{2}\mu^2 \sum_i \Phi_i^2 + \frac{1}{4}\lambda_1 \left( \sum_i \Phi_i^2 \right)^2 + \frac{1}{4}\lambda_2 \sum_i \Phi_i^4 - g \sum_i \Phi_i. \quad (4.54)$$

Imposing  $\frac{\partial \mathcal{V}}{\partial v_\Phi} = 0$  we obtain a set of cubic equations that have at most three solutions:  $\Phi_1, \Phi_2$  and  $\Phi_3$ . In our guess of Eq. 4.51 there are only two different  $\Phi_i$ : 2 and -3, therefore it is a minimum of the potential and breaks  $SO(10)$  in the correct way. Moreover, as we have seen in the last section also D-parity is conserved.

### $\mathbf{G}_{422}^C \rightarrow \mathbf{G}_{3221}^C \rightarrow G_{3221}$ : the breaking of D-Parity

From Eq. 4.24 we see that  $\mathbf{210}$  contains  $(\mathbf{15}, \mathbf{1}, \mathbf{1})_{422}$ . This can be decomposed under  $G_{3221}$  as [68]

$$(\mathbf{15}, \mathbf{1}, \mathbf{1}) = (\mathbf{1}, \mathbf{1}, \mathbf{1})_0 + (\mathbf{3}, \mathbf{1}, \mathbf{1})_{-\frac{4}{3}} + (\bar{\mathbf{3}}, \mathbf{1}, \mathbf{1})_{\frac{4}{3}} + (\mathbf{3}, \mathbf{1}, \mathbf{1}) + (\mathbf{8}, \mathbf{1}, \mathbf{1})_0 \quad (4.55)$$

When the first term of the right hand side gets a VEV we obtain the desired breaking. let us now determine if this breaks also D-parity or not. From the discussion in the last section we notice that the multiplet responsible from this breaking can be written as

$$(\mathbf{15}, \mathbf{1}, \mathbf{1}) = \Phi_{a_1 a_2 a_3 a_4} \quad a = 1, \dots, 6. \quad (4.56)$$

In particular the VEV of the singlet of  $SU(3) \times SU(2)_L \times SU(2)_R \times U(1)_{B-L}$  is

$$\langle \Phi_{1234} \rangle = \langle \Phi_{3456} \rangle = \langle \Phi_{5612} \rangle. \quad (4.57)$$

We can apply the commutation rules for the gamma matrices and prove that this singlet commutes with the operator D. The next breaking can be achieved with  $\mathbf{45}$ . From its decomposition under  $G_{422}$ ,

$$\mathbf{45} = (\mathbf{15}, \mathbf{1}, \mathbf{1}) + (\mathbf{6}, \mathbf{2}, \mathbf{2}) + (\mathbf{1}, \mathbf{3}, \mathbf{1}) + (\mathbf{1}, \mathbf{1}, \mathbf{3}), \quad (4.58)$$

we notice that also  $\mathbf{45}$  contains  $(\mathbf{15}, \mathbf{1}, \mathbf{1})$ . let us write  $\mathbf{45}$  in the notation of Eq. 4.25 and prove that this time  $(\mathbf{15}, \mathbf{1}, \mathbf{1})$  breaks D-parity. Being a 2-rank antisymmetric tensor we can write

$$\mathbf{45} \equiv \Phi_{\mu_1 \mu_2} \quad \mu = 1, \dots, 10, \quad (4.59)$$

and

$$(\mathbf{15}, \mathbf{1}, \mathbf{1}) = \Phi_{a_1 a_2} \quad a = 1, \dots, 6. \quad (4.60)$$

Therefore if the VEV is, for example

$$\langle(\mathbf{1}, \mathbf{1}, \mathbf{1}_0)\rangle = \langle\Phi_{12}\rangle. \quad (4.61)$$

we conclude that this does not break  $G_{3221}$  but only D-parity. Proving that the VEVs of Eq. 4.57 and Eq. 4.61 are indeed minimum need a really lengthy computation (see for example [66, 69] )that can be summarized as:

- Write the most general potential involving all the representations we use for the breaking
- Let all the Higgs get a vev and compute the masses of all the multiplets.
- All the multiplets which does not get a vev can be either Goldstone bosons which are eaten by gauge bosons or physical particles with mass of the same order of the scale of the breaking <sup>¶</sup>
- If all the masses of the multiplets are greater than zero then the vacuum is stable and the VEV correspond to a minimum of the potential.

### $G_{3221} \rightarrow G_{\text{SM}}$ : left-right symmetry breaking

We have already seen this breaking in the last section. Here we are going to embed  $\Delta_R, \Delta_L$  and  $\Phi$  in the representation  $\overline{\mathbf{126}}$ . This step is particularly important because this Higgs not only helps us to arrive finally to the Standard Model group but also because the Higgs we are using appear also in the Yukawa sector linking the breaking scale to the mass of heavy neutrinos and cosmic strings tension  $G\mu$ . Under  $G_{422}$ ,  $\overline{\mathbf{126}}$  decomposes as

$$\overline{\mathbf{126}} = (\mathbf{10}, \mathbf{1}, \mathbf{3}) + (\overline{\mathbf{10}}, \mathbf{3}, \mathbf{1}) + (\mathbf{15}, \mathbf{2}, \mathbf{2}) + (\mathbf{20}, \mathbf{1}, \mathbf{1}). \quad (4.62)$$

If we look at the  $SU(2)_R \times SU(2)_L$  structure we see that the first three terms are good candidates. Let us decompose  $\mathbf{10}$ , the rank-two symmetric tensor representation and  $\mathbf{15}$ , the adjoint representation, for  $SU(4) \rightarrow SU(3) \times U(1)_{B-L}$ :

$$\mathbf{10} = \mathbf{6}\left(\frac{2}{3}\right) + \mathbf{3}\left(-\frac{2}{3}\right) + \mathbf{1}(-2), \quad (4.63)$$

$$\mathbf{15} = \mathbf{8}(0) + \mathbf{3}(0) + \overline{\mathbf{3}}(0) + \mathbf{1}(0). \quad (4.64)$$

---

<sup>¶</sup>This is really important for gauge unification since this multiplets affect the running of the coupling at high scale

In this breaking we need to break  $B - L$  and  $SU(2)_R$ . From the decomposition of Eq. 4.64 we see that it is the last term of the first equation:

$$\Delta_R \equiv (\mathbf{1}, \mathbf{3}, \mathbf{1}) (2). \quad (4.65)$$

We can study also the last breaking down to  $SU(3) \times U(1)_{\text{em}}$ . As we have seen in the previous chapter  $\Phi$  breaks  $SU(2)_L$  and together with  $\Delta_L$  contributes to fermion masses. As we shall see later this is not the whole story since in our model other Higgs bosons contribute to fermion masses making the model realistic.  $\Delta_R$  is responsible for heavy neutrino mass via See-Saw type I and is a singlet of Standard Model group  $SU(3) \times SU(2)_L \times U(1)_Y$

$$\Delta_R = (\mathbf{1}, \mathbf{3}, \mathbf{1}) \rightarrow S \equiv (\mathbf{1}, \mathbf{1}, \mathbf{0}). \quad (4.66)$$

## Recap: breaking chains of $SO(10)$

Let us make a brief summary and study more carefully the breaking chains of the last category. The decompositions of the basic representations of  $SO(10)$  under  $G_{422}$  are [54]

$$\mathbf{16} = (\mathbf{4}, \mathbf{2}, \mathbf{1}) + (\bar{\mathbf{4}}, \mathbf{1}, \mathbf{2}), \quad (4.67)$$

$$\mathbf{45} = (\mathbf{3}, \mathbf{1}, \mathbf{1}) + (\mathbf{6}, \mathbf{2}, \mathbf{2}) + (\mathbf{15}, \mathbf{1}, \mathbf{1}) + (\mathbf{1}, \mathbf{3}, \mathbf{1}), \quad (4.68)$$

$$\mathbf{54} = (\mathbf{1}, \mathbf{1}, \mathbf{1}) + (\mathbf{6}, \mathbf{2}, \mathbf{2}) + (\mathbf{20}, \mathbf{1}, \mathbf{1}) + (\mathbf{1}, \mathbf{3}, \mathbf{3}), \quad (4.69)$$

$$\begin{aligned} \mathbf{210} = & (\mathbf{1}, \mathbf{1}, \mathbf{1}) + (\mathbf{1}, \mathbf{1}, \mathbf{15}) + (\mathbf{2}, \mathbf{2}, \mathbf{6}) + (\mathbf{3}, \mathbf{1}, \mathbf{15}), \\ & + (\mathbf{1}, \mathbf{3}, \mathbf{15}) + (\mathbf{2}, \mathbf{2}, \mathbf{10}) + (\mathbf{2}, \mathbf{2}, \bar{\mathbf{10}}), \end{aligned} \quad (4.70)$$

$$\bar{\mathbf{126}} = (\mathbf{10}, \mathbf{1}, \mathbf{3}) + (\bar{\mathbf{10}}, \mathbf{3}, \mathbf{1}) + (\mathbf{15}, \mathbf{2}, \mathbf{2}) + (\mathbf{20}, \mathbf{1}, \mathbf{1}). \quad (4.71)$$

All the representation that contains  $(\mathbf{15}, \mathbf{1}, \mathbf{1})$  can breaks  $SU(4)$  down to  $SU(3) \times U(1)$ . Let us look at the decomposition of  $\mathbf{15}$ ,  $\mathbf{15}$  and  $\mathbf{10}$  for  $SU(6) \rightarrow SU(3) \times U(1)$  [68]:

$$\mathbf{15} = \mathbf{1}(0) + \mathbf{3}\left(-\frac{4}{3}\right) + \bar{\mathbf{3}}\left(\frac{4}{3}\right) + \mathbf{8}(0), \quad (4.72)$$

$$\mathbf{10} = \mathbf{1}(2) + \mathbf{3}\left(\frac{2}{3}\right) + \mathbf{6}\left(-\frac{2}{3}\right), \quad (4.73)$$

$$\mathbf{6} = \mathbf{3}\left(\frac{2}{3}\right) + \bar{\mathbf{3}}\left(-\frac{2}{3}\right). \quad (4.74)$$

Each multiplet that takes a VEV can be parity odd or parity even. This depend on the embedding in  $SO(6) \times SO(4)$  and one proceed as we did earlier for  $\mathbf{210}$  and  $\mathbf{45}$ . For a general subgroup one has to decompose every representation in that subgroup, if it contains a singlet then one can use that representation to breaks  $SO(10)$  down to the desired subgroup.

SO(10)	$\xrightarrow{Higgs}$	$G_1$	$\xrightarrow{Higgs}$	$G_{SM}$
I1:	$\xrightarrow{45}$	$G_{3221}$	$\xrightarrow{\overline{126}}$	
I2:	$\xrightarrow{210}$	$G_{3221}^C$	$\xrightarrow{\overline{126}}$	
I3:	$\xrightarrow{45}$	$G_{421}$	$\xrightarrow{\overline{126}}$	
I4:	$\xrightarrow{210}$	$G_{421}^C$	$\xrightarrow{\overline{126}, 45}$	
I5:	$\xrightarrow{54}$	$G_{422}^C$	$\xrightarrow{\overline{126}, 45}$	
I6:	$\xrightarrow{210}$	$G_{422}$	$\xrightarrow{\overline{126}}$	

Table 4.1: Breaking chains with one intermediate scale of type (c)

In Tab. 4.1 we can see all the principal breaking chains involving Pati-Salam group with one intermediate scale [25].

### 4.3 Gauge coupling unifications

Let us start studying the vacuum polarization of an abelian theory. The self-energy at 1-loop is [70]

$$i\Pi_2^{\mu\nu} = \text{diagram} = -4e^2 \int \frac{d^4k}{(2\pi)^4} \frac{2k^\mu k^\nu + g^{\mu\nu}(-k^2 + p \cdot k + m^2)}{[(p-k)^2 - m^2 + i\varepsilon][k^2 - m^2 + i\varepsilon]}. \quad (4.75)$$

This integral can be regularized using dimensional regularization. let us rewrite Eq. 4.75 in  $d$  dimension

$$\Pi_2^{\mu\nu} = -8p^2 g^{\mu\nu} \frac{e^2}{(4\pi)^{d/2}} \Gamma\left(2 - \frac{d}{2}\right) \mu^{4-d} \int_0^1 dx x(1-x) \left(\frac{1}{m^2 - p^2 x(1-x)}\right)^{2-\frac{d}{2}} \quad (4.76)$$

Now we can explicit the pole using  $d = 4 - \epsilon$  for  $\epsilon \rightarrow 0$ :

$$\Pi_2^{\mu\nu} = -\frac{e^2}{2\pi^2} p^2 g^{\mu\nu} \int_0^1 dx x(1-x) \left[ \frac{2}{\epsilon} + \ln\left(\frac{\tilde{\mu}^2}{m^2 - p^2 x(1-x)}\right) + \mathcal{O}(\epsilon) \right]. \quad (4.77)$$

We can regard the vacuum polarization diagram as a correction to the photon propagator. For example what we call dressed propagator at 1-loop can be expressed as

$$iG_{\mu\nu} = iG_{\mu\nu}^0 + iG_{\mu\nu}^0 i\Pi_{2\mu\nu} iG_{\mu\nu}^0 + \dots \quad (4.78)$$

Plugging the expressions for the bare propagator and  $\Pi_{\mu\nu}^2$ :

$$iG_{\mu\nu}^0 = \frac{i}{p^2} \left( g^{\mu\nu} + \frac{p^\mu p^\nu}{p^2} \right), \quad (4.79)$$

$$i\Pi_{\mu\nu}^2 = i \left( -p^2 g^{\mu\nu} + p^\mu p^\nu \right) e^2 \Pi^2(p^2). \quad (4.80)$$

Expressing the propagator in terms of the Fourier transform of the potential we obtain at one loop the following correction for the potential

$$\tilde{V}(p) = e^2 \frac{1 - e^2 \Pi^2(p^2)}{p^2}. \quad (4.81)$$

Now we renormalize the Feynman diagram measuring the value of the potential at an arbitrary energy scale  $p_0$ . In that way we can define the renormalized charge as:

$$e_R^2 \equiv p_0^2 \tilde{V}(p_0^2) = e^2 - e^4 \Pi^2(p_0^2) + \dots \quad (4.82)$$

Both the self-energy  $\Pi_2$  and the bare charge  $e^2$  can be regarded as infinite and in this way the infinite terms cancel out. We can compute now the potential at any scale starting

from the renormalized charge. The physical relevant quantity that can be predicted after renormalization is the difference between the potential measured at different scales

$$\tilde{V}(Q^2) - \tilde{V}(Q_0^2) = \frac{1}{Q^2} \frac{e_R^4}{12\pi^2} \ln \frac{Q_0^2}{Q^2}, \quad (4.83)$$

where the potential at a certain scale is

$$\tilde{V}(Q^2) = \frac{e_{eff}(Q^2)}{Q^2}. \quad (4.84)$$

From Eq. 4.83 and Eq. 4.84 we obtain the expression for the effective charge at 1-loop:

$$e_{eff}^2(Q^2) = e_R^2 \left( 1 + \frac{e_R^2}{12\pi^2} \ln \frac{Q^2}{\mu} \right), \quad (4.85)$$

where we defined the renormalized charge at scale  $\mu$ . We can consider higher order corrections considering all 1PI diagrams

$$iG^{\mu\nu} = \text{wavy line} + \text{wavy line with one loop} + \text{wavy line with two loops} + \dots \quad (4.86)$$

Repeating the discussion, we obtain that the effective charge is:

$$e_{eff}^2(Q^2) = \frac{e_R^2}{1 - \frac{e_R^2}{12\pi^2} \ln Q^2 \mu^2}. \quad (4.87)$$

This is called *running coupling*. In the following for deriving again this formula we are going to use the renormalization group, hence it is convenient to rewrite 4.87 as

$$\alpha_{em}^{-1}(Q^2) = \alpha_{em}^{-1}(\mu^2) - \frac{1}{3} \ln \frac{Q^2}{\mu^2}, \quad (4.88)$$

where we have used

$$\alpha_{em} \equiv \frac{e^2}{4\pi^2}. \quad (4.89)$$

## Renormalization group

We can arrive at Eq. 4.89 in a much more elegant way. The principle that makes renormalization consistent is that the value of an observable cannot depend on the renormalization scale  $\mu$ , i.e. the scale at which we defined the renormalized coupling. let us reobtain the running coupling equations for QED with this approach. The renormalized lagrangian for QED is

$$\mathcal{L} = -\frac{1}{4} Z_3 F_{\mu\nu} F^{\mu\nu} + i Z_2 \bar{\psi} \not{\partial} \psi - m_R Z_2 Z_m \bar{\psi} \psi - \mu^{\frac{4-d}{2}} e_R Z_e Z_2 \sqrt{Z_3} \bar{\psi} A \psi, \quad (4.90)$$

where

$$Z_i = 1 + \delta_i, \quad (4.91)$$

and  $\delta_i$  is the  $i$ -th counterterm that depend on the renormalization scheme used.

The renormalized coupling now is <sup>¶</sup>

$$e_R = \frac{1}{Z_e} \mu^{\frac{d-4}{2}} e^0, \quad (4.92)$$

$$Z_e = 1 + \delta_e = 1 + \frac{e_R^2}{16\pi^2} \frac{4}{3\epsilon}. \quad (4.93)$$

The bare charge does not depend on scale  $\mu$  and thus we have

$$0 = \mu \frac{d}{d\mu} e^0 = \frac{\epsilon}{2} + \frac{\mu}{e_R} + \frac{\mu}{Z_e} \frac{dZ_e}{d\mu}. \quad (4.94)$$

At 1-loop we obtain

$$\mu \frac{de_R}{d\mu} = \frac{e_R^3}{12\pi^2} \equiv \beta(e_R). \quad (4.95)$$

This a differential equation called RGE equation and one can prove, using  $\alpha = \frac{e^2}{4\pi}$ , that Eq. 4.89 is a solution. Therefore for determining how a coupling run one has to proceed in the following way:

- Renormalize the theory computing counterterms
- Find the beta function for the theory and the RGE equation
- Solve the equation

## RGE equations for $G_1 \otimes G_2 \dots \otimes G_N$

Let us extend our discussion to a more general gauge group which is the tensor product between arbitrary non abelian theories [71]. Our goal is to find an expression for the running at two-loop.

In the last section the procedure used for determine the beta function requires to compute all the counterterms of the theory and then find  $Z_e$ . As the model gets more complicated this procedure can become quite lengthy. Here we are going to use a faster method for computing the beta function: the background field method [72].

Following Ref. [73] we are going to call the gauge couplings as  $g$ , the background field

---

<sup>¶</sup>We are using  $\overline{MS}$  renormalization scheme

$A$  and we are going to use  $\alpha_p \equiv \frac{g_p^2}{4\pi^2}$ .

let us start from a Yang-Mills theory.

We label the gauge field as  $\mathcal{A}$  and we separate it into two components a slow varying classical field  $A$  and a quantum field  $Q$ . The ordinary generating functional for the gauge theory is

$$Z[J] = \int \mathcal{D}\mathcal{A} \det \frac{\delta G^a}{\delta \omega^b} \exp i \int d^4x \left( -\frac{1}{4} (F_{\mu\nu}^a)^2 - \frac{1}{2\alpha} (G^a)^2 + J_\mu^a \mathcal{A}_\mu^a \right), \quad (4.96)$$

where the second term of the action is a gauge-fixing term. From the generating functional we can compute the effective action  $\Gamma[\mathcal{A}]$ . In the background field we have instead

$$\tilde{Z}[J, A] = \int \mathcal{D}Q \det \frac{\delta G^a}{\delta \omega^b} \exp i \int d^4x \left( -\frac{1}{4} (F_{\mu\nu}^a)^2 - \frac{1}{2\alpha} (G^a)^2 + J_\mu^a Q_\mu^a \right). \quad (4.97)$$

In this case the effective action is called:

$$\tilde{\Gamma}[\tilde{Q}, A], \quad \tilde{Q} = \frac{\delta W}{\delta J_\mu^a}. \quad (4.98)$$

It is possible to prove that  $\tilde{\Gamma}[0, A]$  is equivalent to the ordinary effective action  $\Gamma[\mathcal{A}]$ . With this method only three quantities need to be renormalized, the gauge coupling, the background field and the gauge fixing constant:

$$g = Z_g g^0 \quad A = Z_a^{\frac{1}{2}} a^0 \alpha = Z_\alpha \alpha^0. \quad (4.99)$$

Imposing gauge invariance on  $\tilde{\Gamma}[0, A]$  one can find  $Z_g = Z_a^{-\frac{1}{2}}$ . The beta function is defined as

$$\beta = -g\mu \frac{d}{d\mu} \ln Z_g, \quad (4.100)$$

while  $Z_a$  appear in the anomalous dimension definition

$$\gamma_A = \frac{1}{2}\mu \frac{d}{d\mu} \ln Z_a. \quad (4.101)$$

Therefore we can relate the beta function to the anomalous dimension and noticing the convenience of this method. We do not have anymore to compute vertex diagrams but only the two point function of the background field. We can write  $Z_A$  as

$$Z_A = 1 + \sum_{i=1}^{\infty} \frac{Z_A^{(i)}}{\epsilon^i}. \quad (4.102)$$

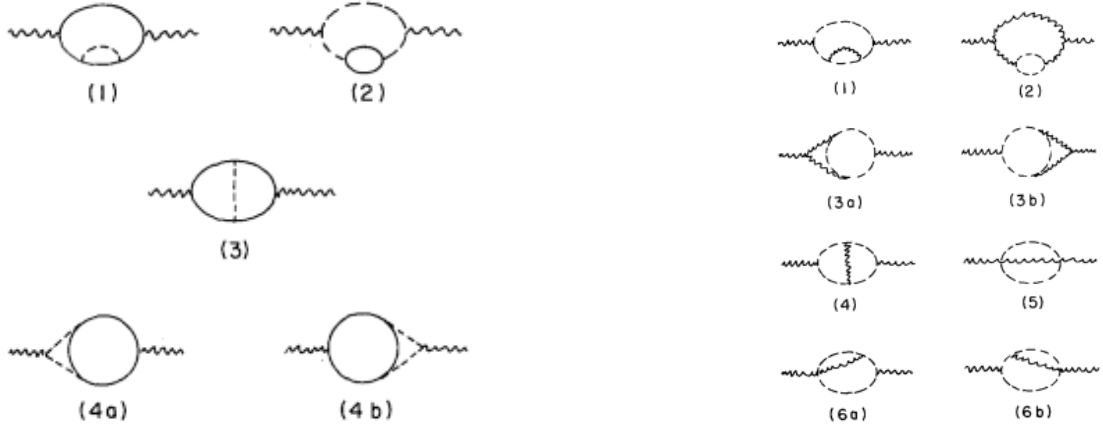


Figure 4.1: Left: Gauge field wave function renormalization diagram of order  $g^2 Y^2$ . Right: Gauge field wave renormalization diagram of order  $g^4$ . Picture taken from Ref. [73]

Differentiating we obtain

$$\beta \left( 2 - g \frac{\partial}{\partial g} \right) Z_A^{(i)} = -g^2 \frac{\partial}{\partial g} Z_A^{(i+1)}. \quad (4.103)$$

From this relation we obtain the beta function at 2-loop for a simple Yang-Mills theory without fermions

$$\beta = -g \left( A \left( \frac{g}{4\pi} \right)^2 + B \left( \frac{g}{4\pi} \right)^4 \right). \quad (4.104)$$

We can easily extend the discussion to a tensor product of non abelian gauge groups and adding fermion and scalars in arbitrary representations. The Feynman diagrams which contribute to  $Z_A$  are in Fig. 4.1. The resulting expression for the beta function is: [73] [71]

$$\begin{aligned} \beta_p = & \frac{g_p^2}{(4\pi)^2} \left\{ -\frac{11}{3} C_2(G_p) + \frac{4}{3} \kappa S_2(F_p) + \frac{1}{3} \eta S_2(S_p) - \frac{2\kappa}{(4\pi)^2} Y_4(F_p) + \right. \\ & \frac{g_p^2}{(4\pi)^2} \left[ -\frac{34}{3} (C_2(G_p))^2 + (4C_2(F_p) + \frac{20}{3} C_2(G_p)) \kappa S_2(F_p) + \right. \\ & \left. \left. (4C_2(S_p) + \frac{2}{3} C_2(G_p)) \eta S_2(S_p) \right] \right. \\ & \left. + \frac{g_q^2}{(4\pi)^2} 4 [\kappa C_2(F_q) S_2(F_p) + \eta C_2(S_q) S_2(S_p)] \right\}, \quad (4.105) \end{aligned}$$

$\kappa$  can be either 1,  $\frac{1}{2}$  for Dirac and Weyl fermions and similarly  $\eta$  1 or  $\frac{1}{2}$  for complex or real scalars. The other coefficients are taken from group theory:

- $C_2$  is the quadratic Casimir operator  $T_A T_A$  where  $T$  are the generators of the group. It is equal to a constant  $C_2(R)$  times the identity, where  $R$  is the representation

- $S_2$  is the Dynkin index and it is defined as

$$\text{Tr } T_A T_B = S_2(R) \delta_{AB}. \quad (4.106)$$

The index  $p$  run through the gauge sectors and at two-loop also different gauge sectors contribute to the running of a given gauge coupling. We can rewrite 4.105 in a more compact way\*\* as

$$\mu \frac{dg_i}{d\mu} = \beta_i, \quad (4.107)$$

and

$$\beta_i = \frac{g_i^2}{4\pi^2} \left( b_i + \sum_j b_{ij} \frac{g_j^2}{4\pi^2} \right). \quad (4.108)$$

The coefficients  $b_i$  and  $b_{ij}$  depends on the matter content of the model used and they consider respectively all the contributes of 1-loop diagrams and 2-loop diagrams of the eq. 4.105.

## Matching at one loop

Our goal is studying how couplings run through different intermediate scales and determine if they reach unification at a certain scale. To do that we have already seen that for different scales we have different models.

let us study how we can match the coupling from two different gauge group at a certain scale  $M$ . Following Ref. [71] let us start studying the spontaneous breaking of a group  $G$  into a subproduct  $\tilde{G} = G_1 \otimes G_2 \dots \otimes G_N$ . We are going to call  $\alpha$  the index for the full theory generators,  $A$  the broken generators and  $a$  the generators of the light gauge fields. We can study the latter gauge group with an effective field theory integrating out the heavy gauge fields. let us call the fields belonging to the effective theory  $\phi$  and the heavy fields we are integrating out  $\Phi$ , the new action is then

$$\tilde{S}[\phi] = \int \mathcal{D}\Phi S[\phi, \Phi]. \quad (4.109)$$

There is a caveat regarding gauge fixing since we want the effective theory to be invariant under  $\tilde{G}$ . For doing that we need first to insert a gauge fixing term that fix only the gauge of the heavy fields. This extra term takes the following form

$$\Delta S = -\frac{1}{2} \int d^4x \sum_A f_A^2, \quad (4.110)$$

---

\*\*This is valid also when at most one  $U(1)$  is present

where

$$f_A = \frac{1}{\sqrt{\xi}} \left( \partial^\mu A_{A\mu} + g C_{ABa} A_B^\mu A_{a\mu} + ig\xi \lambda_i (t_S^A) y \phi J' \right), \quad (4.111)$$

and  $C_{ABa}$  are the completely antisymmetric structure constants of the theory,  $\phi_i$  are the scalars that break  $G$  of which  $\lambda_i$  is the VEV and  $T_S^A$  are the broken generators in the scalar representation. In this way we have obtained a gauge invariant effective field theory. We can apply this integration all over the heavy gauge fields for finding the renormalized gauge coupling  $g_i$  of  $\tilde{G}$  at scale  $\mu \approx M$ . In order to do that let us start with the kinetic terms of the full theory

$$\begin{aligned} \mathcal{L} = & -\frac{1}{4} F_\alpha^{\mu\nu} F_{\alpha\mu\nu} = -\frac{1}{4} \left( \tilde{F}_A^{\mu\nu} - g \sum_t C_{ABct} A_B^\mu A_{c1}^\nu - \right. \\ & \left. g \sum_t C_{AbtC} A_{bt}^\mu A_C^\nu \right)^2 - \frac{1}{4} \sum_t \left( \tilde{F}_{a1}^{\mu\nu} - g C_{a_iBC} A_B^\mu A_C^\nu \right)^2, \end{aligned} \quad (4.112)$$

where:

$$\tilde{F}_{A\mu\nu} = (\partial_\mu A_{A\nu} - \partial_\nu A_{A\mu} - g C_{ABC} A_{B\mu} A_{C\nu}), \quad (4.113)$$

$$\tilde{F}_{a_i\mu\nu} = (\partial_\mu A_{a_i\nu} - \partial_\nu A_{a_i\mu} - g C_{abc} A_{b\mu} A_{c\nu}). \quad (4.114)$$

Integrating out the heavy field and considering 1-loop contribution the kinetic term takes the non canonical expression [74]

$$\mathcal{L} = -\frac{1}{4} (1 - l_i) \tilde{F}_{a_i}^{\mu\nu} \tilde{F}_{a_i\mu\nu}. \quad (4.115)$$

This extra term is due to the contributions on the vacuum polarization diagram of the heavy field. Since it is not canonically normalized we need to rescale the potential  $A_{a_i}^\mu$  and the coupling  $g_i$  because we want the Yang Mills curl to be gauge invariant

$$A_{a_i}^\mu = (1 - l_i)^{\frac{1}{2}} A_\alpha^\mu, \quad (4.116)$$

$$g_i = (1 - l_i)^{-\frac{1}{2}} g. \quad (4.117)$$

From the second equation we obtain the matching rule at 1-loop we just need to compute  $l_i$  that can be expressed as

$$l_i = g^2 \left( \lambda_i + \frac{\lambda'_i}{\epsilon} \right) + \dots \quad (4.118)$$

The renormalized couplings in terms of the bare ones are

$$g^o \mu^{2-\frac{d}{2}} = g(\mu) - b_G \frac{g^3(\mu)}{\epsilon} + \dots, \quad (4.119)$$

$$g_i^o \mu^{2-\frac{d}{2}} = g_i(\mu) - b_i \frac{g_i^3(\mu)}{\epsilon} + \dots \quad (4.120)$$

We obtain

$$g_i(\mu) = g(\mu) + \frac{1}{2} \lambda_i(\mu) g^3(\mu). \quad (4.121)$$

Rewriting the couplings using  $\alpha$ , computing  $\lambda_i$  solving the Feynman diagrams of the vacuum polarization and neglecting the logarithmic terms we obtain [71]

$$\alpha_p^{-1} - \frac{C_2(G_p)}{12\pi} = \alpha_G^{-1} - \frac{C_2(G)}{12\pi}. \quad (4.122)$$

## General considerations

We can finally study the running of the couplings for any breaking chain of  $SO(10)$ . It is convenient to organize the breaking chains according to the number of the intermediate scales used, we are going to describe the cases with one, two and three intermediate scales. We denote the intermediate scales as  $M_i$  and the grand unification scale as  $M_U$ . The gauge unification constraint implies correlation between the scales which we are going to study. Between breaking chain with the same number of intermediate scales the differences are given not only between models with different intermediate gauge groups, but also between models which use different Higgs representation to achieve some breaking, this is because to different Higgs representation correspond a different matter content, therefore a different  $\beta$  function. In general one proceeds starting from the experimental values of the Standard Model gauge couplings at scale  $M_Z$ : [75]

$$\alpha_3 = 0.1184, \quad \alpha_2 = 0.033819, \quad \alpha_1 = 0.010168, \quad (4.123)$$

then we let them run using Eq. 4.107 until the first intermediate scale  $M_1$ . We then match the couplings using Eq. 4.122 and iterate the process until the reaching of the grand unification scale  $M_U$ .

We scan trough all the combinations of intermediate scales such that:  $M_1 \leq \dots \leq M_U$  [25]

**S(10)  $\rightarrow$   $\mathbf{G}_1 \rightarrow \mathbf{G}_{SM}$**  As we can see from Tab. 4.2 from Ref. [25], there is only one solution for each breaking scale except for I6 which does not achieve grand unification. There are no free parameters and therefore this models are highly predictive

**S(10)  $\rightarrow$   $\mathbf{G}_2 \rightarrow \mathbf{G}_1 \rightarrow \mathbf{G}_{SM}$**  In this case  $M_2$  is a free parameter which depends on  $M_1$  and  $M_U$ . There exists then an interval of values of  $M_1$  for which we can achieve grand unification.

	$M_1$ [GeV]	$M_U$ [GeV]
I1:	$1.617 \times 10^{10}$	$5.660 \times 10^{15}$
I2:	$8.630 \times 10^{10}$	$1.410 \times 10^{15}$
I3:	$1.634 \times 10^{11}$	$2.902 \times 10^{14}$
I4:	$4.368 \times 10^9$	$3.500 \times 10^{16}$
I5:	$1.143 \times 10^{13}$	$2.772 \times 10^{14}$
I6:	excluded	

Table 4.2:  $M_1$  and  $M_U$  imposed by gauge unification from the breaking chain of  $SO(10)$  with one intermediate step.

$\mathbf{S}(10) \rightarrow \mathbf{G}_3 \rightarrow \mathbf{G}_2 \rightarrow \mathbf{G}_1 \rightarrow \mathbf{G}_{SM}$  In this case there is another free parameter,  $M_3$ . We proceed fixing  $M_1$  and finding the interval of values of  $M_U$  consistent with gauge unification. Spanning in this interval we found all the possible values of  $M_2$  and  $M_3$ . Then we span all over the  $M_1$  interval. The result is a region in the parameter space  $M_1, M_2, M_3, M_U$  consistent with gauge unification. We are going to see an example of this procedure in the next section, in which we shall study in detail the breaking chain *III4*

## Application to our model

let us focus on the breaking chain we have already studied:

$$SO(10) \xrightarrow{54} G_{422}^C \xrightarrow{210} G_{3221}^C \xrightarrow{45} G_{3221} \xrightarrow{\overline{126}} G_{SM} \quad (4.124)$$

When we have discussed about the matching of the coupling we have said how passing from  $G$  to a subgroup  $\tilde{G}$  we integrate out all the heavy fields. Therefore we keep account for scalar representation  $\phi$  in the  $\beta$  function expression only when  $m_\phi > M_i$ , we do not consider threshold effect [76] and we assume that all the masses of the physical scalars have the same order of magnitude of the intermediate scale in which the associate representation gets a VEV. let us now describe in details step by step the running of the couplings toward unification.

In Tab. 4.3 we can see the numerical values for  $b_i$  and  $b_{ij}$  at each step of the breaking chain, we automatically add at each steps the gauge bosons of the model and from now on we'll talk with more details only about the Higgses multiplets used.

$SO(10)$	broken at $Q = M_X$
↓	$\{b_i\} = \begin{pmatrix} \frac{10}{3} \\ \frac{26}{3} \\ \frac{26}{3} \end{pmatrix}, \quad \{b_{ij}\} = \begin{pmatrix} \frac{4447}{6} & \frac{249}{2} & \frac{249}{2} \\ \frac{1245}{2} & \frac{779}{3} & 48 \\ \frac{1245}{2} & 48 & \frac{779}{3} \end{pmatrix}$
$G_3$	broken at $Q = M_3$
↓	$\{b_i\} = \begin{pmatrix} -7 \\ -2 \\ -2 \\ 7 \end{pmatrix}, \quad \{b_{ij}\} = \begin{pmatrix} -26 & \frac{9}{2} & \frac{9}{2} & \frac{1}{2} \\ 12 & 31 & 6 & \frac{27}{2} \\ 12 & 6 & 31 & \frac{27}{2} \\ 4 & \frac{81}{2} & \frac{81}{2} & \frac{115}{2} \end{pmatrix}$
$G_2$	broken at $Q = M_2$
↓	$\{b_i\} = \begin{pmatrix} -7 \\ -\frac{8}{3} \\ -2 \\ \frac{11}{2} \end{pmatrix}, \quad \{b_{ij}\} = \begin{pmatrix} -26 & \frac{9}{2} & \frac{9}{2} & \frac{1}{2} \\ 12 & \frac{37}{3} & 6 & \frac{3}{2} \\ 12 & 6 & 31 & \frac{27}{2} \\ 4 & \frac{9}{2} & \frac{81}{2} & \frac{61}{2} \end{pmatrix}$
$G_1$	broken at $Q = M_1$
↓	$\{b_i\} = \begin{pmatrix} -7 \\ -\frac{19}{6} \\ \frac{41}{10} \end{pmatrix}, \quad \{b_{ij}\} = \begin{pmatrix} -26 & \frac{9}{2} & \frac{11}{10} \\ 12 & \frac{35}{6} & \frac{9}{10} \\ \frac{44}{5} & \frac{17}{10} & \frac{199}{50} \end{pmatrix}$
$G_{SM}$	

Table 4.3: Decomposition of the matter multiplet 16 in each step of the breaking chain.

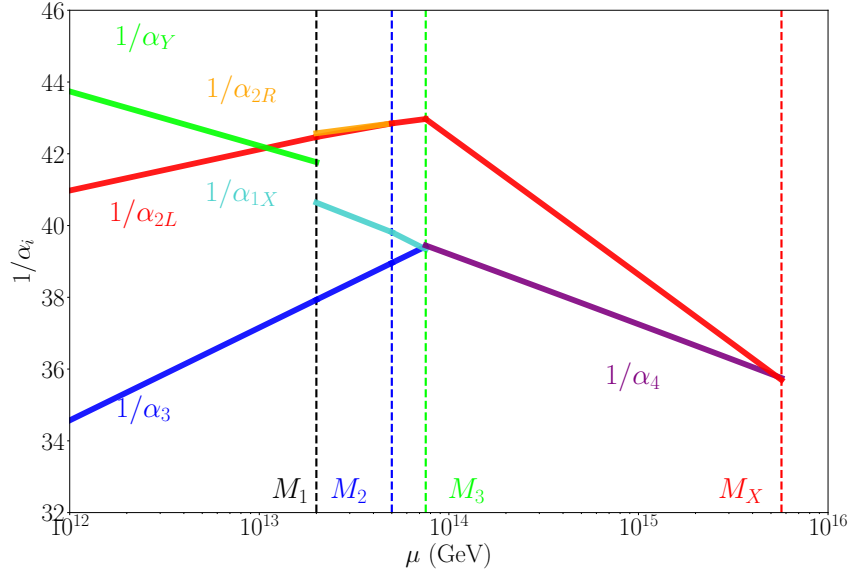


Figure 4.2: An example of the RG running of gauge couplings in the breaking chain  $SO(10) \rightarrow G_3 \rightarrow G_2 \rightarrow G_1 \rightarrow G_{SM}$ . The first and second lowest intermediate scales are fixed at  $M_1 = 2 \times 10^{13}$  GeV and  $M_2 = 5 \times 10^{13}$  GeV, the remaining scales  $M_3$  and  $M_X$ , as well as gauge couplings  $\alpha_{2R}$ , are determined by the gauge unification at  $M_X$ .

- From  $M_Z$  to  $M_1$  the couplings run without considering any addition to the particle content of the Standard Model.
- We impose the matching of the couplings at scale  $M_1$  using Eq. 4.122.
- From  $M_1$  to  $M_2$  we need to consider also the submultiplets of the  $\overline{\mathbf{126}}$  representation together with  $\mathbf{10}$ . The sub-multiplets that contribute to the running are two  $(\mathbf{1}, \mathbf{2}, \mathbf{2}, \mathbf{0})$  (one from  $\overline{\mathbf{126}}$  and one from  $\mathbf{10}$  needed in the Yukawa lagrangian) and one  $(\mathbf{1}, \mathbf{3}, \mathbf{1}, -\mathbf{1})$ . These are  $\Phi$  and  $\Delta$  of the left-right symmetry breaking, among them there is the Standard Model Higgs and the singlet  $S$ .
- We impose the matching at the scale  $M_2$
- From  $M_2$  to  $M_3$  we still have the Higgses mentioned above. Now we have also  $(\mathbf{1}, \mathbf{3}, \mathbf{1}, \mathbf{1})$  due to D-parity and  $(\mathbf{1}, \mathbf{1}, \mathbf{1}, \mathbf{0}_{odd})$  which breaks D-parity in  $G_2 \rightarrow G_1$ .
- We impose the matching at  $M_3$
- From  $M_3$  to  $M_U$  we embed  $(\mathbf{1}, \mathbf{2}, \mathbf{2}, \mathbf{0})$  in  $(\mathbf{15}, \mathbf{2}, \mathbf{2})$ ,  $(\mathbf{1}, \mathbf{2}, \mathbf{2})$ ,  $(\mathbf{1}, \mathbf{3}, \mathbf{1}, \mathbf{1})$  and  $(\mathbf{1}, \mathbf{3}, \mathbf{1}, -\mathbf{1})$  in  $(\mathbf{10}, \mathbf{3}, \mathbf{1})$  and  $(\mathbf{10}, \mathbf{3}, -\mathbf{1})$ . We add also the 45 and the 210 singlets embedded in

(15, 1, 1) In Figure 4.2 we see an example of running couplings reaching grand unification for fixed values of the intermediate scales. In Figure 4.3, instead, we can see the correlation between the intermediate scales and the region in the parameters space which is compatible with gauge unification.

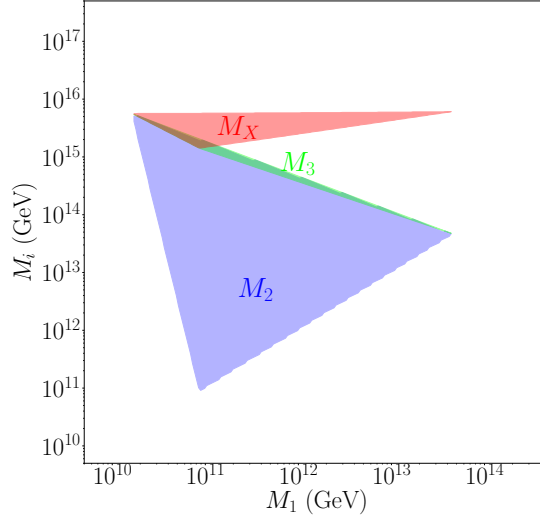


Figure 4.3: Left panel: regions of  $M_2$ ,  $M_3$ ,  $M_X$  as functions of  $M_1$  allowed by gauge unification; Right panel: prediction of proton lifetime as functions of  $M_1$ , with exclusion upper bound of Super-K and future sensitivity of Hyper-K indicated.

## 4.4 Proton decay

One of the most striking prediction of GUT theories is proton decay. Up to now we are using constraints from proton decay non observation to put a lower bound on grand unification scale. In this section we are going to see it in detail. In general heavy SO(10) gauge bosons mediate baryon number violating interactions that cause proton decay as we can see in Fig. 4.4.

Without specifying the model or even the GUT theory we can use an effective field theory to describe this phenomenon. There can be four independent operators that at low energy describe proton decay interaction [77]:

$$\begin{aligned} \mathcal{L}_{\text{eff}} = & \epsilon^{ijk} \epsilon_{\alpha\beta} \left( \frac{1}{\Lambda^2} \left( \overline{u_R^{jc}} \gamma^\mu Q_\alpha^k \right) \left( \overline{d_R^{ic}} \gamma_\mu L_\beta \right) + \frac{1}{\Lambda^2} \left( \overline{u_R^{jc}} \gamma^\mu Q_\alpha^k \right) \left( \overline{e_R^c} \gamma_\mu Q_\beta^i \right) \right. \\ & \left. + \frac{1}{\Lambda^2} \left( \overline{d_R^{jc}} \gamma^\mu Q_\alpha^k \right) \left( \overline{u_R^{ic}} \gamma_\mu L_\beta \right) + \frac{1}{\Lambda^2} \left( \overline{d_R^{jc}} \gamma^\mu Q_\alpha^k \right) \left( \overline{\nu_R^c} \gamma_\mu Q_\beta^i \right) + \text{h.c.} \right) \end{aligned} \quad (4.125)$$

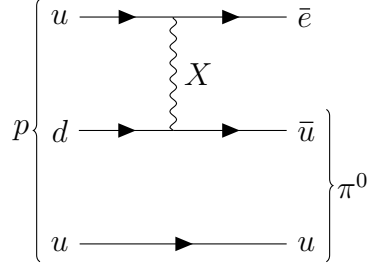


Figure 4.4:  $p \rightarrow \pi^0 + e^c$  mediated by a heavy gauge bosons

where  $\Lambda \approx g_U M_U/2$ . In this notation  $i, j, k$  are color index and  $\alpha, \beta$  flavour index. For computing the proton lifetime in function of the grand unification scale we can proceed in the same way one does with the muon decay. The scattering amplitude for such a diagram is

$$i|\mathcal{M}| = \begin{array}{ccc} & u & d \\ & \searrow & \nearrow \\ e & & u \\ & \nearrow & \searrow \end{array} . \quad (4.126)$$

Applying the Feynman rules for the external legs and working on the kinematics one find approximatively:

$$\Gamma_p \approx = \frac{g^4}{M_U^4} m_p^5. \quad (4.127)$$

A more detailed computation led to [25]

$$\Gamma(p \rightarrow \pi^0 + e^+) = \frac{m_p}{32\pi} \left(1 - \frac{m_{\pi^0}^2}{m_p^2}\right)^2 A_L^2 \times \left[ A_{SL} \Lambda_1^{-2} (1 + |V_{ud}|^2) |\langle \pi^0 | (ud) RuL | p \rangle|^2 + A_{SR} (\Lambda_1^{-2} + |V_{ud}|^2 \Lambda_2^{-2}) |\langle \pi^0 | (ud) LuL | p \rangle_0|^2 \right], \quad (4.128)$$

where  $A_L A_{SR} A_{SL}$  are long range and short range enhancement factors that depend on the breaking chain because we want quantity at the same energy scale and then we need to run the proton mass at  $M_Z$  and then run all the relevant quantities up to the grand unification scale.  $\langle \pi^0 | (ud) RuL | p \rangle$  is the hadronic matrix element computed with lattice QCD simulations [78] and  $V_{ud}$  is an element of the  $V_{CKM}$  matrix. The prediction for the lifetime of the proton decay it is, generally: <sup>††</sup>:

$$\tau \simeq 6.9 \times 10^{35} \times \left( \frac{M_U}{10^{16} \text{GeV}} \right)^4 \text{ yr}. \quad (4.129)$$

<sup>††</sup>Not considering the differences between different breaking chain

So that by searching for proton decay we can look for the value of the grand unification scale. As we have said in the last chapter the grand unification scale is correlated to the other intermediate scales, especially with  $M_1$ . Therefore constraints from proton decay become constrain upon the intermediate scale  $M_1$  that controls leptogenesis scale and cosmic string production [24]. For breaking chain with only one intermediate scale we are able to tell directly if the breaking chain can be excluded. The current bound from Super-Kamiokande is  $\tau > 1.6 \times 10^{34}$  that translates in:  $M_X > 4 \times 10^{15}$  GeV. Looking at Tab. 4.2 we see that the only breaking chains which are not excluded are  $I1$  and  $I4$ . When two intermediate scales are present there is one free parameter and thus we have a line for each breaking chain which is possible to test. From the figure ?? we can see how  $II3,4,5,7,8$  are still consistent with the Super-K bound and for example  $II3$  and  $8$  will be completely tested by the next generation experiment HyperKamiokande which will arrive at testing proton decay lifetime up to  $\tau \sim 10^{35}$ .

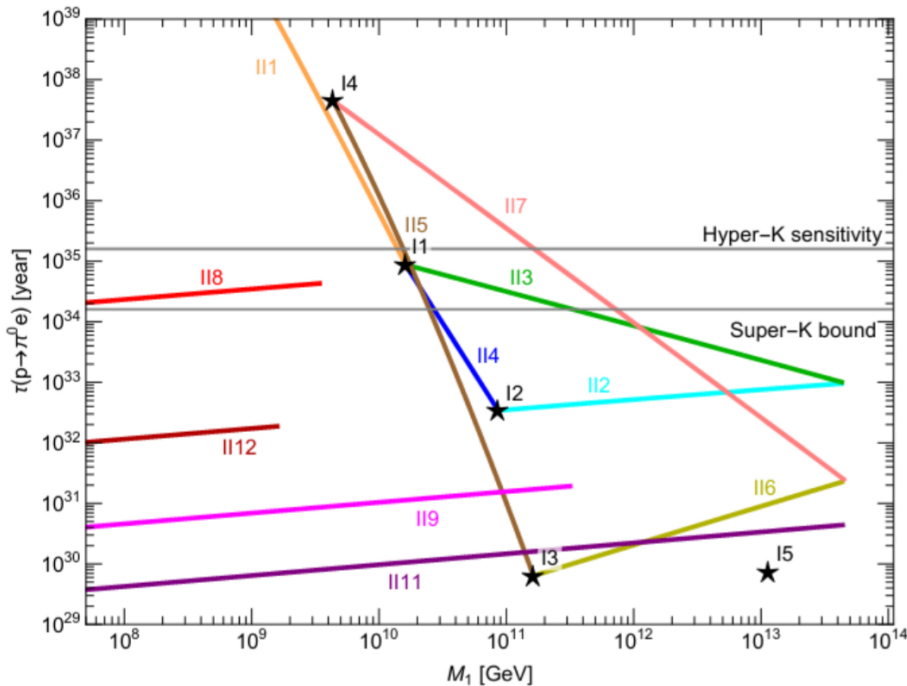


Figure 4.5: Correlation between  $M_1$  and proton lifetime for breaking chains with one (black stars) and two (lines) intermediate scale. The lower region has already been tested by Super-K and Hyper-K will test  $\tau$  up to  $10^{35}$ . Figure taken from [25]

For three intermediate scale there is a region that correlates  $M_U$  and  $M_1$  since there are two free parameters. In Fig. 4.6 we can see how part of the parameter space of our breaking chain can be consistent with Super-K bound and that it will be completely tested by Hyper-K.

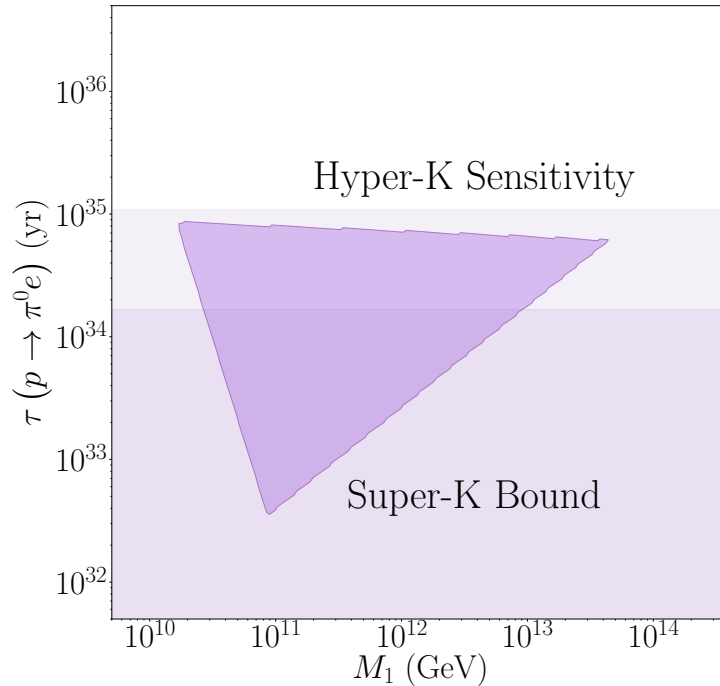


Figure 4.6: Correlation region between  $M_1$  and proton lifetime for the breaking chain of our model. We can see that Hyper-K will be able to test the whole parameter space

In the following chapters we are going to see how the parameter space can be furtherly tested by cosmic strings experiments.

## 4.5 Yukawa sector

Let us now compute fermion masses and study the Yukawa lagrangian. As we have seen earlier the tensor product between two spinorial representations is:

$$\mathbf{16} \times \mathbf{16} = \mathbf{10} + \mathbf{120} + \overline{\mathbf{126}}. \quad (4.130)$$

There are different combination of Higgses that can be used in order to generate fermion masses [79, 80, 81, 82, 83], we are going to use  $\mathbf{10}$ ,  $\mathbf{120}$ ,  $\overline{\mathbf{126}}$ . The most

general Yukawa Lagrangian can be written as:

$$\mathcal{L} = Y_{10}\overline{\mathbf{16}}_F 10_H 16_F + Y_{120}\overline{\mathbf{16}}_F 120_H 16_F + Y_{\overline{\mathbf{126}}}\overline{\mathbf{16}}_F 126_H 16_F + \text{h.c.} \quad (4.131)$$

With respect to the flavour indices we have that  $Y_{10}$  and  $Y_{126}$  are symmetric and  $Y_{120}$  is antisymmetric. We have therefore that the symmetric terms have 6 free parameters each that contribute to the direct mass terms and the mixing angles while the latter has 3 free parameters that contributes only to the mixing angles. For reducing the parameter space we assume all three Yukawa couplings to be real. The decompositions of  $\mathbf{10}$  and  $\overline{\mathbf{126}}$  down to the subgroups of our breaking chain is:

$$\begin{aligned} SO(10) : & \quad 10 & \quad \overline{\mathbf{126}} \\ G_3 : & \quad \rightarrow (1, 2, 2) & \quad \rightarrow (15, 2, 2) + (\overline{\mathbf{10}}, 3, 1) + (10, 1, 3), \\ G_2 : & \quad \rightarrow (1, 2, 2, 0)_1 & \quad \rightarrow (1, 2, 2, 0)_2 + (1, 3, 1, 1) + (1, 1, 3, -1), \\ G_1 : & \quad \rightarrow (1, 2, 2, 0)_1 & \quad \rightarrow (1, 2, 2, 0)_2 + (1, 3, 1, 1) + (1, 1, 3, -1), \\ G_{SM} : & \quad \rightarrow (1, 2, \mp 1/2)_{h_{10}^{u,d}} & \quad \rightarrow (1, 2, \mp 1/2)_{h_{\overline{\mathbf{126}}}^{u,d}} + (1, 1, 0)_S, \end{aligned} \quad (4.132)$$

while for  $\mathbf{120}$  we have:

$$\begin{aligned} SO(10) : & \quad 120 \\ G_3 : & \quad \rightarrow (1, 2, 2) + (15, 2, 2), \\ G_2 : & \quad \rightarrow (1, 2, 2, 0)'_1 + (1, 2, 2, 0)'_2, \\ G_1 : & \quad \rightarrow (1, 2, 2, 0)'_1 + (1, 2, 2, 0)'_2, \\ G_{SM} : & \quad \rightarrow (1, 2, \pm 1/2)_{h_{120}^{u,d}, h_{120}^{u',d'}}. \end{aligned} \quad (4.133)$$

We can write the Standard Model Yukawa Lagrangian in terms of the Higgs submultiplets we have used as:

$$\mathcal{L}_Y = Y_{10} [(\bar{Q}u + \bar{L}\nu_R) h_{10}^u + (\bar{Q}d + \bar{L}e_R) h_{10}^d] +$$

$$\begin{aligned} & \frac{1}{\sqrt{3}} Y_{\overline{126}} \left[ (\bar{Q}u - 3\bar{L}\nu_R) h_{\overline{126}}^u + (\bar{Q}d - 3\bar{L}e_R) h_{\overline{126}}^d \right] + \\ & Y_{120} \left[ (\bar{Q}u + \bar{L}\nu_R) h_{120}^u + (\bar{Q}d + \bar{L}e_R) h_{120}^d + \right. \\ & \left. \frac{1}{\sqrt{3}} (\bar{Q}u - 3\bar{L}\nu_R) h_{120}^{\prime u} + (\bar{Q}d - 3\bar{L}e_R) h_{120}^{\prime d} \right]. \end{aligned} \quad (4.134)$$

This is not enough since we need to add another piece, the mass of the right-handed neutrino generated by the singlet  $S$ :

$$\mathcal{L}_{\nu_R} = \bar{L} Y_{\overline{126}} \bar{\nu}_R S \nu_R + \text{h.c.} \quad (4.135)$$

We can rewrite those Higgses as a linear combination of mass eigenstates  $\hat{h}_i = \sum_j V_{ij} h_j$  where we call  $h_{SM} = \hat{h}_1 = \sum_j V_{1j} h_j$ . We call

$$h_j = \{\tilde{h}_{10}^u, \tilde{h}_{126}^u, \tilde{h}_{120}^u, \tilde{h}_{120}^{\prime u}, h_{10}^d, h_{126}^d, h_{120}^d, h_{120}^{\prime d}\}, \quad (4.136)$$

where  $\tilde{h} = i\sigma_2 h$ . In terms of  $h_{SM}$  the langrangian is, as usual:

$$\mathcal{L}_Y = Y_u \bar{Q} \tilde{h}_{SM} u_R + Y_d \bar{Q} h_{SM} d_R + Y_\nu \bar{L} \tilde{h}_{SM} \nu_R + Y_e \bar{L} h_{SM} e_R + \text{h.c.} \quad (4.137)$$

Confronting Eq. 4.134 with Eq. 4.137 we can find the expression of the ordinary Yukawa couplings

$$Y_u = Y_{10} V_{11} + \frac{1}{\sqrt{3}} Y_{\overline{126}} V_{12} + Y_{120} \left( V_{13} + \frac{1}{\sqrt{3}} V_{14} \right), \quad (4.138)$$

$$Y_d = Y_{10} V_{15} + \frac{1}{\sqrt{3}} Y_{\overline{126}} V_{16} + Y_{120} \left( V_{17} + \frac{1}{\sqrt{3}} V_{18} \right), \quad (4.139)$$

$$Y_\nu = Y_{10} V_{11} - \sqrt{3} Y_{\overline{126}} V_{12} + Y_{120} \left( V_{13} - \sqrt{3} V_{14} \right), \quad (4.140)$$

$$Y_e = Y_{10} V_{15} - \sqrt{3} Y_{\overline{126}} V_{16} + Y_{120} \left( V_{17} - \sqrt{3} V_{18} \right), \quad (4.141)$$

and from Eq. 4.142

$$M_{\nu_R} = Y_{\overline{126}} \nu_S, \quad (4.142)$$

we can compute the mass of the light neutrino via the See-Saw mechanism:

$$M_\nu = -Y_\nu M_{\nu_R}^{-1} Y_\nu \nu_{SM}^2 \quad (4.143)$$

## 4.6 Scan of the parameter space

Following [84] we can parametrize the Yukawa couplings using two real symmetric matrices  $h$  and  $f$ , one real antisymmetric matrix  $h'$  and five free parameters  $r_1$ ,

$r_2, r_3, c_\nu$  and  $c_e$  and  $m_0$ .

$$\begin{aligned} Y_u &= h + r_2 f + i r_3 h', & Y_d &= r_1(h + f + i h'), & Y_\nu &= h - 3r_2 f + i c_\nu h', \\ Y_e &= r_1(h - 3f + i c_e h'), & M_{\nu R} &= f \frac{\sqrt{3} r_1}{V_{16}} v_S. \end{aligned} \quad (4.144)$$

Confronting it with Eq. 4.141 we obtain:

$$\begin{aligned} h &= Y_{10} V_{11}, \quad f = Y_{126} \frac{V_{16} V_{11}^*}{\sqrt{3} V_{15}}, \quad c_e = \frac{V_{17} - \sqrt{3} V_{18}}{V_{17} + V_{18}/\sqrt{3}}, \quad c_\nu = \frac{V_{13}^* - \sqrt{3} V_{14}^* V_{15}}{V_{17} + V_{18}/\sqrt{3} V_{11}^*}, \\ r_1 &= \frac{V_{15}}{V_{11}^*}, \quad r_2 = \frac{V_{12}^* V_{15}}{V_{16} V_{11}^*}, \quad r_3 = \frac{V_{13}^* + V_{14}^*/\sqrt{3} V_{15}}{V_{17} + V_{18}/\sqrt{3} V_{11}^*}, \quad h' = -i Y_{120} \left( V_{17} + V_{18}/\sqrt{3} \right) \frac{V_{11}^*}{V_{15}}, \end{aligned} \quad (4.145)$$

For the light neutrino matrix we have:

$$M_\nu = m_0 Y_\nu f^{-1} Y_\nu, \quad (4.146)$$

where  $m_0 = -\frac{V_{16}}{\sqrt{3} r_1} \frac{v_S^2 M}{v_S}$ . Our goal is to use this parametrization to express  $Y_e$  and  $M_\nu$  in terms of  $Y_u$  and  $Y_d$ , in this way we will be able to predict the lepton masses from knowing the quark masses.

We want to scan all over the parameter space of  $\{r_1, r_2, c_\nu, c_e, m_0\}$  to see for which points the predictions fit with the experimental data. We start assuming  $r_3 = 0$  thus assuming  $Y_u$  to be real and use the basis in which it is diagonal: We have:

$$Y_u = h + r_2 f = \text{diag}\{\eta_u y_u, \eta_c y_c, \eta_t y_t\}, \quad (4.147)$$

Then we can express  $Y_d$  in terms of  $Y_u$ :

$$Y_d = P_a V_{\text{CKM}} \text{diag}\{\eta_d y_d, \eta_s y_s, \eta_b y_b\} V_{\text{CKM}}^\dagger P_a^*, \quad (4.148)$$

where  $\eta_{d,s,b} = \pm 1$  represent the signs of eigenvalues. We can express  $h, h'$  and  $f$  in terms of the Yukawa matrices for up and down quarks:

$$h = -\frac{Y_u}{r_2 - 1} + \frac{r_2 \text{Re} Y_d}{r_1(r_2 - 1)}, \quad f = \frac{Y_u}{r_2 - 1} - \frac{\text{Re} Y_d}{r_1(r_2 - 1)}, \quad h' = i \frac{\text{Im} Y_d}{r_1}.$$

Finally plugging these expressions in 4.141 we finally find:

$$Y_\nu = -\frac{3r_2 + 1}{r_2 - 1} Y_u + \frac{4r_2}{r_1(r_2 - 1)} \text{Re} Y_d + i \frac{c_\nu}{r_1} \text{Im} Y_d,$$

$$Y_e = -\frac{4r_1}{r_2-1}Y_u + \frac{r_2+3}{r_2-1}\text{Re}Y_d + ic_e\text{Im}Y_d. \quad (4.149)$$

The light neutrino mass matrix can be expressed as

$$M_\nu = m_0 \left( \frac{8r_2(r_2+1)}{r_2-1}Y_u - \frac{16r_2^2}{r_1(r_2-1)}\text{Re}Y_d + \frac{r_2-1}{r_1}(r_1Y_u + ic_\nu\text{Im}Y_d)(r_1Y_u - \text{Re}Y_d)^{-1}(r_1Y_u - ic_\nu\text{Im}Y_d) \right) \quad (4.150)$$

This is the starting point for the scan.

## Numerical parameters

Now we'll try to predict the lepton sector observables using quark masses and mixing as input. The free parameters in the quark sector are the quark masses, three mixing angles and one phase from  $V_{\text{CKM}}$ . There is also a small parameter  $\theta$  related to the strong CP problem which we will not consider. In the extended lepton sector the free parameters are the lepton masses, the squared difference of the neutrino masses  $\Delta m_{12}^2$  and  $\Delta m_{13}^2$ , and the mixing angles plus the phases of the  $U_{\text{PMNS}}$  matrix. We are going to use the following best fit values [82, 85]:

$$\begin{aligned} y_u^{\text{bf}} &= 2.54 \times 10^{-6}, & y_c^{\text{bf}} &= 1.37 \times 10^{-3}, & y_t^{\text{bf}} &= 0.43, \\ y_d^{\text{bf}} &= 6.56 \times 10^{-6}, & y_s^{\text{bf}} &= 1.24 \times 10^{-4}, & y_b^{\text{bf}} &= 5.7 \times 10^{-3}, \\ y_e^{\text{bf}} &= 2.70 \times 10^{-6}, & y_\mu^{\text{bf}} &= 5.71 \times 10^{-4}, & y_\tau^{\text{bf}} &= 9.7 \times 10^{-3}, \end{aligned} \quad (4.151)$$

and:

$$\theta_{12}^{q,\text{bf}} = 0.227, \quad \theta_{23}^{q,\text{bf}} = 4.858 \times 10^{-2}, \quad \theta_{13}^{q,\text{bf}} = 4.202 \times 10^{-3}, \quad \delta^{q,\text{bf}} = 1.207. \quad (4.152)$$

For neutrino sector we are using the best-fit values from NuFIT 5.0 [42] with  $1\sigma$  uncertainty, we have already presented this results in the first chapter distinguishing from first and second octant and obtaining two sets of parameters. We are going to do the scan for both the first and second octant separately.

## Numerical analysis

The scan is divided in two steps. The first step is to find which points in the parameter space correctly fit charged lepton masses. Using Eq. 4.149 we obtain

that  $Y_e$  depend on the continuous parameter  $(a_1, a_2, r_1, r_2, c_\nu)$  and on the sign  $eta_i$ . It has to satisfy the following relations:

$$\begin{aligned}\text{Tr} [Y_e Y_e^\dagger] &= y_e^2 + y_\mu^2 + y_\tau^2, \\ \text{Tr} [Y_e Y_e^\dagger Y_e Y_e^\dagger] &= y_e^4 + y_\mu^4 + y_\tau^4, \\ \text{Det} [Y_e Y_e^\dagger] &= y_e^2 y_\mu^2 y_\tau^2,\end{aligned}\tag{4.153}$$

We scan over  $a_1, a_2$  in the range  $[0, 2\pi]$ , for all the possible sign combinations and for each point in this parameter space we solve the constrains equations and find  $r_1, r_2, c_e$ . In order to do that we use the first equation for writing  $r_1$  as a function of  $r_2$ . We find

$$r_1 = \frac{(r_2 + 3) \sum y_d - (r_2 - 1) \sum y_e}{4 \sum y_u}.\tag{4.154}$$

We then solve numerically the other two equations in order to find  $r_2$  and  $c_e$ . After the first step we have many points of the parameter space  $(a_1, a_2, r_1, r_2, c_\nu)$  which gives the correct lepton masses. We use this values to compute the unitary matrix which diagonalize  $Y_e$ :  $V_e$ . There are still two free parameters in the definition of  $M_\nu$ : these are  $c_\nu$  and  $m_0$ . We compute the observables in the neutrino sector starting from  $U_{\text{PMNS}} = V_e^\dagger V_\nu$  matrix which depends only on one free parameter:  $c_\nu$ . We have

$$\sin \theta_{13} = |(U_{\text{PMNS}}) e3|, \quad \tan \theta_{12} = \left| \frac{(U_{\text{PMNS}}) e2}{(U_{\text{PMNS}}) e1} \right|, \quad \tan \theta_{23} = \left| \frac{(U_{\text{PMNS}}) \mu 3}{(U_{\text{PMNS}})_{\tau 3}} \right|.\tag{4.155}$$

We call  $\{Y^{sq} = Y_\nu Y_\nu^\dagger\}$  and the squared values of the eigenstates of  $Y_\nu$  are respectively  $Y_3^{sq}, Y_2^{sq}$  and  $Y_1^{sq}$ . For a fixed value of  $c_\nu$  we compute  $m_0$  from the ratio  $\Delta m_{12}^2 / Y_2^{sq} - Y_2^{sq}$  or from the ratio  $\Delta m_{23}^2 / Y_3^{sq} - Y_2^{sq}$  and we decide randomly which value to choose between those two. <sup>‡‡</sup> For each point we computed the chi squared:

$$\chi^2 = \sum_n \left[ \frac{\mathcal{O}_n(\mathcal{P}_m) - \mathcal{O}_n^{\text{bf}}}{\sigma \mathcal{O}_n} \right]^2.\tag{4.156}$$

We first have done a general scan for  $\chi^2 < 100$  of which the results are shown in Fig. 4.7. The two-dimensional subspaces of  $a_1 - a_2$  and  $m_0 - c_\nu$  are shown respectively in the top and in the bottom of the left panel while in the right panel we have  $\theta_{23} - \delta$  in the top and  $M_{N_1} - M_{N_3}$  in the bottom. The most of the points

---

<sup>‡‡</sup>For the points which fit correctly the observables the two values are almost the same.

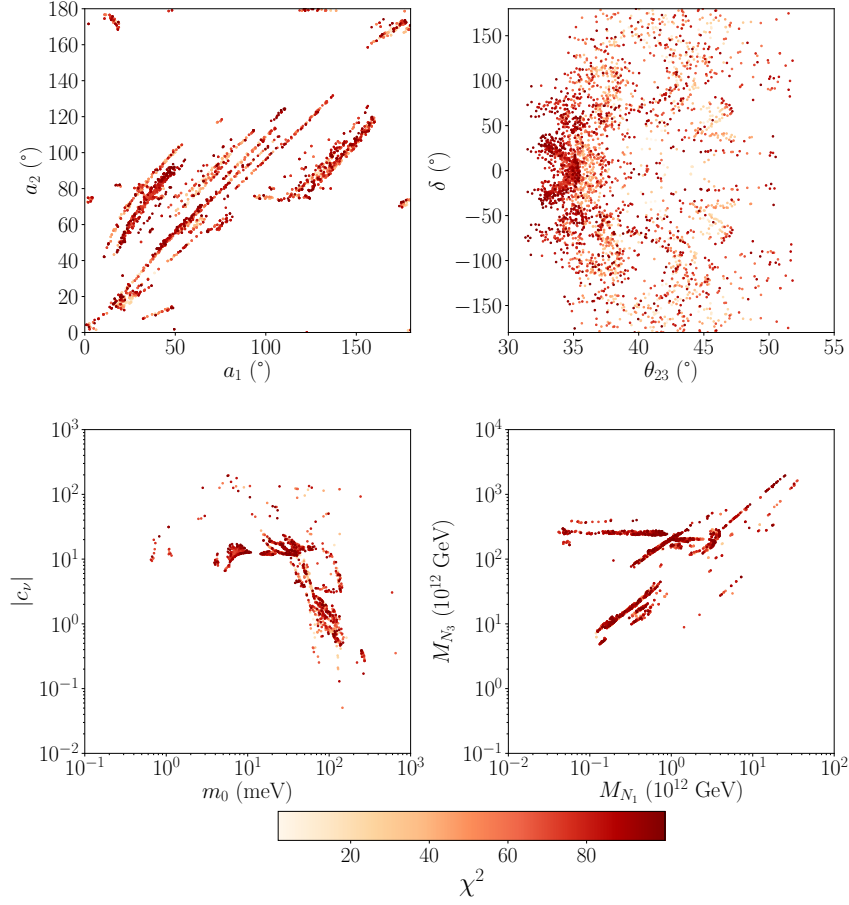


Figure 4.7: Two-dimensional correlations between theory inputs (left two panels) and predicted observables (right two panels) for  $\chi^2 < 100$  for  $\theta_{23} \leq 45$  deg. Consistency with gauge unification is not considered

have  $M_{N_3} \sim 10^{15}$  GeV as expected from assuming  $Y_{\overline{126}} \sim \mathcal{O}(1)$  and from the see-saw model, but it is important to consider the bound on heavy neutrino mass imposed by proton decay. For the breaking chain of our model, type IIIc the proton decay bound on  $M_1$  is:

$$M_1 < 4.4 \times 10^{13} \text{ GeV} \quad (4.157)$$

From 4.142 we require  $Y_{126} \leq 1$  and therefore we have included only those points who satisfy

$$M_{N_3} < 4.4 \times 10^{13} \text{ GeV}. \quad (4.158)$$

Therefore we need to exclude the points not allowed by proton decay but we can also notice that there is an island which satisfies the proton decay bound, gauge

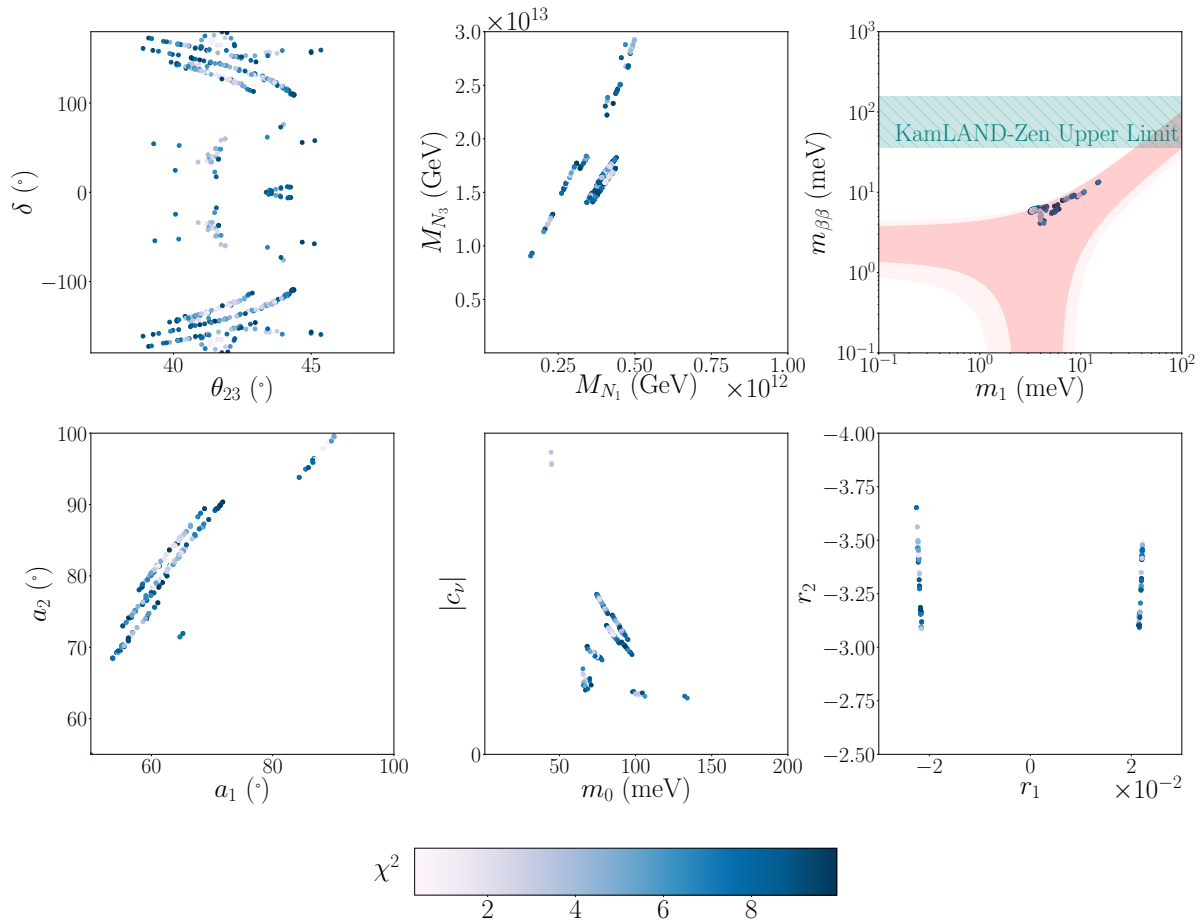


Figure 4.8: The predicted observables (top left two panels), the effective neutrino mass prediction (top right panel) and two-dimensional correlations between theory inputs (bottom panels) for  $\chi^2 < 10$  and  $\theta_{23} \leq 45$  deg. Consistency with gauge unification is considered.

unification and predicts the correct fermion masses. We then have made a more dense scan around this island refining the range of the parameter space of  $a_1$ ,  $a_2$  and  $c_\nu$ , in particular noticing that most of the points which satisfies all the constraints have  $a_1, a_2$  in the range (50 deg, 100 deg) and  $c_\nu$  in the range (1, 10). In this last scan we imposed the proton decay bound and we have required  $\chi^2 < 10$ . We can see the results for the first and the second octant respectively in Fig. 4.8 and in Fig. 4.9. For each of the figure in the bottom panels we have plotted two-dimensional subspaces of the parameter spaces, from left to right we have:  $(a_1, a_2)$ ,  $(m_0, c_\nu)$  and  $(r_1, r_2)$ . In the top panels we have the plot the points in function of

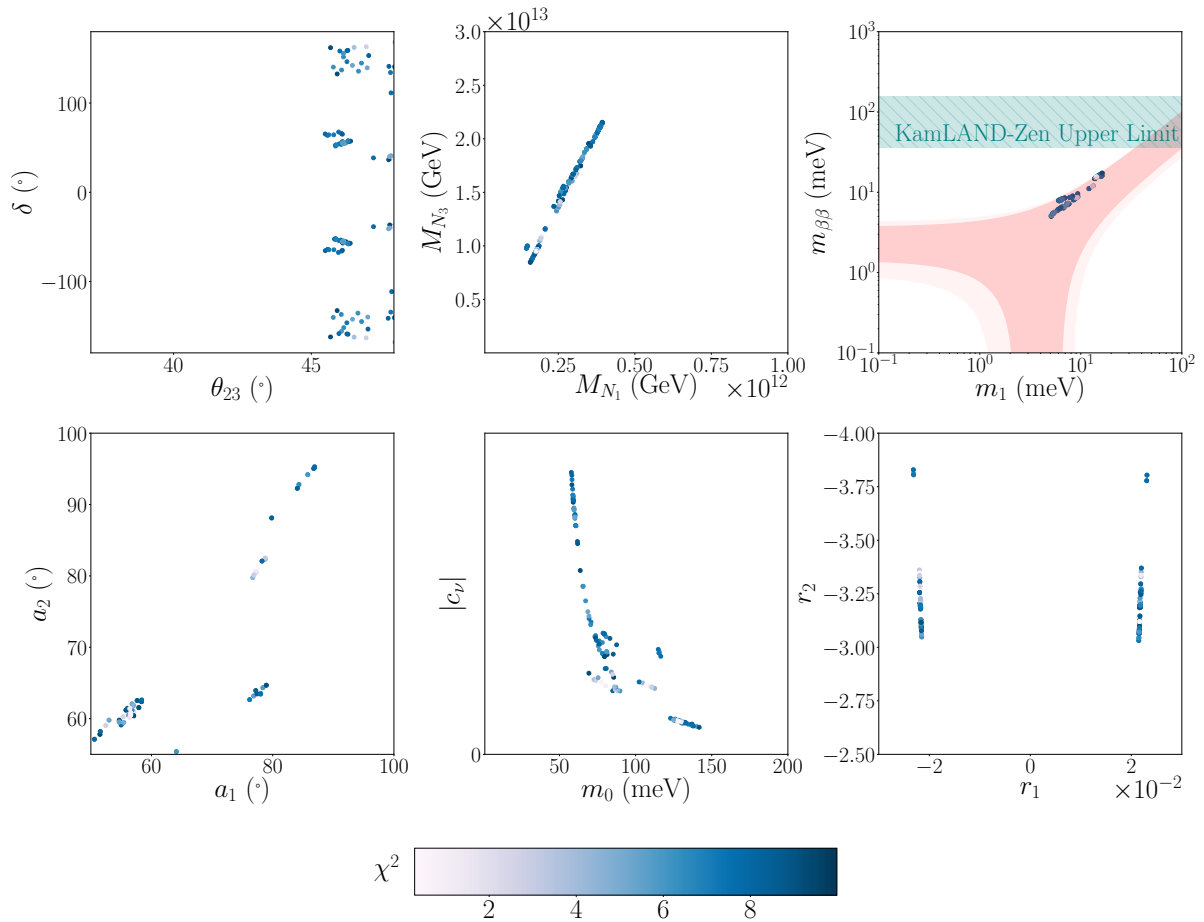


Figure 4.9: The predicted observables (top left two panels), the effective neutrino mass prediction (top right panel) and two-dimensional correlations between theory inputs (bottom panels) for  $\chi^2 < 10$  and  $\theta_{23} \geq 45$  deg. Consistency with gauge unification is considered.

the observables: from left to the right we have  $(\theta_{23}, \delta)$ ,  $(M_{N_1}, M_{N_3})$  and  $(m_1, m_{\beta\beta})$ , in which the effective mass parameter can be tested with neutrinoless double- $\beta$  decay and it is defined as:

$$m_{\beta\beta} = \left| \sum_{i=1}^3 m_i (U_{PMNS})_{ei}^2 \right|. \quad (4.159)$$

Both in the first and second octant we can notice an interesting correlation between  $r_1$  and  $r_2$ , we can derive analytically this correlation following [26]. The input variables of our scan, the Yukawa couplings of the quark sector, have the following

hierarchy that can be expressed in terms of the Cabibbo angle

$$y_u : \tilde{y}_c : y_t \sim \theta_C^8 : \theta_C^4 : \theta_C^0, \quad (4.160)$$

$$y_d : y_s : y_b \sim \theta_C^8 : \theta_C^6 : \theta_C^3, \quad (4.161)$$

$$\theta_{13}^q : \theta_{23}^q : \theta_{12}^q \sim \theta_C^3 : \theta_C^2 : \theta_C^1. \quad (4.162)$$

$$(4.163)$$

From Eq. 4.149 we have

$$\text{Tr } Y_e = -\frac{4r_1}{r_2 - 1} \text{Tr } Y_u + \frac{r_2 + 3}{r_2 - 1}, \quad (4.164)$$

keeping account of the hierarchy we find

$$\frac{\tilde{y}_\tau}{\tilde{y}_b} \simeq \frac{r_2 + 3}{r_2 - 1} p - \frac{4r_1}{r_2 - 1}, \frac{\tilde{y}_t}{\tilde{y}_b}, \quad (4.165)$$

where  $\tilde{y}_i = \eta_i y_i$  and

$$p = 1 - \frac{\tilde{y}_\mu}{\tilde{y}_\tau} + \frac{r_2 + 3}{r_2 - 1} \frac{\tilde{y}_s}{\tilde{y}_\tau} \quad (4.166)$$

keeps account of the contribution of the smaller Yukawa couplings. We obtain the following linear relation which is the one we can see in Fig. 4.8 and Fig. 4.9

$$r_2 \approx \frac{-4\tilde{y}_t}{\tilde{y}_\tau - \tilde{y}_b p} r_1 + \frac{\tilde{y}_\tau + 3\tilde{y}_b p}{\tilde{y}_\tau - \tilde{y}_b p}. \quad (4.167)$$

## 4.7 Benchmark point: BP1

It is worth to show an example and compute all the relevant quantities for the benchmark point BP1. This point has  $\chi^2 = 0.33$  and, as we shall see later, predicts the correct amount of baryon asymmetry. The parameters  $(a_1, a_2, r_1, r_2, c_e, c_\nu, m_0)$  for this model and the predicted observables in the neutrino sector are shown in Table 4.4 and we obtain from them the following expression for  $h$ ,  $h'$  and  $f$ :

$$h = 10^{-2} \begin{pmatrix} -0.1934 & 0.1343 & -0.0845 \\ 0.1343 & 0.3924 & -0.0995 \\ -0.0845 & -0.0995 & -33.7016 \end{pmatrix},$$

$$f = 10^{-2} \cdot \begin{pmatrix} -0.1934 & 0.1343 & -0.0845 \\ 0.1343 & 0.3924 & -0.0995 \\ -0.0845 & -0.0995 & -33.7016 \end{pmatrix},$$

Inputs	$a_1$	$a_2$	$c_\nu$	$m_0$	$(\eta_u, \eta_c, \eta_t; \eta_d, \eta_s, \eta_b)$
	$63.57^\circ$	$84.17^\circ$	-1.945	82.82 meV	$(+, +, -; +, -, +)$
Outputs	$\theta_{13}$	$\theta_{12}$	$\theta_{23}$	$\delta$	$m_1$
	$8.53^\circ$	$32.7^\circ$	$41.9^\circ$	$-125^\circ$	3.36 meV
$(\chi^2 = 0.33)$	$m_{\beta\beta}$	$M_{N_1}$	$M_{N_2}$	$M_{N_3}$	
	5.83	$4.23 \cdot 10^{11}$ GeV	$5.32 \cdot 10^{11}$ GeV	$1.66 \cdot 10^{13}$ GeV	

Table 4.4: Inputs and predictions of neutrino masses and mixing parameters of BP1 fully satisfy all experimental data. Charged fermion masses and CKM mixing are all fixed at experimental best-fit values. Neutrino masses with normal ordering are predicted.

$$h' = 10^{-2} \cdot \begin{pmatrix} 0. & -0.0693 & 0.0025 \\ 0.0693 & 0. & -1.4430 \\ -0.0025 & 1.4430 & 0. \end{pmatrix}.$$

Plugging this expression into 4.144 we have:

$$Y_u = \begin{pmatrix} 2.54 \cdot 10^{-6} & 0 & 0 \\ 0 & -0.00137 & 0 \\ 0 & 0 & -0.428 \end{pmatrix}, \quad (4.168)$$

$$Y_d = 10^{-2} \cdot \begin{pmatrix} 0.0056 & -0.0039 + 0.0014i & 0.0024 - 0.0i \\ -0.0039 - 0.0014i & -0.0100 & 0.0029 + 0.0281i \\ 0.0024 + 0.0i & 0.0029 - 0.0281i & 0.5686 \end{pmatrix}, \quad (4.169)$$

$$Y_e = 10^{-2} \cdot \begin{pmatrix} -0.0018 & 0.0012 - 0.0111i & -0.0008 + 0.004i \\ 0.0012 + 0.0111i & -0.0003 & -0.0009 - 0.2304i \\ -0.0008 - 0.0004i & -0.0009 + 0.2304i & 0.9155 \end{pmatrix}, \quad (4.170)$$

$$Y_\nu = 10^{-2} \cdot \begin{pmatrix} -0.7743 & 0.5374 + 0.1348i & -0.3379 - 0.0049i \\ 0.5374 - 0.1348i & 1.1586 & -0.3979 + 2.8068i \\ -0.3379 + 0.0049i & -0.3979 - 2.8068i & -6.4066 \end{pmatrix}, \quad (4.171)$$

$$M_\nu = 10^{-2} \cdot \begin{pmatrix} -0.5269 + 0.0i & 0.3628 + 0.0090i & -0.0434 - 0.0446i \\ 0.3628 + 0.0090i & 0.7407 - 0.0058i & -0.3755 - 2.417i \\ -0.0434 - 0.0446i & -0.3755 - 2.4168i & -2.9181 + 2.0125i \end{pmatrix} eV. \quad (4.172)$$

As we have said from the Yukawa coupling we predicts the observables in the neutrino sector and this gives  $\chi^2 = 0.33$ , moreover using the See-Saw Type I formula we obtain for the light neutrino masses:

$$M_{\nu_R} = 10^{13} \cdot \begin{pmatrix} -0.0354 & 0.0246 & -0.0154 \\ 0.0246 & 0.0467 & -0.0182 \\ -0.0154 & -0.0182 & 1.6650 \end{pmatrix} GeV. \quad (4.173)$$

Moreover, the three associated eigenvalues are given in tab:benchmark. Finally, we note that the heaviest right-handed neutrino mass is given by  $1.6 \times 10^{13}$  GeV. This is lower than the lowest intermediate scale  $M_1$  and thus consistent with proton decay measurement.

# Leptogenesis

One of the crucial questions that Standard Model does not answer in a satisfying manner is why there is more matter than antimatter. In principle during matter formation both antimatter and matter should have been produced with the same rate except for quantum fluctuations. This fails to explain the observed value of matter-antimatter asymmetry which is  $\eta_B = 6.15 \times 10^{-9}$  [86] where  $\eta_B = \frac{n_b - n_{\bar{b}}}{n_\gamma}$ . This is approximately nine orders of magnitude bigger than the results obtained assuming the origin of this asymmetry to be caused just by random fluctuations. In this chapter we are going to study a mechanism that could explain this asymmetry and we are going to see how to embed it on  $SO(10)$ .

## 5.1 Sakharov conditions

There are three main conditions that a model need to satisfies to predict baryogenesis. [87] These are baryon number violation, CP violation, and that a baryon asymmetry can only be generated by an out of equilibrium process.

### Baryon number violation

The first condition is trivial. If a process conserve baryon number then it would not be possible generate an asymmetric production of baryons and antibaryons. Standard Model is featured by an accidental  $B$  symmetry that can be violated at 1-loop by triangle anomalies. Indeed there are some model of baryogenesis built upon Standard Model as electroweak baryogenesis. We are going to study

leptogenesis, in such a case a lepton asymmetry is first generated and then it is converted into a baryon asymmetry due to a sphaleron process as we are going to see later.

## CP violation

We have studied in the first chapter CP violation in the Standard Model. In the quark sector CP violation comes from  $\delta_q \neq n2\pi$ . We are particularly interested in leptonic CP violation that is originated by three phases:  $\delta, a_1$  and  $a_2$ . These are respectively the Dirac and the two Majorana phases. The first phase is found experimentally by studying neutrino oscillations while the others mainly via  $0\nu\beta\beta$  decay experiments. let us consider a toy model in which a scalar  $X$  decays into two fermions  $\psi$  and  $\bar{\chi}$ :

$$X \rightarrow \psi + \bar{\chi}, \quad (5.1)$$

we want to compute the asymmetry between the production of  $\psi$  and its antiparticle. If we consider the charge conjugated process we obtain the production of  $\bar{\psi}$  with the momentum going in the opposite direction and therefore we need to perform an additional  $P$  transformation. Therefore the production rate of the asymmetry is proportional to the difference between the decay rate and the  $CP$ -transformed corresponding one

$$\frac{d(n_\psi - n_{\bar{\psi}})}{dt} \propto \Gamma_X - \bar{\Gamma}_{\bar{\chi}}. \quad (5.2)$$

Therefore a  $CP$  invariant model cannot generate successfully a baryon asymmetry.

## Non-equilibrium process

Finally let us assume we have  $CP$ -violating ( $CPV$ ) process that violates also baryon asymmetry. For computing the asymmetry we need to consider also the inverse process that might wash out the asymmetry. When we are in thermal equilibrium we have in general

$$\Gamma\{X \rightarrow \psi + \bar{\chi}\} = \Gamma\{\psi + \bar{\chi} \rightarrow X\}. \quad (5.3)$$

Continuing our example we see that even if  $X$  decays and produces a  $\psi$  asymmetry, this is cancelled by the inverse process and the overall  $\psi$  production is zero. Therefore for the production of an asymmetry we need to consider out of equilibrium processes. let us now apply these conditions to the theory of leptogenesis.

## 5.2 Lepton asymmetry

In leptogenesis the baryon asymmetry is generated from a lepton asymmetry generated by the decay of the right handed neutrino which is then converted into a baryon asymmetry by a non-perturbative mechanism, the sphaleron. The ingredients of our model are  $N$ , the right-handed neutrino,  $\Phi$  an Higgs boson and  $l$ , a generic lepton. The lagrangian of the theory is the seesaw type I lagrangian in which  $N$  couples to  $l$  with a Yukawa coupling mediated by  $\Phi$ :

$$\mathcal{L} = Y_\nu \Phi \bar{\nu}_L N_R + M_R \nu_R^T \mathcal{C} \nu_R + \text{h.c.} \quad (5.4)$$

The right-handed neutrino decays and violates lepton number \*:

$$N \rightarrow \bar{\Phi} + l. \quad (5.5)$$

Let us compute the lepton asymmetry generated from this decay in terms of the Yukawa coupling that can be defined as

$$\epsilon_1 = \frac{\Gamma\{N \rightarrow l + \bar{\Phi}\} - \Gamma\{N \rightarrow \bar{l} + \Phi\}}{\Gamma\{N \rightarrow l + \bar{\Phi}\} + \Gamma\{N \rightarrow \bar{l} + \Phi\}}. \quad (5.6)$$

The relevant part of the decay rate we need to compute is the square of the scattering amplitude  $|\mathcal{M}_{\{N \rightarrow l + \bar{\Phi}\}}|^2$ . It is trivial to prove that at three level this quantity is always zero. The scattering amplitude is equal to  $Y_D^2$  for both the decay terms and therefore the difference is zero. The leading order at which we can compute the lepton asymmetry from CP violation is at 1-loop. Looking at Fig. 5.1 there

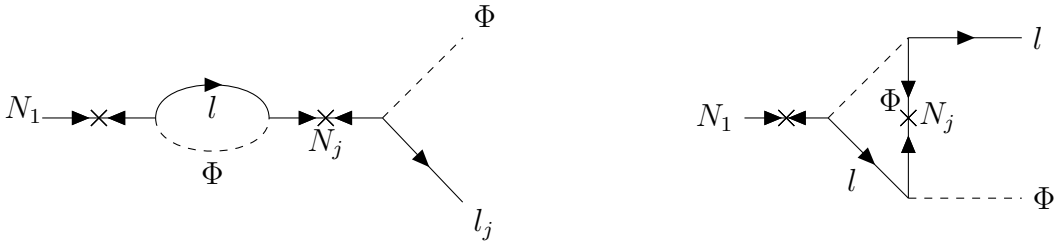


Figure 5.1: Left: Self-energy Feynman diagram. Right: Wave function renormalization Feynman diagram.

are two contributes to the lepton asymmetry, the self-energy diagram and the wave

---

\*The right-handed neutrino is a SM singlet and does not count as a lepton

function renormalization diagram. A lengthy but rather straightforward computation of the Feynman diagrams gives for the asymmetry the following expression [88]:

$$\epsilon_1 = \frac{1}{8\pi} \left[ \sum_k \frac{\text{Im}[(Y_\nu^\dagger Y_\nu)_{k1}^2]}{(Y_\nu^\dagger Y_\nu)_{11}} g\left(\frac{M_k^2}{M_1^2}\right) \right], \quad (5.7)$$

where  $g(x) = \sqrt{x}(1 - (1+x)\ln[(1+x)/x])$ . Here we have considered only the contribution from  $N_1$  and we didn't take account of flavour effects.

### 5.3 Boltzmann equation and $N_1$ -leptogenesis

We have found a  $CP$ -violating process which violates lepton number. Let us study how it generates a lepton asymmetry in a realistic situation and let us compute  $N_L$ . A lepton asymmetry is generated in the early universe with  $T \sim M_{N_1}$  in the most simple case.

#### Boltzmann equation

The Boltzmann equation describes the behaviour of the phase space distribution function  $f(x, p)$  in a non-equilibrium situation [89]. It is stated as

$$L[f] = C[f]. \quad (5.8)$$

The left hand side is the Liouville operator and is defined in a generic curved spacetime as

$$\mathbf{L} = p^\alpha \frac{\partial}{\partial x^\alpha} - \Gamma_{\beta\gamma}^\alpha p^\beta p^\gamma \frac{\partial}{\partial p^\alpha}. \quad (5.9)$$

Since the lepton asymmetry is generated in an expanding universe we are interested in the FRW metric which we shall study in the next chapter. In this case the Liouville operator becomes

$$L[f] = E \frac{\partial f}{\partial t} - \frac{\dot{a}}{a} |\mathbf{p}^2| \frac{\partial f}{\partial E}. \quad (5.10)$$

The number density of a particle species can be determined by its phase space distribution function

$$n(t) = \frac{g}{2\pi^3} \int d^3p f(E, t), \quad (5.11)$$

where  $g$  is the number of degrees of freedom of the particle we are studying. Using Eq. 5.10 we obtain

$$\frac{dn}{dt} + 3\frac{\dot{a}}{a}n = -\frac{g}{2\pi^3} \int C[f] \frac{d^3p}{E}. \quad (5.12)$$

Let us focus on the right handed term, in which  $C[f]$  is called the collision factor. If we want to study how the number density of a particle  $\psi$  is affected by a generic process:  $\psi + a + b + \dots \iff i + j + \dots$  the collision operator is given by [89]

$$\begin{aligned} \frac{g}{2\pi^3} \int C[f] \frac{d^3p_\psi}{E_\psi} &= - \int d\Pi_\psi d\Pi_a d\Pi_b \dots d\Pi_i d\Pi_j \dots \\ &\times (2\pi^4) \delta^4(p_\psi + p_a + p_b + \dots - p_i - p_j - \dots) \\ &\times [|\mathcal{M}|_{\psi+a+b+\dots \rightarrow i+j+\dots}^2 f_a f_b \dots f_\psi (1 \pm f_i)(1 \pm f_j) \\ &\cdot - |\mathcal{M}|_{i+j+\dots \rightarrow \psi+a+b+\dots}^2 f_i f_j (1 \pm f_a)(1 \pm f_b) \dots (1 \pm f_\psi)], \end{aligned} \quad (5.13)$$

where we have used  $d\Pi = \frac{g}{2\pi^3} \frac{d^3p}{2E}$ . There are three RHN, for the moment we do not consider  $N_2$  and  $N_3$  assuming  $M_{N_3}, M_{N_2} \gg M_{N_1}$ . The fact that with hierarchical RHN we can neglect the contribute of the heavier neutrino will be justified later. Therefore, the process we need to consider is  $N_1 \longleftrightarrow l + \bar{\Phi}$ . We need two equation: one for the number density of  $N_1$  and one for  $B - L$  asymmetry which is the equivalent of using lepton asymmetry since in this situation there are no baryon number violating processes, indeed in this case we have  $n_{B-L} = -n_L$ . Following [89] we assume to be in kinetical equilibrium and thus assume the phase space distribution function to be

$$f = \frac{n}{n^{eq}} f^{eq} = \frac{n}{n^{eq}} e^{-E/T}. \quad (5.14)$$

In such a case, respectively for  $N_1$  and  $B - L$ , Eq. 5.12 becomes

$$\dot{n}_{N_1} + 3Hn_{N_1} = \left( \frac{n_{N_1}}{n_{N_1}^{eq}} - 1 \right) (\gamma_D + \gamma_{H_t} + \gamma_{H_s}), \quad (5.15)$$

$$\dot{n}_{B-L} + 3Hn_{B-L} = \epsilon \left[ \frac{n_{N_1}}{n_{N_1}^{eq}} - 1 \right] \gamma_D - \frac{n_{B-L}}{n_l^{eq}} \left[ \gamma_N + \frac{n_{N_1}}{n_{N_1}^{eq}} \gamma_{H_s} + \gamma_{H_t} \right], \quad (5.16)$$

where  $\gamma$  is related to the thermal averaged decay rate as

$$\gamma = n^{eq} \Gamma, \quad (5.17)$$

and the thermal averaged decay rate is related to the zero temperature decay rate using [?]

$$\Gamma(m/T) = \tilde{\Gamma} \frac{K_1(m/T)}{K_2(m/T)}, \quad (5.18)$$

where  $\tilde{\Gamma}$  is the decay rate at  $T = 0$ . The subscripts indicate all the process considered for the lepton asymmetry generation. Indeed the decay of  $N_1$  is not the only one that generates a lepton asymmetry. There are also  $\Delta L = 1$  scattering in the  $s$ -channel and in the  $t$ -channel and  $\Delta L = 2$  scattering. It is important also to consider the second term in the right hand side of the second equation. This term describe the washout effect on the lepton asymmetry given by the inverse decay of  $N_1$  and it is of particular importance for a quantitative description of the process, indeed there can be different cases in which this term may be or may be not in equilibrium. Before of doing that we can rewrite Eq. 5.16 in a more compact way following the conventional notation used, for example, in Ref. [90] and [91]. It is convenient to use instead of  $n$ , the number of particle per comoving frame which contains one photon at the time  $t_*$  in which the leptogenesis starts to happen, that is [92]

$$N = nR_*^3(t), \quad R_*(t_*) = (n_\gamma^e q(t_*))^{-\frac{1}{3}}. \quad (5.19)$$

Moreover, let us introduce  $z = M_1/T$  and describe the evolution of the system in terms of the temperature, the new equations are then [91] [90]

$$\frac{dN_{N_1}}{dz} = -(D + S)(N_{N_1} - N_{N_1}^{eq}), \quad (5.20)$$

$$\frac{dN_{B-L}}{dz} = -\epsilon_1 D(N_{N_1} - N_{N_1}^{eq}) - W N_{B-L}, \quad (5.21)$$

where we have called  $D = \frac{\Gamma_D(z)}{Hz}$  the decay rate, and with the same convention we have called  $S$  all the scattering terms and  $W$  the washout term.

## Analytic approximations, weak and strong washout

As we have already said the inverse decays produces a washout of the lepton asymmetry. This washout can be quantified by introducing the parameter

$$K \equiv \frac{\Gamma_D(z = \infty)}{H(z = 1)}, \quad (5.22)$$

where we can regard as the numerator simply as the decay rate at zero temperature of  $N_1$ . The decay rate can be written as [90]

$$\Gamma_D = \frac{1}{8\pi}(Y_\nu Y_\nu^\dagger)_{11}M_1. \quad (5.23)$$

We can introduce the effective neutrino mass

$$\tilde{m}_1 = \frac{(Y_\nu Y_\nu^\dagger)_{11}}{v^2 M_1} \quad (5.24)$$

to relate better the washout parameter with the neutrino mass. In such a case we can rewritten  $K$  as

$$K = \frac{\tilde{m}_1}{m_*}, \quad (5.25)$$

where  $m_* \sim 1.08 \times 10^{-3}$  eV and it is the equilibrium neutrino mass.

The solution to the Boltzmann equation for  $N_{B-L}$  is [91]

$$N_{B-L}(z) = N_{B-L}^i e^{-\int_{z_i}^z dz' W(z')} - \frac{3}{4}\epsilon_1 \kappa(z). \quad (5.26)$$

The first term takes account for the contribution of an eventual initial  $B-L$  asymmetry that is being washed out by inverse decays. The second term is proportional to  $\epsilon_1$  and to a function  $\kappa(z)$  which is called efficiency factor. The behaviour of this function depend on  $K$  and we are going to study carefully some particular cases that can be studied analytically. The exact integral expression for the efficiency factor is [91]

$$\kappa(z) = -\frac{4}{3} \int_{z_i}^z dz' \frac{D}{D+S} \frac{dN_{N_1}}{dz'} e^{-\int_{z'}^z dz'' W(z'')}. \quad (5.27)$$

In order to understand better the dynamics of the generation of the lepton asymmetry is better to do not consider scatterings but only decays and inverse decays. We have thus

$$\kappa(z) = \frac{4}{3} \int_{z_i}^z dz' \frac{dN_{N_1}}{dz'} e^{-\int_{z'}^z dz'' W(z'')}. \quad (5.28)$$

Using Eq. 5.18 we can write the explicit expressions in terms of the Bessel functions

$$D = \frac{K_1(z)}{K_2(z)} z K, \quad W = \frac{1}{4} K z^3 K_1(z). \quad (5.29)$$

We can use an analytical approximation for the Bessel functions and plug it in 5.29, we find

$$D \simeq K \frac{z^2}{\frac{15}{8} + z}, \quad W \simeq K \frac{1}{4} z^2 \sqrt{1 + \frac{\pi}{2}} z e^{-z}. \quad (5.30)$$

Let us call  $T_d$  the temperature at which decays start enter into equilibrium, it corresponds to the condition  $\Gamma_D(z_d)/Hz_d = 2$ . This gives us an expression for  $z_d \equiv \frac{M_1}{T_d} \simeq \sqrt{2/K}$  for  $K \ll 1$  and  $z_d \simeq (15/4K)^{\frac{1}{3}}$  for  $K \gg 1$ . The inverse decays enter in equilibrium when  $W \geq 1$ . The maximum value of  $W$  is for  $T \equiv T_{max}$  and is  $W \simeq 0.3K$ . This is the reason of why we called  $K$  the washout parameter. When  $K$  is large inverse decays enters in equilibrium and wash out an eventual initial asymmetry, when it is small, in particular for  $K \leq 3$  inverse decays never enters in equilibrium and a initial asymmetry survives to the process. The two cases are called respectively strong and weak washout and they depend exclusively on the parameter  $K$ . For  $K \ll 1$  the we have that decays enters in equilibrium at small temperature since from the earlier discussion we find  $z_d \gg 1$ . In the expression for the efficiency factor  $W$  can be neglected and one finds

$$\kappa(z) = \frac{4}{3}(N_1^i - N_1). \quad (5.31)$$

The  $B - L$  asymmetry then depends only on the initial condition

$$N_{B-L} \sim N_{B-L}^i - \epsilon_1(N_1^i - N_1). \quad (5.32)$$

Therefore the weak washout regime is not a very predictive model. It is more predictive instead the strong washout regime in which an initial abundance of  $N_1$  is completely washed out and therefore does not need to be assumed.

## Dynamical initial abundance of $N_1$

A better way to proceed is assuming  $N_{N_1}^i = N_{B-L}^i = 0$  and compute  $N_{N_1}$  abundance directly from the Boltzmann equation considering the contributes of decays and inverse decays. Let us first define  $z_{eq}$  the time in which the abundance of  $N_1$  is the same as if it was in equilibrium

$$N_{N_1}(z_{eq}) = N_{N_1}^{eq}(z_{eq}). \quad (5.33)$$

Let us first solve the first of the Boltzmann equation for  $z \leq z_{eq}$ . In the case of strong washout,  $K \gg 1$  we have that  $z_{eq} \sim z_d \sim (6/K)^{\frac{1}{3}}$  and the solution for  $z \ll z_{eq}$  is

$$N_{N_1}(z) = \frac{3}{4} \left( 1 - e^{\frac{1}{6}Kz^3} \right). \quad (5.34)$$

The inverse decays enter in equilibrium in the interval  $z_{in} < z < z_{out}$  where  $z_{in} \sim 2/\sqrt{K}$ . For  $z < z_{eq}$  the decays are not in equilibrium and therefore the abundance of  $N_{N_1}$  differs from the equilibrium abundance. In this case the efficiency factor is given by

$$\kappa(z) \simeq \frac{2K}{75} z^5. \quad (5.35)$$

We are interested in computing  $N_{B-L}$  in the limit  $z \rightarrow 0$  and therefore we want the asymptotic behaviour of  $\kappa(z)$  for  $z \leq z_{eq}$ . Using the first of the Boltzmann equation and noticing that now decays keeps  $N_{N_1}$  near the equilibrium abundance we have at first order in  $1/K$

$$\frac{dN_{N_1}^{eq}}{dz} = -\frac{3}{2Kz} W_{ID}(z). \quad (5.36)$$

The efficiency factor for  $z > z_{eq}$  becomes then

$$\begin{aligned} \kappa(z) &= \frac{2}{K} \int_{z_i}^z dz' \frac{1}{z'} W_{ID}(z') e^{-\int_z^{z'} dz'' W_{ID}(z'')} \\ &\equiv \int_{z_i}^z dz' e^{-\psi(z', z)}. \end{aligned} \quad (5.37)$$

The main contribute to this integral is around the region in which  $\psi(z', z)$  has a minimum, that we call  $z_B$ . The condition from which we can find  $z_B$  is

$$W_{ID}(z_B) = \frac{K_2(z)}{K_1(z)}(z_B) - \frac{3}{z_B}. \quad (5.38)$$

We can see that for  $K \gg 1$  we have also  $z_B \gg 1$  and this implies  $W_{ID}(z_B) \sim 1$ . Therefore when  $z$  starts to approach  $z_B$ ,  $W_{ID}$  approaches 1 from above and that means that inverse decays goes out from equilibrium for  $z > z_B$ , in other words this means that  $z_B \sim z_{out}$ . The analytic approximation of the efficiency factor in the strong washout regime for  $z > z_d$  is

$$\kappa(z) \simeq \frac{2}{K\bar{z}} \left( 1 - e^{-\int_{z_i}^z dz' W_{ID}(z')} \right), \quad \bar{z} = \min\{z, z_B\}, \quad (5.39)$$

and we can notice it become constant as soon as  $W_{ID}$  becomes negligible therefore for  $z > z_B$ . We say that the efficiency factor freeze out at  $z \sim z_B$  and we have for  $K \gg 1$

$$\kappa(z_B) = \kappa_f(\infty) \simeq \frac{2}{z_B(K)K}, \quad (5.40)$$

where [91] [90]

$$z_B(K) \simeq \frac{1}{2} \ln \left( 1 + \left[ \ln \left( \frac{3125K^2}{1024} \right) \right]^5 \right). \quad (5.41)$$

In the weak washout regime, instead, we have that  $z_{eq} \gg 1$ . We have

$$N_{N_1}(z_{eq}) \simeq \frac{9\pi}{16} K \equiv N(K). \quad (5.42)$$

For  $z > z_{eq}$  decays dominate and wash out is exponentially suppressed and thus can be neglected. The efficiency factor is  $\kappa(z) = \kappa^+(z) + \kappa(z)^-$  where

$$\kappa^-(z) = -2(1 - e^{-\frac{2}{3}N(K)}), \quad (5.43)$$

$$\kappa^+(z) = \frac{4}{3}(N(K) - N_{N_1}(z)). \quad (5.44)$$

For  $z \gg 1$  the asymptotic value of the efficiency factor is zero in such a rough approximation. We need to consider washout for  $z < z_{eq}$  that produce an abundance of  $N_1$  and we have

$$\kappa_f(\infty) \simeq \frac{9\pi^2}{64} K^2. \quad (5.45)$$

Keeping in mind the expression of  $N_{B-L}$  of Eq. 5.26 we have

$$N_{B-L}(\infty) = -\frac{3}{4}\epsilon_1\kappa_f(\infty). \quad (5.46)$$

In order to compute the baryon asymmetry we just need to see how this  $B - L$  asymmetry is converted into a baryon asymmetry via a sphaleron process.

## 5.4 Sphalerons

The lepton asymmetry generated by the decay of  $N$  is converted into a baryon asymmetry during the electroweak phase transition at temperature around  $T = 100 - 300$  GeV. [93] This happen because of a non-perturbative process called sphalerons. In the Standard Model both  $B$  and  $L$  symmetry are accidentally conserved at tree level. Due to anomalies the asymmetry  $B + L$  is violated while  $B - L$  is conserved due to anomalies cancellation. Due to  $B - L$  conservation one could promote this symmetry into a gauge symmetry and extend Standard Model with an extra  $U(1)$  symmetry.

## The vacuum structure of a non-abelian gauge theory

Let us take a vacuum configuration in which we have  $F_{\mu\nu} = 0$ . This implies, in general, the vector potential to have the following configuration

$$A_0 = 0, \quad A_i = \frac{i}{g}(\partial_i \mathbf{U})\mathbf{U}^{-1}. \quad (5.47)$$

The converse instead, does not necessarily hold, and therefore even if the vector potential assumes a pure gauge configuration this still implies that has observable consequences and that  $F_{\mu\nu} \neq 0$ . This is due to the non trivial topology of the vacuum of a non abelian theory.

We can define the winding number to be [94]

$$m = \int \text{Tr} (\epsilon^{ijk} (\partial_i \mathbf{U})\mathbf{U}^{-1} (\partial_j \mathbf{U})\mathbf{U}^{-1} (\partial_k \mathbf{U})\mathbf{U}^{-1}) d^3x. \quad (5.48)$$

It can be proven that it is invariant if we transform continuously  $\mathbf{U}$  and that it is a integer. This makes  $m$  a topological invariant and we can decompose  $\mathbf{U}(x)$  in homotopy classes. Two matrices belong to the same homotopy class if one can be obtained from a continuous transformation of the other, therefore they are characterized by the same winding number. Therefore there are many vacuum configurations each one characterized by a different vacuum number. A vacuum transition can happen either via tunnel effects at  $T = 0$  via an instanton process or at higher temperature via a sphaleron process. Let us now look at the consequences of this vacuum transition.

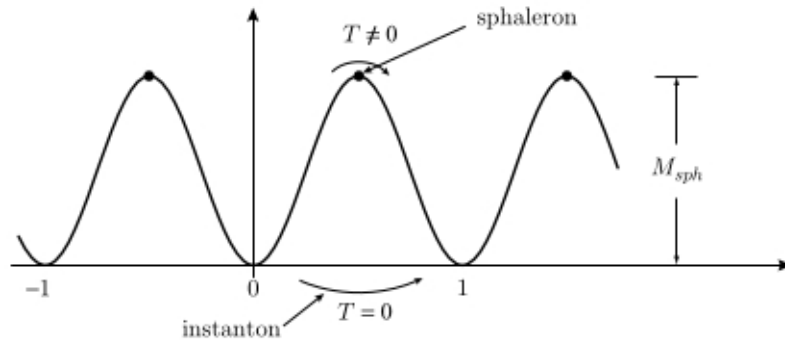


Figure 5.2: Different vacuum corresponds to different winding numbers. The transition can happen either via instantons or sphalerons. Picture taken from [94].

## Anomalies and fermion number violation

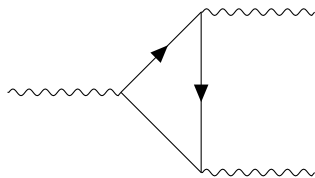


Figure 5.3: Feynman diagram of the triangle loop anomaly.

An anomaly is a symmetry at classical level which gets broken by quantum effects. The Standard Model is characterized by the chiral anomaly which violates  $B$  and  $L$  at quantum level. Such an anomaly can be studied equivalently non-perturbatively using path integrals or with Feynman diagrams, computing the so-called triangle loops of Fig. 5.3. Even if we are only at 1-loop level the results obtained computing this loops is the exact one. Due to the non-perturbative origin of this anomaly there is a link between the vacuum structure and this anomaly. At classical level we have

$$\partial_\mu J_{L(R)}^\mu = 0, \quad (5.49)$$

where  $J_\mu = \bar{\psi}\gamma_\mu\psi$ . From computing the triangle loop one obtain for an  $SU(2)$  gauge theory

$$\partial_\mu J_L^\mu = -\frac{g^2}{16\pi} \text{Tr} \left( F\tilde{F} \right), \quad (5.50)$$

where  $F_{\mu\nu} = \tilde{\epsilon}^{\mu\nu\rho\sigma} F_{\rho\sigma}$ . If we consider two configurations with different winding number we obtain

$$\int \text{Tr}(F\tilde{F})d^4x = \frac{16\pi^2}{g^2} \Delta m. \quad (5.51)$$

Therefore a topological vacuum transition implies a finite value for  $\text{Tr}(F\tilde{F})$  and therefore a fermion number violation.

## Baryon asymmetry from sphalerons

From what we have seen before a vacuum transition implies a  $B+L$  violation. Such a transformation needs to satisfies charge, color and energy conservation. Therefore this process generates  $u_l d_l d_l \nu_L$  for each generation out of vacuum. This conversion happens at temperature between 100 and 300 GeV and therefore electroweak interactions are still in equilibrium and keep the system in chemical equilibrium. This

implies that the total chemical potential of the incoming particles is the same as the chemical potential of the outgoing particles. Therefore, we obtain

$$3(\mu_{u_L} + 2\mu_{d_L}) + \sum_i \mu_i = 0, \quad (5.52)$$

where  $\mu_{u_L}$  and  $\mu_{d_L}$  are respectively the chemical potentials of the up and down quark while  $\mu_i$  is the chemical potential of the neutrino of the  $i$ -th generation. In order to proceed computing the baryon asymmetry we need to express the relevant quantities in terms of the chemical potentials. We obtain for the baryon and lepton number and charge operator[93]

$$B = 3(\mu_{u_L} + \mu_{u_R}) + 3(\mu_{d_L} + \mu_{d_R}), \quad (5.53)$$

$$L = \sum_i (\mu_i + \mu_{i_L} + \mu_{i_R}), \quad (5.54)$$

$$Q = 6(\mu_{u_L} + \mu_{u_R}) - 3(\mu_{d_L} + \mu_{d_R}). \quad (5.55)$$

Rewriting everything in terms of  $\mu_W$ , the chemical potential of the  $W$  bosons, setting  $\mu_W = 0$  and  $Q = 0$  we have

$$B = 12\mu_{u_L}, \quad L = -\frac{223}{7}\mu_{u_L}. \quad (5.56)$$

This relation implies

$$N_B = \frac{27}{89}N_{B-L} \equiv a_{sph}N_{B-L}. \quad (5.57)$$

From the last section we have seen how to obtain  $N_{B-L}$  in terms of the asymmetry  $\epsilon_1$  and the efficiency factor. Our goal is to compare our predictions with the value  $\eta_B$  of the baryon asymmetry observed during the recombination time which is  $\eta_B = 6.1 \pm 0.1$  [86]. In terms of the efficiency factor  $\kappa_f$  and the asymmetry  $\epsilon_1$  which we have computed in the last section such quantity can be expressed as

$$\eta_B = \frac{3}{4} \frac{a_{sph}}{f} \epsilon_1 \kappa_f, \quad (5.58)$$

where the factor  $f$  is the dilution factor which takes account of the photon production from the onset time of leptogenesis from which we have defined our comoving volume and the recombination time from when the baryon asymmetry was measured, this value is  $f = \frac{N_\gamma^{\text{rec}}}{N_\gamma^*}$ .

This is the starting point for a meaningful computation of the baryon asymmetry and of course in this discussion many approximations were used, but this is in any

case the main structure of the equation for  $\eta_B$  and we only need to correct it with a more detailed discussion the asymmetry  $\epsilon_1$  and the efficiency factor. In the first instance, the efficiency factor can be solved for any  $K$  numerically, we can take account for flavour and see if also the heavier right handed neutrino contributed to the baryon asymmetry. We will address this further questions going towards a more realistic model in the next section.

## 5.5 Realistic models of leptogenesis

So far, we have studied the simplest of the leptogenesis model, the  $N_1$ -leptogenesis. The main drawbacks of such treatment is that it does not account for flavour, we cannot know if the other heavy neutrinos,  $N_2$  and  $N_3$  contributes to the lepton asymmetry but also the fact that the Boltzmann equation are classical and we neglect quantum effects. Regarding this last topic there is a broad range of quantum phenomena that may affect leptogenesis at a quantum level such as memory effects, phantom effects but in particular the fact that the process happen at finite temperature [95, 96, 97]. An alternative approach to classical Boltzmann equation is to start from first principles with the Kadanoff-Baym equations [98] and then solve them. In the strong washout regime this approach gives approximately the same results of the Boltzmann equation [99] and therefore in this section we are going to study only flavour effects [100, 101, 102] and contribution from the heavier RHN [103].

### Flavour effects and density matrix equations

Until now we did not consider flavour and we treat decays of  $N_1$  to leptons without distinguish between electrons, muons and tauons. This is correct if the temperature at which the process happen is higher than the one at which Yukawa interactions between charged leptons starts getting into equilibrium. In such a case one cannot tell if a lepton is either an electron, a muon or a tauon and there is no need of distinguishing flavour. In such a case one proceed as we have done before. The interaction rate for the Yukawa interaction  $Y_{\alpha\alpha}$  is

$$\Gamma_\alpha = 5 \times 10^{-3} Y_{\alpha\alpha}^2 T. \quad (5.59)$$

The interaction for the tau is getting into equilibrium at  $T \sim 10^{12}$  GeV while for the muon we have  $T \sim 10^9$  GeV. Since the temperature at which leptogenesis happens is of the same order of magnitude of  $M_{N_1}$ , looking at the mass of the lightest RHN one can determine if considering flavour or not. The main change one needs to do is to proceed finding the asymmetry  $\epsilon_{\alpha\alpha}$  and solve the Boltzmann equation for each flavour and sum all the asymmetries only at the end. Assuming the Yukawa interactions for the flavour  $\alpha$  is perfectly in equilibrium and considering only the contribute from  $N_1$ , we proceed as done earlier in this chapter and we find [104]

$$\epsilon_{1\alpha} = \frac{1}{8\pi} \frac{1}{\left(Y_\nu^\dagger Y_\nu\right)_{11}} \sum_{j \neq 1} \Im \left[ \left(Y_\nu^\dagger Y_\nu\right)_{j1} Y_{\nu\alpha 1} Y_{\nu\alpha j}^\dagger \right] g \left( \frac{M_j^2}{M_1^2} \right), \quad (5.60)$$

where  $g(x)$  is defined as we did before <sup>†</sup>. If at this moment we sum over the flavour index  $\alpha$  we would obtain again the unflavoured asymmetry term of Eq. 5.7. In this situation lepton asymmetries evolves differently depending on the flavour and therefore we need to solve the Boltzmann equation for each flavour component. The Boltzmann equation for the flavour  $\alpha$  now is

$$\frac{N_{\Delta\alpha}}{dz} = -\epsilon_{1\alpha} D(N_{N_1} - N_{N_1}^{eq}) - W N_{\Delta\alpha}. \quad (5.61)$$

The main difference between the former case is that even if the sum of the asymmetries is zero these asymmetries evolves differently and a baryon asymmetry may still be generated.

We can still improve this model using the density matrix formalism. In the case we have considered Yukawa interactions are very fast and a charged lepton states remain the same between the production from a decay to the absorption during an inverse decay. In this case such a state can be treated as a pure states and we have an incoherent mixture of states, the flavour asymmetries  $N_{\Delta\alpha}$ .

In general we can see those asymmetries as the diagonal elements of a density matrix. The non diagonal elements of the matrix are quantum correlations and they are not negligible during an intermediate regime in which charged lepton interaction balance Yukawa interactions and the latter are not in equilibrium. For example this happen at  $T \sim 10^{12}$  GeV when there is the one-flavour to two-flavour

---

<sup>†</sup>In this case we are assuming hierarchy between heavy neutrinos and therefore we neglect resonance effects

transition [95].

In such a case the non diagonal elements quantify the interaction between the charged lepton states and the thermal bath. Let us look at an example in which only two flavours are considered that we call  $\tau$  and  $\tau^\perp$ . Following Ref. [105] Let us call respectively  $|1\rangle$  and  $|\bar{1}\rangle$  the leptons and anti-leptons quantum states produced by  $N_1$  decay.

We have that both the states are a linear superposition of flavour states <sup>‡</sup>. We have

$$|1\rangle = \sum_{\alpha} \mathcal{C}_{1\alpha} |\alpha\rangle, \quad |\bar{1}\rangle = \sum_{\alpha} \bar{\mathcal{C}}_{\bar{1}\alpha} |\bar{\alpha}\rangle. \quad (5.62)$$

When charged interaction are not in equilibrium these states propagates as coherent states and we can use the one flavour approximation. For  $T \lesssim 10^{12}$  GeV the coherence is ruined by the interaction with  $\tau$  states and  $|1\rangle$  can collapse down to either  $|\tau\rangle$  or  $|\tau^\perp\rangle$  with probability equal to, respectively  $p_{1\tau} \equiv |\mathcal{C}_{1\tau}|$  and  $p_{1\tau^\perp} \equiv |\mathcal{C}_{1\tau^\perp}|$ . In such a case we are in a two-flavour situation and we have an incoherent mixture of  $|\tau\rangle$  and  $|\tau^\perp\rangle$  states that corresponds to a diagonal density matrix. In the general case we can define also the orthogonal states to  $|1\rangle$  and  $CP|\bar{1}\rangle$ . We have

$$|1^\perp\rangle = -\mathcal{C}_{1\tau^\perp}^* |\tau\rangle + \mathcal{C}_{\infty\tau}^* |\tau^\perp\rangle, \quad CP|\bar{1}^\perp\rangle = -\bar{\mathcal{C}}_{1\tau^\perp}^* |\tau\rangle + \bar{\mathcal{C}}_{\infty\tau}^* |\tau^\perp\rangle. \quad (5.63)$$

Assuming leptons and anti-leptons are produced only trough  $N_1$  decay we define the density matrices in the basis  $l_1 - l_1^\perp$  and the corresponding CP transformed basis as

$$\rho_{ij}^l = \mathcal{P}_{ij}^{(1)} = \text{diag}(1, 0), \quad \bar{\rho}_{ij}^{\bar{l}} = \bar{\mathcal{P}}_{ij}^{(1)} = \text{diag}(1, 0). \quad (5.64)$$

The lepton number density matrix is simply defined as:  $N_{ij}^l = N^l \rho_{ij}^l$  and their evolution is given by

$$\frac{dN_{ij}^l}{dz} = \left( \frac{\Gamma_D}{Hz} N_{N_1} - \frac{\Gamma_{ID}}{Hz} N_{l_1} \right) \rho_{ij}^l, \quad \frac{dN_{ij}^{\bar{l}}}{dz} = \left( \frac{\bar{\Gamma}_D}{Hz} N_{N_1} - \frac{\bar{\Gamma}_{ID}}{Hz} N_{\bar{l}_1} \right) \bar{\rho}_{ij}^{\bar{l}}. \quad (5.65)$$

We define also  $N_{ij}^{B-L} \equiv -\left(N_{ij}^l - N_{ij}^{\bar{l}}\right)$ . In order to find an equation for  $N^{B-L}$  is convenient to rotate the matrices to the  $\tau - \tau^\perp$  basis. We introduce the rotation matrices

$$R_{\alpha i}^{(1)} = \begin{pmatrix} \mathcal{C}_{1\tau} & -\mathcal{C}_{\infty\tau^\perp}^+ \\ \mathcal{C}_{\infty\tau^\perp} & \mathcal{C}_{1\tau}^* \end{pmatrix}, \quad \bar{R}_{\alpha i}^{(1)} = \begin{pmatrix} \bar{\mathcal{C}}_{1\tau} & -\overline{\mathcal{C}_{1\tau^\perp}^*} \\ \bar{\mathcal{C}}_{1\tau^\perp} & \bar{\mathcal{C}}_{1\tau}^* \end{pmatrix}. \quad (5.66)$$

---

<sup>‡</sup>It is important to point out that due to CP violation  $CP|\bar{1}\rangle \neq |1\rangle$

The lepton density matrices in this basis are expressed in terms of the rotated projectors  $\mathcal{P}_{\alpha\beta}^{(1)} = R_{\alpha i}^{(1)} \mathcal{P}_{ij} R^{(1)\dagger}_{\beta j}$ :

$$\mathcal{P}_{\alpha\beta}^{(1)} = \begin{pmatrix} p_{1\tau} & \mathcal{C}_{\infty\tau\perp}^* \mathcal{C}_{\infty\tau} \\ \mathcal{C}_{\infty\tau\perp} \mathcal{C}_{\infty\tau}^* & p_{1\tau\perp} \end{pmatrix}, \quad (5.67)$$

in the same way we can express the projector for the antileptons.

We are going to keep account also for the scattering term and we introduce the parameter  $\Lambda$  which takes account for the charged lepton interactions. The equations for the lepton number density matrices can be written as:

$$\begin{aligned} \frac{dN_{\alpha\beta}^{\ell}}{dz} &= \frac{\Gamma_1}{Hz} N_{N_1} \mathcal{P}_{\alpha\beta}^{(1)} - \frac{1}{2} \frac{\Gamma_1^{ID}}{Hz} \{ \mathcal{P}^{(1)}, N^{\ell} \}_{\alpha\beta} + \Lambda_{\alpha\beta} + G_{\alpha\beta}, \\ \frac{dN_{\alpha\beta}^{\bar{\ell}}}{dz} &= \frac{\bar{\Gamma}_1}{Hz} N_{N_1} \bar{\mathcal{P}}_{\alpha\beta}^{(1)} - \frac{1}{2} \frac{\bar{\Gamma}_1^{ID}}{Hz} \{ \bar{\mathcal{P}}^{(1)}, N^{\bar{\ell}} \}_{\alpha\beta} + \bar{\Lambda}_{\alpha\beta} + \bar{G}_{\alpha\beta}. \end{aligned} \quad (5.68)$$

where the charged Yukawa interactions can be written as:

$$\begin{aligned} \Lambda_{\alpha\beta} &= -i \frac{\text{Re}(\Lambda\tau)}{Hz} \left[ \left( \begin{array}{cc} 1 & 0 \\ 0 & 0 \end{array} \right), N^{\ell} \right]_{\alpha\beta} - \frac{\text{Im}(\Lambda\tau)}{Hz} \begin{pmatrix} 0 & N_{\tau\tau_1^\perp}^{\ell} \\ N_{\tau_1^\perp\tau}^{\ell} & 0 \end{pmatrix}, \\ \bar{\Lambda}_{\alpha\beta} &= +i \frac{\text{Re}(\Lambda\tau)}{Hz} \left[ \left( \begin{array}{cc} 1 & 0 \\ 0 & 0 \end{array} \right), N^{\bar{\ell}} \right]_{\alpha\beta} - \frac{\text{Im}(\Lambda\tau)}{Hz} \begin{pmatrix} 0 & N_{\tau\tau_1^\perp}^{\bar{\ell}} \\ N_{\tau_1^\perp\tau}^{\bar{\ell}} & 0 \end{pmatrix}. \end{aligned} \quad (5.69)$$

and they are given by the imaginary part of the self-energy correction to the charged lepton propagators in the plasma. The first term of the  $\Lambda$  interaction is a commutator that quantifies oscillations in flavour space of the quantum lepton states while the second term keeps account for the damping of the off-diagonal terms. When  $|\Lambda| \gg 1$  we can neglect this terms and come back to the normal Boltzmann equation as we have said earlier. Finally  $G_{\alpha\beta}$  are the gauge interactions between charged leptons, they thermalize the system keeping it in kinetic and chemical equilibrium.

Now we have all the ingredients to find the density matrix equation for  $N_{B-L}$  which are

$$\frac{dN_{\alpha\beta}^{B-L}}{dz} = \varepsilon_{\alpha\beta}^{(1)} D_1 (N_{N_1} - N_{N_1}^{\text{eq}}) - \frac{1}{2} W_1 \{ \mathcal{P}^{0(1)}, N^{B-L} \}_{\alpha\beta} - \frac{\text{Im}(\Lambda\tau)}{Hz} (\sigma_1)_{\alpha\beta} N_{\alpha\beta}^{B-L}. \quad (5.70)$$

The important approximations that have been made are the suppression of the flavour oscillation due to the presence of gauge interactions. The density matrix for the lepton asymmetry is:

$$\varepsilon_{\alpha\beta}^{(1)} = \frac{3}{32\pi(Y_\nu^\dagger Y_\nu)_{11}} \sum_{j \neq 1} \left\{ i \left[ Y_{\nu\alpha 1} Y_{\nu\beta j}^* (Y_\nu^\dagger Y_\nu)_{j1} - Y_{\nu\beta 1}^* Y_{\nu\alpha j} (Y_\nu^\dagger Y_\nu)_{1j} \right] \frac{\xi(x_j/x_1)}{\sqrt{x_j/x_1}} + i \frac{2}{3(x_j/x_1 - 1)} \left[ Y_{\nu\alpha 1} Y_{\nu\beta j}^* (Y_\nu^\dagger Y_\nu)_{1j} - Y_{\nu\beta 1}^* Y_{\nu\alpha j} (Y_\nu^\dagger Y_\nu)_{j1} \right] \right\}. \quad (5.71)$$

Let us come back to the fully flavoured case and see how we can treat the washout keeping account for flavour. In this case there is a washout parameter for each flavour[?]:

$$K_{\alpha\alpha} = K \frac{Y_{\nu 1\alpha} Y_{\nu 1\alpha}^\dagger}{\sum_{\gamma | Y_{\nu 1\gamma}|} } = \left( \frac{\tilde{m}_{\alpha\alpha}}{m_*} \right). \quad (5.72)$$

The sum of the  $K_{\alpha\alpha}$  coincides with the washout parameter of the unflavoured case. One proceed solving the Boltzmann equations of 5.61 for each component  $N_{\alpha\alpha}$ , we can have situations in which all the components have strong washout, some in which all components have weak washout and some mixed situations. Once solve the equations one sum the asymmetries and then convert them into a baryon asymmetry as we have done in the last two sections. For  $T < 10^9$  GeV also the Yukawa interactions between electrons and muons enters in equilibrium and we need to repeat the same procedure but considering all the three flavours:  $\tau$ ,  $\mu$ , and  $e$ .

## Contribute of other neutrinos

We have neglected so far the contribute to leptogenesis of  $N_2$  and  $N_3$ . Important effects may arise when we consider the contributes of more right-handed neutrinos. We are going to study first the conditions on RHN masses that has to be fulfilled to neglect  $N_2$  and  $N_3$  and then what happens if the two lightest right-handed neutrino have approximately the same mass. We have seen that in the strong washout regime one can express the efficiency factor that now we are going to call  $\kappa_{f,1}$  referring to the contribute of  $N_1$  as

$$\kappa_{f,1} = \int_{z_i}^{\infty} e^{-\psi(z)} dz,$$

$$= \int_{z_B(K_1) - \Delta(K_1)}^{z_B(K_1) + \Delta(K_1)} e^{\psi'(z)} dz. \quad (5.73)$$

The main contribute to the integral is given by the region near the minimum of  $\psi(z)$ , in the interval  $(z_B(K_1) - \Delta(K_1), z_B(K_1) + \Delta(K_1))$ . We can furtherly assume the integrand to be a Gaussian centered around  $z_B(K_1)$  if  $N_2$  decays are inefficient for  $z \geq z_B(K_1) - \Delta(K_1)$ . In the case of  $N_2$  strong washout we can describe as well the efficiency factor  $\kappa_{f,2}$  as a gaussian centered around  $z_B(K_2) \frac{M_1}{M_2}$ . In such a case  $N_2$  decays and inverse decays are an independent process and because of the subsequent washout do not affect the final lepton asymmetry. Let us determine the condition on the masses  $M_{N_2}$  and  $M_{N_1}$  for which those values are separated.

Imposing a separation of  $3\sigma$  and therefore assuming  $\Delta \simeq 1.5\sigma \simeq 2$  we start from:

$$(z_B(K_2) + (K_2)) \frac{M_1}{M_2} \leq z_B(K_1) - \Delta(K_1), \quad (5.74)$$

and we obtain the following limit

$$\frac{M_{N_2}}{M_{N_1}} \geq \frac{z_B(K_2) + 2}{z_B(K_1) - 2}. \quad (5.75)$$

In the most conservative assumption with  $K_1 \sim 10$  and  $K_2 \sim 10^4$  one obtain [103]

$$M_{N_2} \geq 5M_{N_1}. \quad (5.76)$$

When the condition is satisfied one can proceed as we have done and consider only the contribute of  $N_1$ .

## 5.6 Application to our model

Now we can compute the baryon asymmetry for all the points of our scan with  $\chi^2 < 10$ . The CP violation is generated spontaneously at higher energy as we will see and we find at low energy a CP violating  $Y_\nu$ , needed for the generation of the lepton asymmetry [106, 107]. We are going to consider the contributes of all three neutrinos and use density matrix which account for flavour, even if we will not consider finite density effects and in general quantum effects becomes they are negligible in the strong washout regime which our scan seems to prefer for all the points.

### 5.6.1 Spontaneous CP violation in SO(10)

One of the assumption of our model is that above a certain scale CP symmetry holds and it is only broken spontaneously at lower scales. This happen when a singlet of  $G_2 = SU(3) \times SU(2)_L \times SU(2)_R \times U(1)_{B-L} \times z_2^C$  embedded in **45** takes an imaginary VEV. The potential of **45** without considering the interaction term with the other Higgs bosons is

$$\mathcal{V}(\Phi) = -\frac{1}{2}\mu_{45}^2 \text{Tr} \Phi^2 + \lambda_{45}^1 (\text{Tr} \Phi^2)^2 + \lambda_{45}^2 \Phi^4, \quad (5.77)$$

and assuming  $\Phi_{12}$  takes a VEV we can see that the following VEV can be pure imaginary and that it breaks D-parity. In the last chapter we defined the lightest Higgs mass eigenstate which correspond to the Standard Model Higgs as a linear combinations of the various Higgs representations

$$h_j = \{\tilde{h}_{10}^u, \tilde{h}_{126}^u, \tilde{h}_{120}^u, \tilde{h}_{120}^{u'}, h_{10}^d, h_{126}^d, h_{120}^d, h_{120}^{d'}\}, \quad (5.78)$$

with coefficients  $V_{ij}$ .

Then we can see how this CP violation appears in the term  $Y_\nu$  we need for leptogenesis starting from the expression

$$Y_\nu = Y_{10}V_{11} - \sqrt{3}Y_{126}V_{12} + Y_{120} \left( V_{13} - \sqrt{3}V_{14} \right). \quad (5.79)$$

The last two terms of the equation can be fixed to be pure imaginary from the term in the potential **45** · **10** · **120**. When **45** takes the imaginary term this can be seen as an imaginary contribute to the mass term of  $h_1$ . Indeed we can write  $h_1 = h_{10}^u + h_{120}^u + \dots$  and in the mass term we find the following term

$$V_{11}V_{13}h_{10}^u h_{120}^u, \quad (5.80)$$

but this is exactly one of the pure imaginary term which appear in the interaction potential between **10**, **120** and **45** and therefore we can set  $V_{13}$  as a pure imaginary term. We can proceed in a similar way for  $V_{14}$ ,  $V_{17}$  and  $V_{18}$  <sup>§</sup> From this it follows that  $Y_\nu$  has a CP violating phases that comes from  $V_{13}$  and  $V_{14}$  being imaginary.

---

<sup>§</sup>In the last two cases the interaction potential we need to consider in the one among **120**,  $\overline{\mathbf{126}}$  and **45**.

## 5.6.2 3DME equations

The equations we have used for computing baryon asymmetry are the density matrix equation with all three flavours. We did not do the assumption of hierarchical heavy neutrinos and we considered all the three flavours. Extending the discussion we have done earlier we have that the  $N_{B-L}$  matrix and the projector are defined as [?]

$$N^{B-L} = \begin{pmatrix} N_{\tau\tau} & N_{\tau\mu} & N_{\tau e} \\ N_{\mu\tau} & N_{\mu\mu} & N_{\mu e} \\ N_{e\tau} & N_{e\mu} & N_{ee} \end{pmatrix}, \quad \mathcal{P}^{(i)0} = \frac{1}{\left(\tilde{Y}_\nu^\dagger \tilde{Y}_\nu\right)_{ii}} \begin{pmatrix} \left|\tilde{Y}_{\nu\tau i}\right|^2 & \tilde{Y}_{\nu\tau i} \tilde{Y}_{\nu\mu i}^* & \tilde{Y}_{\nu\tau i} \tilde{Y}_{\nu e i}^* \\ \tilde{Y}_{\nu\tau i}^* \tilde{Y}_{\nu\mu i} & \left|\tilde{Y}_{\nu\mu i}\right|^2 & \tilde{Y}_{\nu\tau i}^* \tilde{Y}_{\nu e i} \\ \tilde{Y}_{\nu e i} \tilde{Y}_{\nu\tau i}^* & \tilde{Y}_{\nu\mu i} \tilde{Y}_{\nu\tau i}^* & \left|\tilde{Y}_{\nu e i}\right|^2 \end{pmatrix}. \quad (5.81)$$

The CP-asymmetry matrix, describing the decay asymmetry generated by  $N_i$  is denoted by  $\epsilon_{\alpha\beta}^{(i)}$ , and may be written this time as:

$$\begin{aligned} \epsilon_{\alpha\beta}^{(i)} = & \frac{3}{32\pi \left(\tilde{Y}_\nu^\dagger \tilde{Y}_\nu\right)_{ii}} \sum_{j \neq i} \left\{ i \left[ \tilde{Y}_{\nu\alpha i} \tilde{Y}_{\nu\beta j}^* \left(\tilde{Y}_\nu^\dagger \tilde{Y}_\nu\right)_{ji} - \tilde{Y}_{\nu\beta i}^* \tilde{Y}_{\nu\alpha j} \left(\tilde{Y}_\nu^\dagger \tilde{Y}_\nu\right)_{ij} \right] \frac{\xi(x_j/x_i)}{\sqrt{x_j/x_i}} \right. \\ & \left. + i \frac{2}{3(x_j/x_i - 1)} \left[ \tilde{Y}_{\nu\alpha i} \tilde{Y}_{\nu\beta j}^* \left(\tilde{Y}_\nu^\dagger \tilde{Y}_\nu\right)_{ij} - \tilde{Y}_{\nu\beta i}^* \tilde{Y}_{\nu\alpha j} \left(\tilde{Y}_\nu^\dagger \tilde{Y}_\nu\right)_{ji} \right] \right\}, \end{aligned} \quad (5.82)$$

where  $x_i \equiv M_{N_i}^2/M_{N_1}^2$  and Greek and Roman indices denote charged lepton flavour and right-handed neutrino generation indices, respectively, and

$$\xi(x) = \frac{2}{3}x \left[ (1+x) \ln \left( \frac{1+x}{x} \right) - \frac{2-x}{1-x} \right]. \quad (5.83)$$

Finally we can states the density matrix Boltzmann equations we have used for our model:

$$\begin{aligned} \frac{dN_{\alpha\beta}^{B-L}}{dz} = & \sum_{i=1}^3 \epsilon_{\alpha\beta}^{(i)} D_i (N_{N_i} - N_{N_i}^{\text{eq}}) - \frac{1}{2} W_i \{ \mathcal{P}^{(i)0}, N^{B-L} \}_{\alpha\beta} \\ & - \frac{\text{Im}(\Lambda_\tau)}{Hz} \left[ \begin{pmatrix} 1 & 0 & 0 \\ 0 & 0 & 0 \\ 0 & 0 & 0 \end{pmatrix}, \left[ \begin{pmatrix} 1 & 0 & 0 \\ 0 & 0 & 0 \\ 0 & 0 & 0 \end{pmatrix}, N^{B-L} \right] \right]_{\alpha\beta} \\ & - \frac{\text{Im}(\Lambda_\mu)}{Hz} \left[ \begin{pmatrix} 0 & 0 & 0 \\ 0 & 1 & 0 \\ 0 & 0 & 0 \end{pmatrix}, \left[ \begin{pmatrix} 0 & 0 & 0 \\ 0 & 1 & 0 \\ 0 & 0 & 0 \end{pmatrix}, N^{B-L} \right] \right]_{\alpha\beta}, \end{aligned}$$

where  $z = M_{N_1}/T$  is the evolution parameter,  $H$  is the Hubble expansion rate, and the decay and washout terms are given by

$$D_i(z) = K_i x_i z \frac{\mathcal{K}_1(z_i)}{\mathcal{K}_2(z_i)}, \quad W_i(z) = \frac{1}{4} K_i \sqrt{x_i} \mathcal{K}_1(z_i) z_i^3, \quad (5.84)$$

where  $z_i \equiv \sqrt{x_i} z$ ,  $\mathcal{K}_1$  and  $\mathcal{K}_2$  are modified Bessel functions of the second kind with the decay asymmetry  $K_i$  given by

$$K_i \equiv \frac{\tilde{\Gamma}_i}{H(T = M_{N_i})}, \quad \tilde{\Gamma}_i = \frac{M_{N_i} \left( \tilde{Y}_\nu^\dagger \tilde{Y}_\nu \right)_{ii}}{8\pi}, \quad (5.85)$$

respectively. The thermal widths of the charged leptons,  $\Lambda_\tau$ ,  $\Lambda_\mu$ , has been introduced earlier and are important in intermediate regime in which the fully flavoured approximation does not hold.

### 5.6.3 Results

For each point in our parameter scan, we have solved eq:DME which provides the baryon-to-photon ratio using the publicly available tool ULYSSES [109] and the associated ‘‘3DME’’ code which accounts for the decays and washout of all three right-handed neutrinos. We show our results in Fig. 5.4 where all the points have  $\chi^2 < 10$  and satisfy the proton decay bounds. We observe that for both octants, many low  $\chi^2$  points achieve thermal leptogenesis successfully, and their baryon-to-photon ratio is  $\eta_B \approx 10^{-10}$ . Interestingly, the predicted baryon-to-photon ratio shows little dependence on  $\delta$  but has a very constrained prediction for the effective Majorana mass,  $4 \lesssim m_{\beta\beta} \text{ (meV)} \lesssim 10$ . This indicates that the predicted Majorana phases are highly constrained within our model.

For all the points with  $\chi^2 < 10$ , we found leptogenesis is always in the strong washout regime  $K_1 \gg 1$  (for the benchmark point  $K_1 \approx 130$ ) since the Yukawa couplings (Eq. 4.171) are not very small. As we are in the strong washout regime, neglecting finite density effects is a good approximation [110]. For the above benchmark point, the lightest two masses of right-handed neutrinos are  $M_{N_1} = 4.23 \cdot 10^{11}$  GeV and  $M_{N_2} = 5.32 \cdot 10^{11}$  GeV and the baryon-to-photon ratio is  $\sim 6.11 \times 10^{-10}$ . Next generation  $0\nu\beta\beta$  experiments such as Legend-1000 [111], nEXO [112], NEXT-HD [113], DARWIN[114], SNO+II [115] and CUPID-Mo [116] will allow to test further test the results of our scan. The most sensitive

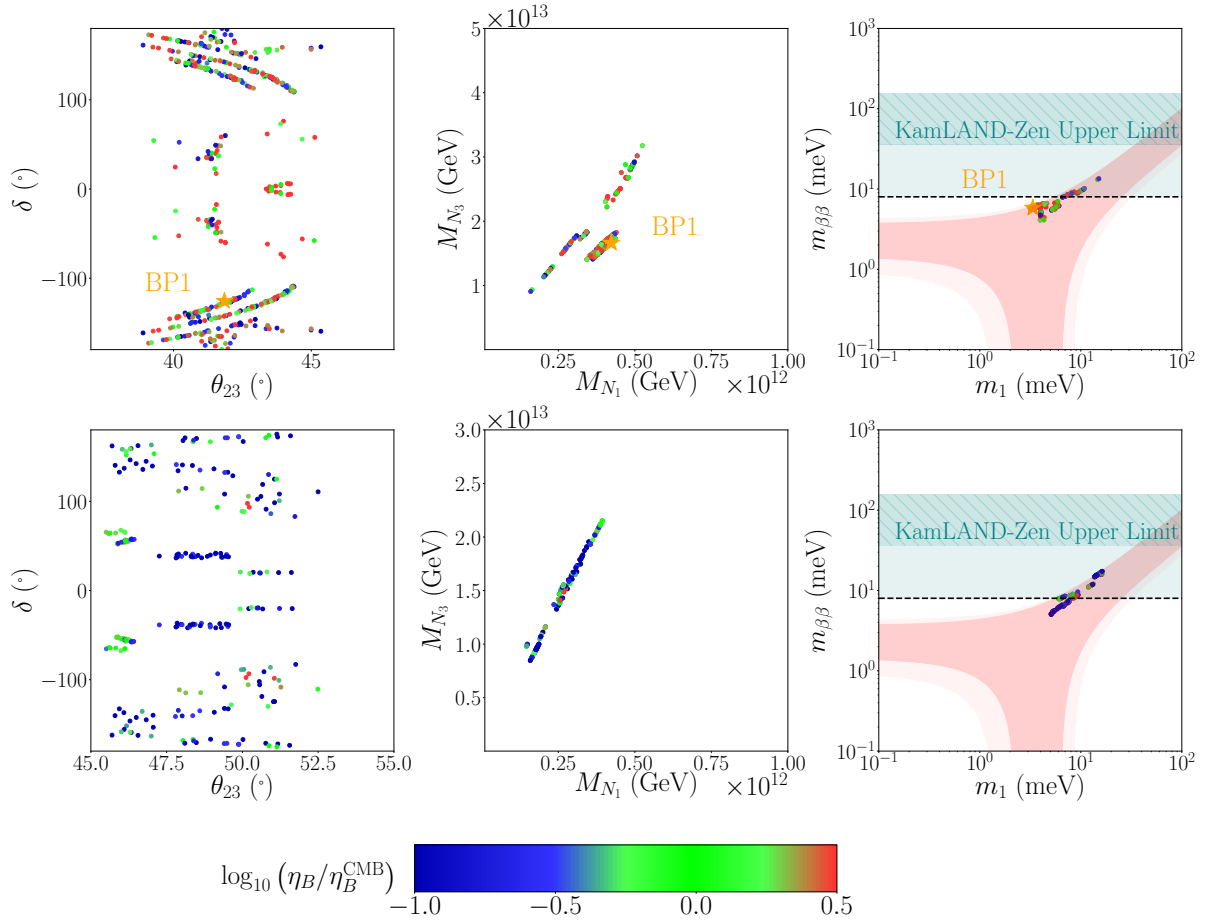


Figure 5.4: The top (bottom) left and centre panels are the two-dimensional correlations between predicted observables for  $\chi^2 < 10$  and  $\theta_{23} \leq 45^\circ$  ( $\theta_{23} \geq 45^\circ$ ). The top (bottom) rightmost panel shows the predictions for the effective neutrino mass for  $\theta_{23} \leq 45^\circ$  ( $\theta_{23} \geq 45^\circ$ ). The colour of the points denotes the ratio of the predicted baryon-to-photon ratio to the experimentally observed best-fit value as measured using CMB data  $\eta_B^{\text{CMB}} = 6.15 \times 10^{-10}$  [108]. Consistency with gauge unification is considered. In the leftmost plots, the dashed line labels the sensitivity of the next generation experiments on  $0\nu\beta\beta$  decay. The orange star is the benchmark point BP1

experiments will probe  $m_{\beta\beta}$  down to  $8 - 10\text{meV}$  which, as we can see from Fig. 5.4, covers a significant fraction of the points of our scan.

# Cosmic strings

Cosmic strings may be produced during early universe phase transitions as a particular type of topological defects during a spontaneous symmetry breaking. GUT theories predict a variety of topological defects such as domain walls and magnetic monopoles [?]. This is one of the main problems of such models since for most of the models both domain walls and magnetic monopoles becomes the dominant component in the total energy of the universe and this is not what we observe experimentally. In general one solves this problem setting a reheating scale after the inflation after the production of this topological defects so that they are washed out. A cosmic string network instead can evolve in a scaling solutions, that is with its energy density being a constant fraction of the energy density of the universe and therefore being compatible with the current cosmological observation. The main signature of this network is a stochastic gravitational wave background produced by oscillating loops of strings. In this chapter we are going to introduce the basic features of cosmic strings.

## 6.1 Topological defects and string solutions

Let us start from a toy model of a scalar theory with a  $U(1)$  gauge symmetry breaking. [?] We are going to work in cylindrical coordinates  $\{\rho, \theta, z\}$ . The lagrangian is

$$\mathcal{L} = -\frac{1}{4}F_{\mu\nu}F^{\mu\nu} + \frac{1}{2}(D_\mu\phi)^*(D_\mu\phi) - \mathcal{V}(\phi), \quad (6.1)$$

where

$$\mathcal{V}(\phi) = \frac{\lambda^2}{2}(\phi^2 - v^2)^2. \quad (6.2)$$

Instead of considering a special vacuum configuration such as simply  $\Phi = v$ , let us consider all the possible vacuum configurations. Those configurations form the so-called vacuum manifold

$$\mathcal{M}_0 = \{\phi_s : \phi_s = ve^{i\theta}, \theta \in [0, 2\pi]\}, \quad (6.3)$$

which is isomorphic to  $S^1$ . Let us now compute the linear energy density of the string

$$\frac{E}{L} = \int dS \left[ \frac{1}{2} |D_i \phi|^2 + \mathcal{V}(\phi) \right]. \quad (6.4)$$

From imposing  $\frac{E}{L}$  to be finite we conclude that

$$|\phi| \xrightarrow{\infty} v, \quad (6.5)$$

$$D_\mu \phi \xrightarrow{\infty} 0. \quad (6.6)$$

The trivial solution is when we choose  $\phi(\infty) = v$ . In this case we would have a trivial map and the linear energy density would be zero: nothing interesting happen. Another configuration at infinity might be

$$\phi_s(\infty) = ve^{i\theta}. \quad (6.7)$$

Therefore also the boundary conditions form a manifold omeomorphic to  $S^1$ . In this way  $\phi_s$  induces a non trivial map between the vacuum manifold and the boundary conditions

$$\phi_s : \mathcal{M}_0 \rightarrow \mathcal{M}_\infty. \quad (6.8)$$

In general the most general configuration is  $\phi(\infty) = ve^{in\theta}$ . In the last two configurations the linear energy is greater than zero, hence bigger than the energy of the trivial vacuum solution. It is crucial understanding why these solutions are stable. Let us write  $\phi = \phi_1 + i\phi_2$  and consider the following conserved current

$$j^\mu = \mathcal{C}\epsilon^{\mu\nu\rho} \partial_\nu \Phi_a \partial_\rho \Phi_b \epsilon_{ab}. \quad (6.9)$$

It is trivially conserved due to the presence of the Levi-Civita tensor

$$\partial_\mu j^\mu = \mathcal{C}\epsilon^{\mu\nu\rho} [\partial_\mu \partial_\nu \Phi_a \partial_\rho \Phi_b \epsilon_{ab} + \partial_\nu \Phi_a \partial_\mu \partial_\rho \Phi_b \epsilon_{ab}] = 0. \quad (6.10)$$

This implies the existence of a conserved quantity

$$Q = \int dS j^0. \quad (6.11)$$

We can write

$$j^0 = \mathcal{C}\epsilon_{ij}\epsilon_{ab} [\partial_i(\Phi_a\partial_j\Phi_b)] \equiv \mathcal{C}\epsilon_{ij}\partial_iV_j, \quad (6.12)$$

therefore the conserved charge can be written as

$$Q \oint dx_i V_i. \quad (6.13)$$

we can place the path of integration at infinity and therefore using  $\Phi_s = ve^{i\theta}$ . This implies:

$$\Phi_a = \frac{x_a}{\rho}. \quad (6.14)$$

Plugging this expression in 6.13 we obtain:

$$Q = 2\pi\mathcal{C}v^2 \equiv 1, \quad (6.15)$$

defining the arbitrary constant  $C \equiv \frac{1}{2\pi v^2}$ . For a generic configuration  $\phi_s = ve^{in\theta}$  we have  $Q = n$ . This is called topological charge and it is conserved. Therefore a solution with a certain topological configurations cannot evolve towards a different solution or towards the trivial one. The key for understanding why the string solution is stable is then the topological configuration of the solution originated by the non triviality of the fundamental group of the vacuum manifold, in this case  $S^1$ .

## Details of the string solution

From the second equation of Eq. 6.6 we can derive the expression for the gauge field at infinity

$$A_\mu = \frac{1}{g}\partial_\mu\theta. \quad (6.16)$$

This would seem simply a pure gauge and one could think of removing it with a gauge transformation. This is not the case and this is actually a physical configuration. Let us indeed compute the magnetic flux and prove it is different than zero

$$\Phi = \int d\vec{S}\vec{B} = \oint A_\mu dx^\mu = \frac{2\pi}{g}. \quad (6.17)$$

Because of the boundary condition the magnetic flux is concentrated around the origin and is captured inside a cylindrical region of width  $\delta$ . Plugging the expression of the magnetic flux in Eq. 6.4 we can find

$$\delta \simeq \frac{1}{v} \frac{1}{\sqrt{g\lambda}}. \quad (6.18)$$

The exact string solution can be written in term of two function  $f(\rho)$  and  $\alpha(\rho)$  which can be found numerically.

$$\phi_s(\rho) = e^{in\theta} f(\rho), \quad (6.19)$$

$$A_{sa}(\rho) = -\epsilon_{ab} x_b \frac{n}{e\rho^2} \alpha(\rho), \quad a, b = 1, 2. \quad (6.20)$$

## 6.2 String dynamics

The action of a gauge theory which allow string solutions is [117]

$$S = \int d^4y \sqrt{-g} |D_\mu \phi|^2 - \frac{1}{4} F_{\mu\nu} F^{\mu\nu} - \mathcal{V}(\phi). \quad (6.21)$$

where  $\mathcal{V}(\phi)$  is defined in Eq. 6.2. Our goal is to study the basic properties of a string network and we do not need the detailed description of the solutions of 6.20 We can find an effective action, an approximation of 6.21 in which the only important thing is the stringy configuration of the fields and not the details of the gauge theory. Let us derive this effective action following [117]. In the last section we have seen that the solution is concentrated around the zero of the Higgs field. The zeros of the Higgs field swept out a worldsheet on which we define the coordinate  $\zeta^0$  and  $\zeta^1$ . Let us define two tangent vectors in a certain point of the worldsheet  $x_a^\mu, a = 1, 2$  and two vectors orthogonal to these tangent vectors which we call  $\eta_\mu^A, A = 1, 2$ . These two vectors are also orthonormal:  $g^{\mu\nu} \eta_\mu^A \eta_\nu^B = 0$ . We parametrize any point  $y^\mu$  near a point of the worldsheet  $x^\mu(\zeta^\alpha)$  introducing other two radial coordinates  $\rho^A, A = 1, 2$  as

$$y^\mu(\zeta^\alpha, \rho^A) = x^\mu(\zeta) + \rho^A \eta_A^\mu(\zeta). \quad (6.22)$$

This mapping is single valued if we assume its curvature radius  $R$  to be much greater than  $\rho$  The fields solution near the worldsheet is

$$\phi(y) = \phi_s(\rho), \quad (6.23)$$

$$A^\mu(y) = n_B^\mu(\zeta) A_{sB}(\rho), \quad (6.24)$$

where  $\phi_s$  and  $A_s$  are the solution of 6.20. Now we want to change from the coordinates  $y$  to  $\xi = (\zeta^\alpha, \rho^A)$ . The jacobian is

$$\sqrt{-g} \det \left( \frac{\partial y}{\partial \xi} \right) = (-\det M_{\alpha\beta})^{\frac{1}{2}}, \quad (6.25)$$

where:

$$M_{\alpha\beta} = \left( g_{\mu\nu} \frac{\partial y^\mu}{\partial \xi^\alpha} \frac{\partial y^\nu}{\partial \xi^\beta} \right) = \text{diag}(\gamma_{ab}, -\delta_{AB}) + \mathcal{O}\left(\frac{r}{R}\right). \quad (6.26)$$

We can integrate out the perpendicular modes integrating out  $\rho^A$ ,  $A = 1, 2$  from the action 6.21. Remembering the expression for the linear energy density this give exactly  $\frac{E}{L} \equiv \mu$ . The new action is, therefore

$$S = -\mu \int d^2\zeta \sqrt{-\gamma}. \quad (6.27)$$

This is the so-called Nambu-Goto action.

The equation of motion for a string in a general metric are

$$\left( \frac{dx^\mu}{d\zeta^a} \right)_{;a} + \Gamma_{\nu\sigma}^\mu \gamma^{ab} \frac{dx^\nu}{d\zeta^a} \frac{dx^\sigma}{d\zeta^b} = 0, \quad (6.28)$$

while the energy-momentum tensor is

$$T^{\mu\nu} \sqrt{-g} = \mu \int d^2\zeta \sqrt{-\gamma} \gamma^{ab} \frac{dx^\mu}{d\zeta^a} \frac{dx^\nu}{d\zeta^b} \delta^{(4)}(x^\sigma - x^\sigma(\zeta^a)). \quad (6.29)$$

## Strings in flat spacetime

In a flat spacetime we fix  $g_{\mu\nu} = \eta_{\mu\nu}$ . The Nambu-Goto action is invariant for reparametrization of the world sheet, so that we can choose a convenient parametrization gauge fixing the coordinates. One convenient way is that of choosing the conformal gauge imposing

$$\gamma_{01} = 0, \quad \gamma_{00} + \gamma_{11} = 0, \quad (6.30)$$

and fixing  $\zeta^0 = t$  to remove the residual gauge symmetry. In this way the worldsheet metric is

$$\gamma_{ab} = \sqrt{-\gamma} \eta_{ab}. \quad (6.31)$$

We can describe the string with a three dimensional vector  $\mathbf{x}(\zeta, t)$ . The equation of motion are

$$\dot{x} \cdot x' = 0, \quad (6.32)$$

$$\dot{x}^2 + x'^2 = 0, \quad (6.33)$$

$$\ddot{x} - x'' = 0, \quad (6.34)$$

where the dot and ' means, respectively, derivative with respect to  $\zeta^0$  and  $\zeta^1$ . From the first equation we see that  $\dot{x}$  is perpendicular to the string and therefore is the transverse velocity of the string. From the second equation we can see that the most general solution to Eq. 6.34 is

$$\mathbf{x}(\zeta, t) = \frac{1}{2} [\mathbf{a}(\zeta - t)(\zeta + t) + \mathbf{b}(\zeta + t)]. \quad (6.35)$$

For the aim of this project it is interesting to study carefully the closed string solution, an oscillating loop with length  $L$  with  $0 < \zeta < L$  as boundary conditions. The condition on  $\mathbf{a}$  and  $\mathbf{b}$  are, in the loop center of mass frame of reference

$$\mathbf{a}(\zeta + L) = \mathbf{a}(\zeta), \quad \mathbf{b}(\zeta + L) = \mathbf{b}(\zeta). \quad (6.36)$$

Let us study some features of an oscillating loop [118]. If both  $\mathbf{a}$  and  $\mathbf{b}$  are continuous functions the loop is said to be smooth. This is not always the case and in general when some discontinuities are present the loop are featured by the presence of cusps and kinks. This will affect the emission of gravitational waves and therefore it is worth to give some examples.

- Let us start from noticing that in a smooth loop there is a point moving at the velocity of light. We have indeed [117]

$$\dot{x}^2(\zeta, t) = \frac{1}{4} [a'(\zeta - t) - b'(\zeta + t)]^2 \quad (6.37)$$

The constraints given by the periodicity of  $\mathbf{a}$  and  $\mathbf{b}$  are

$$\int_0^L \mathbf{a}' d\zeta = \int_0^L \mathbf{b}' d\zeta = 0. \quad (6.38)$$

If for some values of  $\zeta_a$  the two functions intersect, that is if  $\mathbf{a}'(\zeta_a) = \mathbf{b}'(\zeta_a)$  then we have  $\dot{x}^2 = 1$ , that is we have a point with luminal velocity. We can assume this point to be around  $\zeta = t = 0$  and in this case the shape of the loop around that point will be

$$x(\zeta, 0) = \frac{1}{4} (\mathbf{a}_0'' + \mathbf{b}_0'') \zeta^2 + \frac{1}{12} (\mathbf{a}_0''' + \mathbf{b}_0''') \zeta^3 + \dots \quad (6.39)$$

We can see that if  $\mathbf{a}_0'' + \mathbf{b}_0'' \neq 0$  then the loop develop what is called a *cusp*.

- When instead the two functions are discontinuous or have discontinuous derivatives we said we have a *kink*. An example is [119]

$$a(\zeta) = \begin{cases} \left(\frac{L}{2\pi}\zeta - \frac{L}{4}\right) \hat{\mathbf{u}}, & 0 \leq \zeta < \pi, \\ \left(\frac{3L}{4} - \frac{L}{2\pi}\zeta\right) \hat{\mathbf{u}}, & \pi \leq \zeta < 2\pi \end{cases}, \quad (6.40)$$

$$\mathbf{b}(\zeta) = \begin{cases} \left(\frac{L}{2\pi}\zeta - \frac{L}{4}\right) \hat{\mathbf{v}}, & 0 \leq \zeta < \pi \\ \left(\frac{3L}{4} - \frac{L}{2\pi}\zeta\right) \hat{\mathbf{v}}, & \pi \leq \zeta < 2\pi \end{cases}. \quad (6.41)$$

where  $\hat{\mathbf{u}}$  and  $\hat{\mathbf{v}}$  are arbitrary unit vectors. In such an example the loops is featured with 4 kinks. As we shall see later, in general kinks are generated when loop intersect with each other during a network evolution.

## Oscillating loop in an expanding universe

Now we can describe the dynamics of an oscillating loop in the FRW metric using the comoving time

$$ds^2 = a^2(\tau) (d\tau^2 - d\mathbf{x}^2). \quad (6.42)$$

Now we impose as gauge conditions:

$$\zeta^0 = \tau, \quad \dot{x} \cdot x' = 0. \quad (6.43)$$

From Eq. 6.20 we obtain that the equations of motion for the string now are

$$\ddot{\mathbf{x}} + 2\frac{\dot{a}}{a}(1 - \dot{\mathbf{x}}^2)\dot{\mathbf{x}} = \epsilon^{-1}(\epsilon^{-1}\mathbf{x}')', \quad (6.44)$$

$$\mathbf{x}'' \cdot \dot{\epsilon} = -2\frac{\dot{a}}{a}\epsilon\dot{\mathbf{x}}^2, \quad (6.45)$$

where

$$\epsilon = \left(\frac{\mathbf{x}'^2}{1 - \dot{\mathbf{x}}^2}\right)^{1/2}. \quad (6.46)$$

## Frictional force

In the equation of motion we have considered so far we have assumed a string moving in the vacuum. For a realistic study of the string evolution in the early universe we need to consider the motion of a string in a plasma of temperature  $T$ . We can picture the interactions between a string and the plasma as scattering between the string and

particle with momentum  $q \sim T$ . The cross section can be approximated roughly to be  $\sim T^{-1}$ .

This interaction can be modeled using a frictional force [117]

$$\mathbf{F} = n\sigma_t v_T \Delta \mathbf{P}, \quad (6.47)$$

where  $\Delta \mathbf{p}$  is the average momentum transfer per collision,  $v_T$  is the particles thermal velocity and the number density of the particles is  $n \sim T^3$  in a radiation-dominated era. This gives, in a first approximation [120]

$$\mathbf{F} \sim -T^3 \mathbf{v}. \quad (6.48)$$

With a more detailed computation in which we plug the exact cross section for a particle interaction we have

$$\sigma_t = 2q^{-1} \sin^2(\pi\nu), \quad (6.49)$$

where  $\nu$  is the phase change due to the Bohm-Aharonov effect when a particle is transported around the string. The number of particles of momentum  $k$  is

$$n_k = n_{FD/BE}(\gamma(k + \mathbf{k} \cdot \mathbf{v}/T)), \quad (6.50)$$

where  $n$  can be either a Bose-Einstein or a Fermi-Dirac distribution. The force per unit length is

$$\mathbf{F} = -\beta T^3 \gamma \mathbf{v}, \quad (6.51)$$

where

$$\beta = 2\pi^{-2} \zeta(3) \sum_a b_a \sin^2(\pi\nu_a) \quad (6.52)$$

and the sum is over the particles species. Following [121, 122] we rewrite the equation above as:

$$F^i = -\frac{\mu}{l_F} \frac{v^i}{\sqrt{1-v^2}} \quad (6.53)$$

$$l_F = \frac{\mu}{\beta T^3} \quad (6.54)$$

We have assumed  $T \gg m$ , that is massless particles. In the local frame of the string we have also  $F^0 = 0$ . Let us rewrite the equation of motion in case of a frictional force. We can rewrite the formula above in a covariant way:

$$F^\nu = \frac{\mu}{l_F} (u^\nu - x^\nu_{,a} x^{\sigma,a} u_\sigma) \quad (6.55)$$

The generalization of Eq. 6.28 are then:

$$x_{,a}^{\nu;a} + \Gamma_{\sigma\tau}^{\nu} x_{,a}^{\sigma} x^{\tau,a} = \left( \frac{1}{l_F} \right) (u^{\nu} - x_{,a}^{\nu} x^{\sigma,a} u_{\sigma}) \quad (6.56)$$

In the case of a string in an expanding universe, applying the same gauge conditions we have applied above we obtain

$$\ddot{\mathbf{x}} + \left( 2\frac{\dot{a}}{a} + \frac{a}{\ell_f} \right) (1 - \dot{\mathbf{x}}^2) \dot{\mathbf{x}} = \frac{1}{\epsilon} \left( \frac{\mathbf{x}'}{\epsilon} \right)', \quad (6.57)$$

$$\dot{\epsilon} + \left( 2\frac{\dot{a}}{a} + \frac{a}{\ell_f} \right) \dot{\mathbf{x}}^2 \epsilon = 0, \quad (6.58)$$

where  $\epsilon$  is defined as above. These are the realistic equations of motion of a string in a plasma at temperature  $T$ .

## String interactions

Before of studying how a cosmic network evolves in the early Universe we still need to understand what happens when two strings intersect. Until now we have used an effective action, the Nambu-Goto action which works only for a non interacting string. In general the equations that governs the behaviour of two intersecting strings for a simple abelian model are

$$(\partial_{\mu} - ieA_{\mu})(\partial^{\mu} - ieA^{\mu})\phi + \frac{\lambda}{2}\phi(\phi\bar{\phi} - \eta^2) = 0, \quad \partial_{\mu}F^{\mu\nu} = j^{\nu}, \quad (6.59)$$

where  $j^{\nu} \equiv 2e \text{Im} [\bar{\phi}(\partial^{\nu} - ieA^{\nu})\phi]$ . These equations has been solved numerically [117] for studying the behaviour of the interaction between two vortices. The results applied to a 3-dimensional case and thus to string interactions can be summarized in the following way. When two strings intersect there are three possibilities:

- They can reconnect, that is at the intersection points an end of a string it is separated by the other end and then reconnect with an end of the opposite string
- They do not interact. There can be indeed some kind of string for which there are topological constraints that prevent them from reconnecting
- They get entangled.

From now on we are going to assume that the kind of strings formed by our model always reconnect when they interacts. In general this can happen with probability  $p$ , for example when the network considered is generated by fundamental superstrings which

are quantum object. The probability of interconnection affect the gravitational wave background spectrum. We are going to assume  $p = 1$ : the strings always reconnect. When they do so each of the ends are moving with different velocities and then  $\mathbf{x}'(\zeta, t)$  and  $\dot{\mathbf{x}}(\zeta, t)$  rapidly vary around the point of interconnection. This forms a discontinuities and therefore a kink, which moves at the speed of light. Following the example of Eq. 6.41 the kinks generated by a discontinuity in  $\mathbf{a}'$  has velocity

$$\frac{d\mathbf{x}}{dt} = \frac{1}{2}\mathbf{b}' \left( 1 + \frac{d\zeta}{dt} \right) = \mathbf{b}', \quad (6.60)$$

therefore having  $|\dot{x}| = 1$ .

In a network of long string these are going to intersect, reconnects and form closed loops. These loops are going to either self-interact or interact with other loops or with some long strings thus producing smaller loops. The goal of the next section is studying in details how this happen.

### 6.3 String network evolution

One of the main drawback of topological defects formation is that when they evolve may become the dominant contribution to the energy of the Universe and this is not observed. The typical feature of a cosmic string network is that instead of doing so, it evolves following a scaling solution in which its energy density is a constant fraction of the total energy of the universe. This is particularly important because it makes a cosmic strings network compatible with the current observation. In this section we are going to study in a detailed way how a cosmic strings network is generated and its scaling behaviour.

#### Phase transition

Before of studying in details how cosmic strings network are generated in the early universe it is important to come back discussing spontaneous symmetry breaking at finite temperature. Considering a simple scalar theory we can use the effective action to compute the potential considering loop corrections. Using then finite temperature Green functions we find the effective potential at finite temperature [123]

$$V_{eff}(\phi, T) = V(\phi) + \sum_n F_n, \quad (6.61)$$

where

$$F_n = \pm \int \frac{d^3k}{(2\pi)^3} \ln(1 \mp \exp -\epsilon_k/T) \quad (6.62)$$

and  $V(\phi)$  is the usual potential. At high temperature  $T \gg 1$  we can write

$$V_{eff}(\phi, T) = V(\phi) + \frac{\lambda + 3g^2}{12} T^2 \phi^2 - \frac{2\pi^2}{45} T^4 \quad (6.63)$$

where  $\lambda$  is the coupling for the quartic interaction and  $g$  is the gauge coupling. We can rewrite the expression above as

$$V_{eff}(\phi, T) = m^2(T)\phi^2 + \frac{\lambda}{4}\phi^4. \quad (6.64)$$

If we now compute the minimum for the potential we can see that for  $T$  greater than a certain critical value  $T_c$  the symmetry is restored and the vacuum is not anymore  $\langle a\phi_0 \rangle = \eta e^{i\theta}$  but  $\langle \phi_0 \rangle = 0$ . Indeed

$$m^2(T) = \frac{\lambda}{12} (T^2 - 6\eta^2), \quad (6.65)$$

and we have a VEV different than zero only in  $m^2(T)$  is smaller than zero. The critical temperature in this case is  $T_c = \sqrt{6}\eta$  and then we can see that it is of the same order of magnitude of the breaking scale. During the Universe expansion  $T$  decreases until it goes below  $T_c$ , we say it occur a phase transition. In our breaking chain, for example, there are three phase transitions corresponding to each breaking scale  $M_i$ . There are two possibilities when we talk about phase transitions: we can have a smooth transition, so that the VEV pass smoothly from zero to  $\eta$ , in this case we have a second-order phase transition. On the other hand there can be some discontinuities in the potential at  $T_c$  and in this case we have a first-order phase transition and one cannot compute analitically the critical temperature. The symmetric vacuum may remain in this case a local minimum, called *false vacuum* and there can be therefore a metastable symmetric phase below the critical temperature. We can picture such a transitions with spherical bubbles of the new spontaneously broken phase which appear and then when coalesce the phase transition is completed.

## Kibble mechanism

In a certain region, during a phase transition, an Higgs boson can take a random VEV  $\eta e^{i\theta}$  belonging to the vacuum manifold we have already introduced. The choice of the vacuum

depend on random fluctuations which can be correlated at a scale  $L(t)$  but if we take two regions separated by an Hubble length  $d_H(t) \sim t$  that we are going to call horizon, then a correlation between the two VEVs would violate causality. As the Universe keep expanding the horizon grows and the two region become causally connected. Imposing the boundary conditions at infinity required by imposing finite energy density that we have seen at the beginning of this section, we can see how the only stable solution is a topological defect, in case of a  $U(1)$  breaking, a cosmic string [23]. The linear energy density of the string, its tension, is of the same order of magnitude of the breaking scale. This mechanism generates a network of strings of characteristic length  $L \lesssim d_H(t)$ .

### 6.3.1 Network evolution: VOS model

Let us call  $L$  the characteristic scale of the network. Another parameter that characterize the network is

$$v^2 = \langle \dot{x}^2 \rangle = \frac{\int \epsilon \dot{x}^2 d\sigma}{\int \epsilon d\sigma}. \quad (6.66)$$

The total energy of the string is given by

$$E = \mu a(\tau) \int \epsilon d\sigma. \quad (6.67)$$

The friction is parameterized by the quantity  $l_F$ . We are interested in the evolution of the total energy density of the network:  $\rho \equiv E/a^3$ . Differentiating (6.67) and using the expression for the quadratic velocity we obtain the equation that governs the evolution of such energy density [121, 122]

$$\frac{d\rho}{dt} + \left[ 2H(1 + v^2) + \frac{v^2}{l_F} \right] \rho = 0. \quad (6.68)$$

This is the first of the set of equation that governs a network. Let us now examine carefully the evolution of long string and the loop production. We express the energy density of long strings in term of the characteristic length

$$\rho_\infty \equiv \frac{\mu}{L^2}. \quad (6.69)$$

Let us compute the loop production rate; because we are studying a scaling solution the loop production rate has to be scale invariant. The probability of producing a loop during the time interval  $\delta t$  is proportional to the probability of a segment of length  $L$  to intersect a segment of length  $l$  going a velocity  $v_\infty$ ; such a probability is  $lv_\infty \delta t / L^2$ . We

multiply the probability above with the probability of having a loop produced with length between  $l$  and  $l + dl$ , this probability is given by an unknown scale invariant function that we call  $w(l/L)$ . Then the loss rate of  $\rho_\infty$  due exclusively to the loop production is

$$\frac{d\rho_\infty}{dt}_{loops} = \rho_\infty \frac{v_\infty}{L} \int w\left(\frac{l}{L}\right) \frac{l}{L} \frac{dl}{dL} = \tilde{c}v_\infty \frac{\rho_\infty}{L}. \quad (6.70)$$

Subtracting this term from (6.68) and using  $\rho_\infty = \mu/L^2$  we can find an equation for the evolution of the characteristic length of the network

$$2\frac{dL}{dt} = 2HL(1 + v_\infty^2) + \frac{v_\infty^2 L}{l_F} + \tilde{c}v_\infty + 4G\Gamma v^6. \quad (6.71)$$

As we shall study in much detail in the next chapter loops decay while oscillating and emitting gravitational waves. This produces an additional loss of energy that affects the evolution of the characteristic scale that is encoded in the last term of the equation above [124]. Finally for obtaining the last of the equations that describe the evolution of a network, let us derive Eq. 6.66. The if we use the equation of motion Eq. 6.56 we obtain

$$\frac{dv}{dt} = (1 - v^2) \left[ \frac{k}{R} - v \left( 2H + \frac{1}{l_F} \right) \right]. \quad (6.72)$$

The first term inside the square bracket encodes the information of the small scale structure of the string. Indeed until now we have assumed a smooth long string described by the Nambu action. Indeed a string is characterized also by a small structure that affects the evolution of the network. Following [?] an ansatz for  $k$  is

$$k(v) = \frac{2\sqrt{2}}{\pi} (1 - v^2) \left( 1 + 2\sqrt{2}v^3 \right) \frac{1 - 8v^6}{1 + 8v^6}. \quad (6.73)$$

The equation that describe the network evolution are then

$$\frac{d\rho}{dt} + \left[ 2H(1 + v^2) + \frac{v^2}{l_F} \right] \rho = 0, \quad (6.74)$$

$$\frac{d\rho}{dt} + \left[ 2H(1 + v^2) + \frac{v^2}{l_F} \right] \rho = 0, \quad (6.75)$$

$$\frac{d\rho}{dt} + \left[ 2H(1 + v^2) + \frac{v^2}{l_F} \right] \rho = 0, \quad (6.76)$$

$$\frac{dv}{dt} = (1 - v^2) \left[ \frac{k}{R} - v \left( 2H + \frac{1}{l_F} \right) \right]. \quad (6.77)$$

The linear scaling solutions to this set of equations are (for a general epoch with  $a \sim t^\nu$ ) [125]

$$\frac{\xi}{t} = \sqrt{\frac{k(v)(k(v) + \tilde{c})}{4\nu(1-\nu)}} \equiv \xi_s, \quad (6.78)$$

$$v = \sqrt{\left(\frac{k(v)}{k(v) + \tilde{c}}\right) \left(\frac{1-\nu}{\nu}\right)} \equiv v_s. \quad (6.79)$$

Now we can find the loop number density, crucial for the next chapter. The number density of the loop of length  $l$  at time  $t$  is

$$n(l, t) = \int dl' w(l, t') \left(\frac{a(t')}{a(t)}\right)^3, \quad (6.80)$$

where primed quantities are taken at formation time and unprimed quantities at observation time. Eq. 6.79 can be rewritten in terms of a scale invariant term  $x = l/t$

$$n(l, t) = t^{-4} n(x), \quad (6.81)$$

where  $x = \frac{l}{t}$ . Similarly for  $n(l, t)$  also  $w(l, t)$  can be written in terms of  $w(x)$ .

The probability of producing a loop with length between  $l$  and  $l + dl$  is then

$$w(l, t) = t^{-5} w(x). \quad (6.82)$$

A loop oscillates and emits gravitational waves, losing energy. Since the energy of a loop is proportional to its length the loop shrinks as it emits gravitational waves. Its length evolves as

$$l = l' - \Gamma G\mu, \quad (6.83)$$

where  $\Gamma \sim 50$  from numerical simulations [126]. For  $a(t) \sim t^\nu$  we can compute the number density and obtain

$$n(x) = \left[ \frac{1}{(x + \Gamma G\mu)^{3(1-\nu)+1}} \right], \int_x^\infty (x' + \Gamma G\mu)^{3(1-\nu)} w(x') dx'. \quad (6.84)$$

We need to determine the expression of  $w(x)$ . From Eq. 6.77 we find that

$$\int_0^\infty xw(x) = \tilde{c} \frac{v_s}{\xi_s}. \quad (6.85)$$

Now let us assume that all the loops produced at an arbitrary  $t$  have the same length: a fixed fraction of the characteristic scale  $L$ , so that

$$x \equiv l(t)/t = \alpha L(t)/t \equiv \alpha \xi. \quad (6.86)$$

Therefore we have

$$w(x) = \frac{\tilde{c}v}{\alpha\xi^4}\delta(x - \alpha). \quad (6.87)$$

Since assuming all the loops are produced with the same length is a rough approximation we need to make an empirical correction. Comparing our  $w(x)$  with a more accurate numerical simulation one finds that a good empirical description is obtained by multiplying  $w(x)$  by a factor  $\mathcal{F}/f_r \sim 0.1$ . [125, 127] The function we are going to use is

$$w(x) = A\delta(x - \alpha), \quad A \equiv \frac{\tilde{c}v}{\alpha\xi^4} \frac{\mathcal{F}}{f_r}. \quad (6.88)$$

We have all the ingredients to compute the number density of the loops in each epoch. In the radiation-dominated epoch we have  $a(t) \sim t^{\frac{1}{2}}$ . Solving Eq. 6.79 with the VOS solution  $\xi_r = 0.271$  and  $v_r = 0.662$  [?], we obtain

$$n_r(x) = \frac{A_r}{\alpha} \frac{(\alpha + \Gamma G\mu)^{3/2}}{(x + \Gamma G\mu)^{5/2}}, \quad (6.89)$$

where we used  $\Gamma \sim 50$  and  $A_r = \frac{0.1}{\sqrt{2}} = 0.54$ . For the matter dominated era we obtain instead

$$n_m(x) = \frac{A_m}{\alpha} \frac{(\alpha + \Gamma G\mu)}{(\alpha + \Gamma G\mu)^2}, \quad (6.90)$$

where the solution of the VOS model is  $\xi_m = 0.625$  and  $v_m = 0.583$ .

### 6.3.2 Cosmic network simulation

An improvement and more precise result can be achieved with numerical simulation. Let us look in details at the work of Blanco-Pillado, Olum, Shlaer. [128, 129, 130]. Let us start describing the basic steps of the numerical simulation, following [117]. We first discretize the vacuum manifold using three values of theta: 0,  $2\pi/3$  and  $4\pi/3$ . Let us take a lattice and assign randomly a number which can be 0,1 or 2 to all site of the lattice. 0 correspond to  $\theta = 0$ , 1 to  $\theta = 2\pi/3$  and 2 to  $\theta = 4\pi/3$ . A string pass along a cubic surface if the lattice if the pattern of the theta along the vertices is ciclyc, that is:  $\{0, 1, 2, 1\}$ ,  $\{2, 1, 0, 1\}$  and so on. The dimension if the lattice is few hundred times bigger than the characteristic length  $L$ .

We let evolve the system assuming the probability of reconnection to be equal to one. From this simulation we can extract the loop number density function  $w(l, t)$  and the value of  $\alpha$ . Let us look at the main results of Ref. [129] From the simulation we obtain

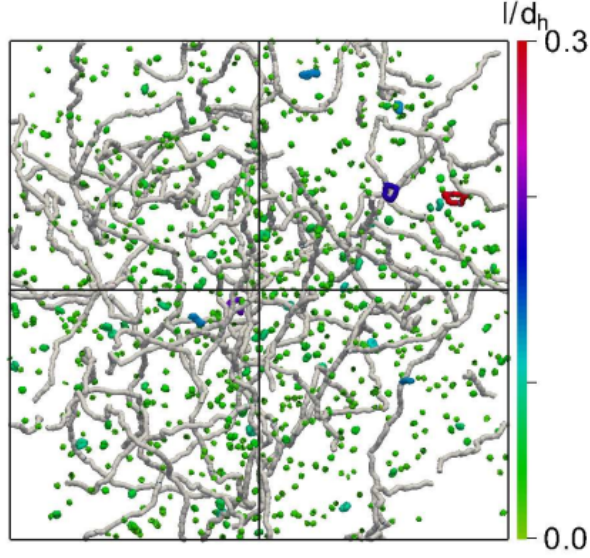


Figure 6.1: Example of an output of the simulation. Picture taken from [128].

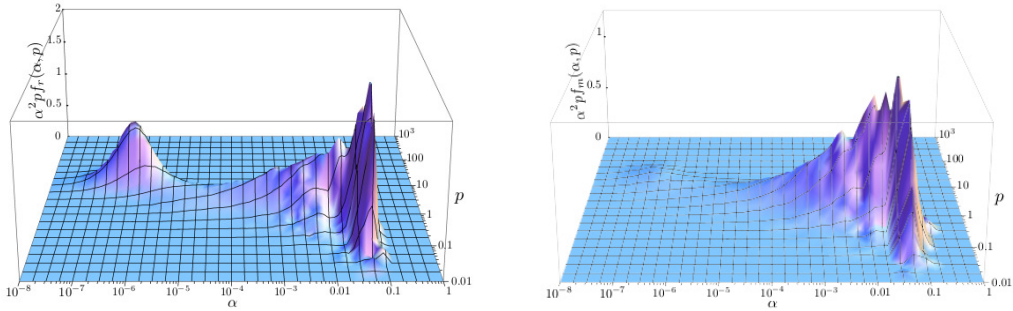


Figure 6.2: Simulation of loop number density with respect to  $\alpha$  and  $p = \frac{v}{\sqrt{1-v^2}}$ . Left: results in radiation dominated epoch. Right: results in matter domination epoch. Picture taken from [129]

numerically the constant in Eq. 6.89 and Eq. 6.90. We obtain for radiation and matter domination epoch, respectively [125]

$$n_r(l, t) = \frac{0.18}{t^{3/2}(l + \Gamma G \mu t)^{5/2}}, \quad (6.91)$$

$$n_m(l, t) = \frac{0.27 - 0.45(l/t)^{0.31}}{t^2(l + \Gamma G \mu t)^2}. \quad (6.92)$$

# Testing SO(10) with a Stochastic Gravitational Waves Background

During each of the spontaneous breaking we encounter from  $SO(10)$  to  $G_{SM}$  topological defects are created. Magnetic monopoles and domain walls are unwanted since they would constitute the largest fraction of the energy density of the universe. We set the inflation scale to be after  $M_3$  and  $M_2$  in order to wash out all the unwanted topological defects. During the breaking  $G_1 \rightarrow G_{SM}$  there is a  $U(1)$  breaking which generates cosmic strings. As we have seen in the previous chapter such a breaking generates a cosmic strings networks, which achieve a scaling solutions and produces small loops which oscillate and decaying producing a Stochastic Gravitational Waves Background. In this chapter we are going to give a quantitative prediction of the signal produced by such a network and determine if it could be observed.

## 7.1 Gravitational Waves

Gravitational waves are perturbations of the spacetime and are caused by some of the most energetic events in the universe such as a black hole collisions. The first signal directly detected has been observed by LIGO in 2016. [131] Let us start studying a small perturbation in the Minkowsky metric

$$g_{\mu\nu}(x) = \eta_{\mu\nu}(x) + h_{\mu\nu}(x). \quad (7.1)$$

Plugging this expression for the metric in the vacuum Einstein equation

$$R_{\mu\nu} = 0, \quad (7.2)$$

we obtain a wave equation for the metric perturbation  $h(x)$

$$h_{\mu\nu} - \frac{\partial^2 h_\nu^\lambda}{\partial x^\lambda \partial x^\nu} - \frac{\partial^2 h_\mu^\lambda}{\partial x^\lambda \partial x^\mu} - \frac{\partial^2 h_\lambda^\lambda}{\partial x^\mu \partial x^\nu}. \quad (7.3)$$

We can use the redundancy due to invariance under reparametrization to fix the gauge

$$\frac{\partial h_\nu^\mu}{\partial x^\mu} = \frac{1}{2} \frac{\partial h}{\partial x^\nu}. \quad (7.4)$$

We simplify Eq. 7.3 as

$$h_{\mu\nu} = 0. \quad (7.5)$$

We can use finally a residual gauge transformation for put the metric perturbation in the transverse traceless gauge so that it will be easier to picture how a gravitational wave affect spacetime. In the TT gauge the metric becomes

$$h_{\mu\nu}^{TT} = \begin{pmatrix} 0 & 0 & 0 & 0 \\ 0 & h_+ & h_x & 0 \\ 0 & h_x & -h_+ & 0 \\ 0 & 0 & 0 & 0 \end{pmatrix}, \quad (7.6)$$

where  $h_x, h_+$  are the two possible polarizations of a gravitational wave.

## 7.2 Stochastic Gravitational Waves Background

The signals observed so far by Advanced Ligo and Virgo all comes from resolved sources such a neutron stars collisions or black holes collisions. If we take all the unresolved signals due to more multiple sources or extend sources that radiate incoherently we obtain a gravitational wave background [132]. This signal must be treated as stochastic. A Stochastic Gravitational Waves Background (SGWB) comes out from all direction and in first approximation can be treated as isotropic. The best way to quantify it is trough its energy density  $\Omega_{GW}$  that can be seen as a part of the total radiation density

$$\Omega_r = \Omega_\gamma + \Omega_{GW} + \Omega_\nu + \dots \quad (7.7)$$

To see how it can be detected Let us come back to the expression for the metric perturbation in the TT gauge of Eq. 7.6. Usually a gravitational waves signal is detected trough the use of an interferometer. The effects of a gravitational waves passing on the proper lenght of the two arms is [133]

$$\Delta L_x = \frac{h_+ L_0}{2}, \quad \Delta L_y = \frac{-h_+ L_0}{2}, \quad (7.8)$$

so that the x-direction shrinks while the y-direction stretch and vice-versa. The main problem of an SGWB is that, not having a definite signal, would appear as noise in a single gravitational wave detector. The main idea is to find a correlation between noise among more different detectors. If we express the detected signal in terms of a gravitational wave strain plus a noise term:

$$s(t) = n(t) + h(t) \quad (7.9)$$

and we see that if we take the correlation between the signals detected by two different detectors we have

$$\langle s_1(t)s_2(t) \rangle = \langle h(t)h(t) \rangle. \quad (7.10)$$

By detecting such a correlation we can observe a SGWB. Such a correlation can be detected as we will see using as we will see pulsar or interferometers for example.

### 7.3 SGWB spectrum from a cosmic string network

In this section we are going to compute and study the signal of an SGWB produced by a cosmic network. In the last chapter we have said that loops oscillate, emit gravitational waves and shrinks, their length vary

$$l' = l - \Gamma G\mu, \quad (7.11)$$

where  $\Gamma$  can be found by numerical simulations as we shall see better later, and  $G\mu$  is a parameter proportional to the string tension. We are interested in computing the spectrum of the SGWB produced by a cosmic string networks. It can be defined as

$$\Omega_{GW} = \frac{f}{\rho_c} \frac{d\rho_{GW}}{df}. \quad (7.12)$$

Since we need to sum all the gravitational wave signal produced by all the loops at all times we need the loop number density we have computed in the last chapter  $n(l, t)$  and an the average power spectrum of GW emission by one loop that can we obtain using numerical simulation [130]. Keeping account of the expansion of the universe which redshift the frequencies from the time of emission until today we find [125]

$$\frac{d\rho_{\text{gw}}}{df}(t_0, f) = G\mu^2 \int_0^{t_0} dt \frac{1}{(1+z(t))^3} \int_0^\infty d\ell \ell n(\ell, t) P((1+z(t))f, t), \quad (7.13)$$

where  $P((1+z)f, t)$  is the average power spectrum. It is useful to work with discrete frequencies  $f = \frac{2k}{l}$ . Therefore we can rewrite Eq. 7.13 as an infinite sum [130]

$$\frac{d\rho_{GW}}{df} = G\mu^2 \sum_{k=1}^{\infty} C_k P_k. \quad (7.14)$$

Rewriting  $l = 2k/f$  we find

$$C_k(f) = \int_0^t \frac{dt}{(1+z)^5} \frac{2n}{f^2} n(l, t). \quad (7.15)$$

Changing the integration variable to  $z$  and using

$$dt = -\frac{dz}{H(z)(1+z)}, \quad (7.16)$$

we obtain

$$C_k(f) = \frac{2n}{f^2} \int_0^{\infty} \frac{dz}{H(z)(1+z)^6} n\left(\frac{2n}{(1+z)f}, t\right), \quad (7.17)$$

this depends on the cosmological epoch in which loops are produced and the number density of the loops.

Let us assume that most of the loops are produced with a length  $l = \alpha t$ . As the length increase when the universe is expanding and the network is scaling loops can oscillate at smaller and smaller frequencies. Therefore earliest loops are the one which contributes to the high frequency spectrum of an SGWB and their whole lifetime happen in the radiation-dominated era. Here we have

$$H(z) = (1+z)^2, \quad t(z) = \frac{1}{2(1+z)^2 H_0 \sqrt{\Omega_r}}, \quad (7.18)$$

where  $H_0 \sim 100 h km/s/Mpc$  and  $h^2 \Omega_r = 4.15 \times 10^{-5}$ . We can reexpress  $n$  in terms of the scale invariant quantity  $x = \frac{l}{t}$ . Changing variable of integration from  $z$  to  $x$  we find

$$C_k = \frac{8H_r^2}{f} dx n(x). \quad (7.19)$$

If we plug everything in the expression of the intensity of the stochastic gravitational waves background using Eq. 7.14 we find

$$\Omega_{GW} = \frac{1}{\rho_c} 8H_r^2 \int dx n(x) \sum_k P_k = \frac{\Gamma}{\rho_c} H_r^2 \int dx n(x). \quad (7.20)$$

We have obtained a flat spectrum in the high-frequency region: this is a crucial feature of the behaviour of an SGWB produced by a cosmic strings network. If we look at the loop number density in the radiation era we can notice that for  $l \gg \Gamma G\mu$  it scales as  $\sim l^{-5/2}$  and therefore the SGWB goes as:  $\Omega_{GW} \sim f^{3/2}$ . Finally the contribution to the SGWB of loops created in the matter dominated era is negligible; for example in Ref. [130] has been found that  $\frac{n_r}{n_m} \sim 10^5$ .

Let us see why until now we have set  $\Gamma = 50$ . The total power emitted by a loop is  $P = \Gamma G\mu^2$ .

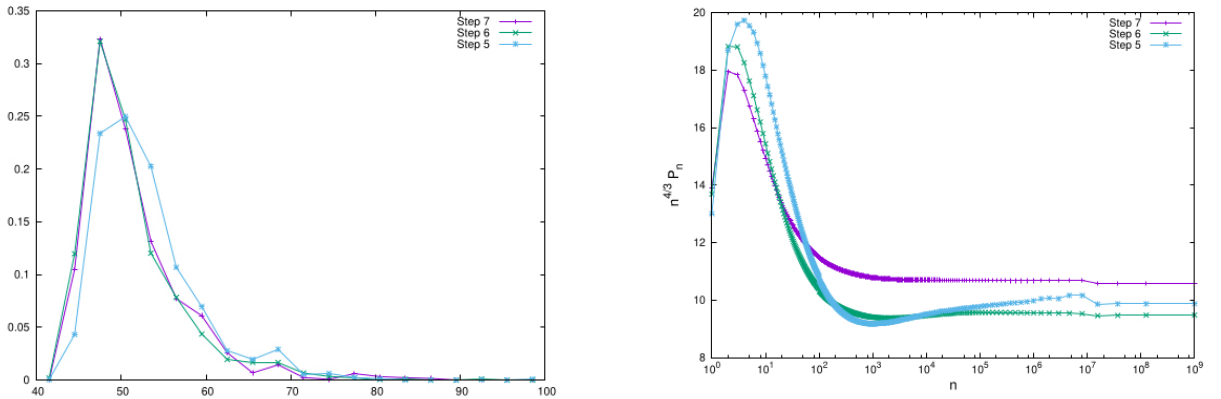


Figure 7.1: Left:  $\Gamma$  for loops in radiation era. We can see that the central value of the distribution is  $\Gamma \sim 50$ . Right:  $n^{4/3} P_n$  averaged for all loops.

Fig. 7.1 shows the results from the simulation of Ref. [130] From this simulation we find  $\Gamma = 50$  that we used so far. Theoretically one can prove that oscillating cusps give a spectrum that scale as:  $P_k = k^{-4/3}$  and kinks instead gives  $P_k = k^{-5/3}$ . In the same simulation has been found also the behaviour of the power spectrum  $P_k$  averaged for all the loops. From this results we find that the relative emission rate per mode is

$$\Gamma^{(k)} = k^{-4/3} \Gamma \sum m^{-4/3}. \quad (7.21)$$

## 7.4 Prediction of our model

In our simulation we have followed [134]. We still compute the spectrum using a discrete set of modes and therefore we can express  $\Omega_{GW}$  as

$$\Omega_{GW} = \sum_k \Omega_{GW}^{(k)}, \quad (7.22)$$

where

$$\Omega_{\text{GW}}^{(k)}(f) = \frac{1}{\rho_c} \frac{2k}{f} \frac{\mathcal{F} \alpha \Gamma^{(k)} G \mu^2}{\alpha(\alpha + \Gamma G \mu)} \int_{t_F}^{t_0} d\tilde{t} \frac{C_{\text{eff}}(t_i^{(k)})}{t_i^{(k)4}} \left[ \frac{a(\tilde{t})}{a(t_0)} \right]^5 \left[ \frac{a(t_i^{(k)})}{a(\tilde{t})} \right]^3 \Theta(t_i^{(k)} - t_F). \quad (7.23)$$

The loop number density here is not the one obtained from numerical simulation but is obtained analytically as we have done in the last chapter assuming  $l = \alpha t$ .  $\mathcal{F}$  is 0.1 and corrects the rough approximation of assuming that all loops are produced with the same length.  $C_{\text{eff}}$  has been obtained from VOS model solution and it is a numerical parameter that quantify how much of the long string energy goes into loop production. This value depend on which era loops are produced we have  $C_{\text{eff}} = 0.39(5.4)$  for matter (radiation) era. The two free parameters that determines uniquely the background spectrum are  $\alpha$  and  $G\mu$ . The standard value used for  $\alpha$  is 0.1 but in our predictions we compare two signals, one for  $\alpha = 0.1$  and one for  $\alpha = 0.01$  in order to show that within an order of magnitude the qualitative predictions of our model are the same. The other free parameter is the string tension expressed by the parameter  $G\mu$ . This can be related to the intermediate scale of our model corresponding to the  $U(1)$  breaking:  $M_1$ . Let us start from the solution of the Abelian-Higgs model of Eq. 6.35. These are

$$\phi_s(\rho) = e^{in\theta} f(\rho), \quad (7.24)$$

$$A_s(\rho) = -\epsilon_{ab} x_b \frac{n}{e\rho^2} \alpha(\rho). \quad (7.25)$$

It is possible to have the analytic approximations of these functions for  $\rho \rightarrow 0$  and  $\rho \rightarrow \infty$ . We have [135]

$$f \simeq \begin{cases} f_0 \xi^{|n|}, \\ 1 - f_1 \xi^{-1/2} \exp(-\sqrt{\beta} \xi), \end{cases} \quad a \simeq \begin{cases} a_0 \xi^2 - \frac{|n| f_0^2}{4(|n|+1)} \xi^{2|n|+2}, & \text{as } \xi \rightarrow 0 \\ 1 - a_1 \xi^{1/2} \exp(-\xi), & \text{as } \xi \rightarrow \infty \end{cases}, \quad (7.26)$$

where  $\xi = m_{Z_R} \rho$  being  $Z_R$  the mass of the  $U(1)$  gauge boson,  $\beta = (m_{\text{P}hi}/m_{Z_R})^2 = \lambda/g^2$ . Plugging this equation in the energy density of the string we find when the Higgs takes an arbitrary VEV  $\sim \eta e^{i\theta}$  where  $\eta$  is also the scale of the phase transition

$$\mu = \pi \eta^2 \epsilon(\beta). \quad (7.27)$$

One can find  $\epsilon(1) = 1$ . Being both  $\Phi$  and  $Z_R$  with unknown mass we are going to set  $\beta = 1$  and therefore  $\mu = \pi \eta^2$ . In the breaking  $G_{3221} \rightarrow G_{SM}$  we define  $M_1$  to be the mass of the gauge boson which acquire mass during the breaking [25]. Being the mass

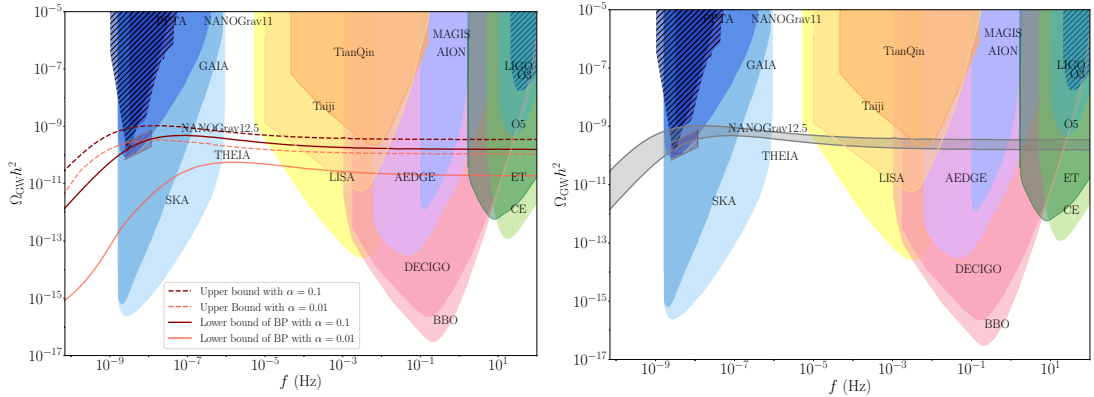


Figure 7.2: Gravitational wave spectrum predicted from the model. Breaking of the intermediate symmetry  $G_1 \equiv SU(3)_c \times SU(2)_L \times SU(2)_R \times U(1)_X$  generate cosmic strings with tension  $\mu$ . We consider the spectrum of gravitational waves background released from the string network with the assumption of Nambu-Goto strings. To be consistent with gauge unification,  $G\mu$  is restricted to be less than  $1.3 \times 10^{-10}$ , referring to  $M_1 = 4.4 \times 10^{13}$  GeV. The lower bound to the GW spectrum for the benchmark point we considered earlier (red lines) is  $G\mu = 2.68 \times 10^{11}$  referring to  $M_1 = 2 \times 10^{13}$  GeV. The GW spectrums of these two bounds are shown in dashed and solid curves, respectively.

of a gauge boson  $M^2 = \alpha\eta^2$  we can assume that both  $SU(2)_R$  and  $U(1)_X$  gauge bosons has the same mass and have

$$M_1^2 \sim (\alpha_{2R} + \alpha_X)\eta^2. \quad (7.28)$$

Therefore

$$G\mu = \frac{1}{2(\alpha_{2R} + \alpha_X)} \frac{M_1^2}{M_{pl}^2}. \quad (7.29)$$

In Fig. 7.2 there are the results of our numerical simulation. The upper bound correspond to  $M_1 = 4.4 \times 10^{13}$  GeV, a constraint given by requiring gauge unification. The main requirement on  $M_1$  is to be greater than the mass of the heavier right handed neutrino:  $M_1 \geq M_{N_3}$ . Therefore for a fixed point in the parameter space we would have a region instead of a line in the plot. In the solid line there is an example of a signal associated to the benchmark point BP1.

In general we can predict a signal for all the breaking chain of  $SO(10)$  and determine whether the model could be still consistent or not. As we can see from our simulation the signal is well within the observational ranges of most of the future GW observatories such as future space-based interferometers (LISA [27], Taiji [136], TianQin [137], BBO [138], DECIGO [139]), atomic interferometers (MAGIS [140], AEDGE [141], AION [142]),

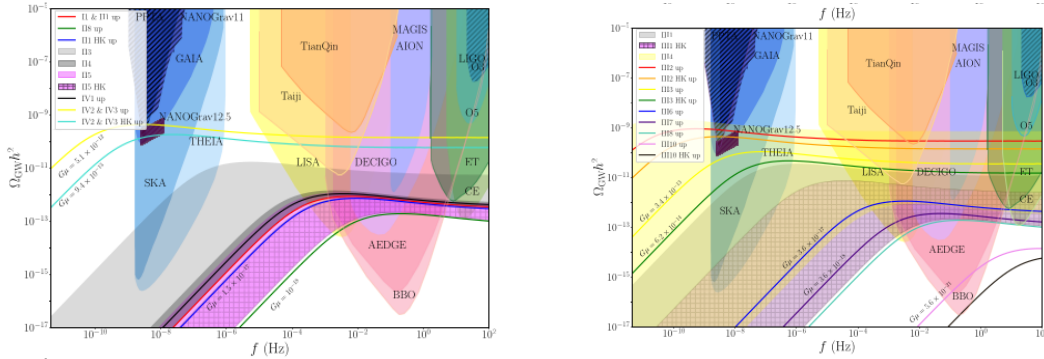


Figure 7.3: Numerical prediction of the signal for some of the breaking chain of  $SO(10)$ . Figure taken from [25]

and ground-based interferometers (Einstein Telescope [143] (ET), Cosmic Explorer [144] (CE)). At lower frequencies an important observational window is given by pulsar timing arrays (PTA) such as EPTA [145] and NANOGrav (11-year data set) [146] which have already probed the nHz regime and provided upper limits through the non-observation of GWs. Future PTA such as SKA [147] will cover even more parameter space, and large-scale surveys of stars such as Gaia [148] and the proposed upgrade, THEIA [149], can be powerful and complementary probes of gravitational waves in the same frequency regime.

Both proton decay and cosmic strings could give us information about the scale  $M_1$  of our model and test  $SO(10)$ . In particular a possible gravitational wave signal observed that could be associated to a cosmic string network could allow us to find a range of  $M_1$  that could subsequently be tested by Hyper-Kamiokande. Also the contrary would hold, a possible signal observed by Hyper-Kamiokande could be strengthened by gravitational waves observation.

## 7.5 $SO(10)$ with Pulsar Time Arrays

The PTA experiment NANOGrav released its 12.5-year dataset [28] which announced the detection of a common-spectrum process that has a characteristic strain given by

$$h_c(f) = A \left( \frac{f}{f_{yr}} \right)^\alpha, \quad (7.30)$$

where  $f_{yr} = yr^{-1}$ . The free parameters of this signal are  $A$  and  $\alpha$ . Similar signals has been observed recently by other PTA experiments such as IPTA, EPTA, and PPTA.

All of these experiments use pulsars for detecting gravitational waves in an indirect way. As a star collapse at the end of its life there could be situations in which it leaves a dense remnants with an extremely intense magnetic field which rotates on itself. This object is called pulsars and emits a signal that we can detect with a well defined period  $\Delta t_0$ . When this signal pass through a gravitational waves the signal becomes slightly delayed and we can measure this delay from the Earth. From a set of well studied pulsar one can find correlations between possible delayed time of arrivals. There are many reasons behind possible correlation therefore it is crucial to model correctly all type of noises that could be interpreted by a GW signal by mistake. Such a method is particularly efficient at low frequencies and ideal for detecting a stochastic background.

The crucial feature of a stochastic gravitational waves background is not a simple waveform and therefore for being detected one has to look for a signal similar to noise but with different correlations. Because all of the four PTA experiments haven't found for the moment a quadrupole strain they haven't yet confirmed the observation of a Stochastic Gravitational Waves Background. Nonetheless it is interesting to assume that this signal comes from a Stochastic Gravitational Waves Background and confront it with our predictions.

Following [150] we have already said that the characteristic strain of the signal detected by PTA experiments could be approximated with a power law mode. In the relevant frequency range  $f = (2.3, 12) \text{ nHz}$  we then fit our signal to a power law model

$$\Omega_{GW}(f) \sim f^2 h_c^2(f) = \Omega_{yr} \left( \frac{f}{f_{yr}} \right)^{5-\gamma} \quad (7.31)$$

$$h_c(f) = A \left( \frac{f}{f_{yr}} \right)^\alpha \quad (7.32)$$

where

$$\Omega_{yr} = \frac{4G}{\rho_c} A^2 f_{yr}^2. \quad (7.33)$$

The signal has been fitted using 5 frequency bins in the interval  $f = (2.3, 12) \text{ nHz}$ . We then plotted the values of  $A$  and  $\gamma$  predicted by our signal with the ones consistent with the signal observed by EPTA, IPTA, PPTA and NANOGrav. We have found that the signal is compatible with PPTA, IPTA and NANOGrav in  $1\sigma$  ranges and with EPTA in  $2\sigma$  range. For NANOGrav, EPTA and IPTA,  $A$  and  $\gamma$  at  $f_* = 5.6 \text{ nHz}$  in  $2\sigma$  ranges are restricted in

$$A = (1.75, 1.95) \times 10^{-15}, \quad \gamma = (4.34, 4.90) \quad (\text{NANOGrav}),$$

$$\begin{aligned}
A &= (1.32, 1.85) \times 10^{-15}, & \gamma &= (4.44, 4.86) & (\text{PPTA}), \\
A &= (1.56, 1.82) \times 10^{-15}, & \gamma &= (4.68, 4.85) & (\text{EPTA}), \\
A &= (1.38, 2.24) \times 10^{-15}, & \gamma &= (4.50, 5.03) & (\text{IPTA}),
\end{aligned} \tag{7.34}$$

respectively.

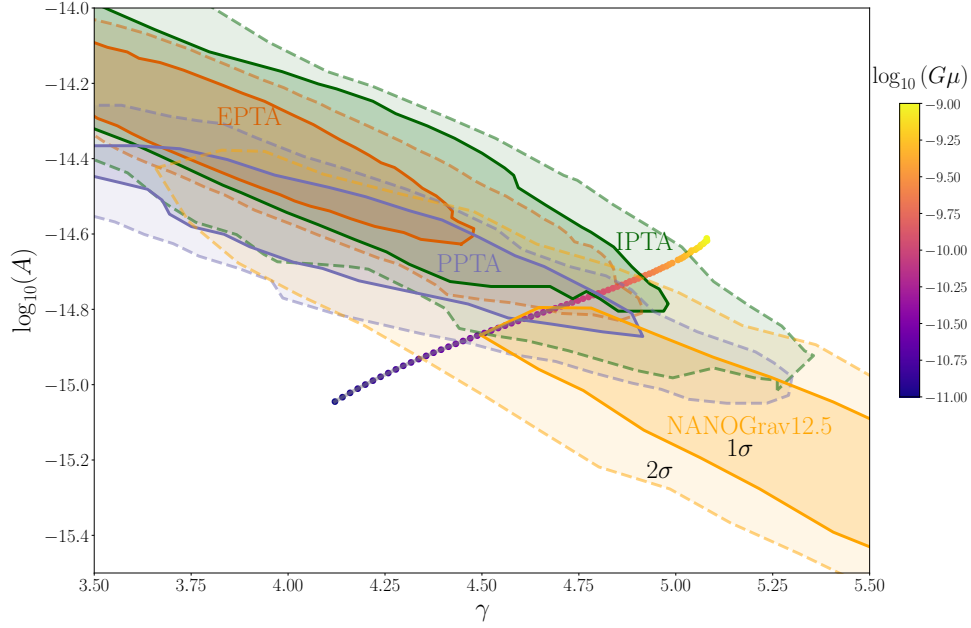


Figure 7.4: Comparison between SGWB signals produced by cosmic strings with  $G\mu$  from  $10^{-11}$  to  $10^{-9}$  the possible  $1\sigma$  and  $2\sigma$  regions hinted by EPTA, PPTA, IPTA and NANOGrav. The SGWB signal has been fitted for three frequencies: 2.4 nHz, 5.4 nHz and 12 nHz. The simulation shows that the signal is compatible with NANOGrav, PPTA and IPTA at  $1\sigma$  while with EPTA at  $2\sigma$ .

We then computed again the GW signal for our model in the narrowed frequency interval and we compared with the regions allowed by the PTA experiments. Looking at Fig. 7.5 we can see how this model is consistent with the signal predicted by NANOGrav, EPTA, IPTA and PPTA.

## Interplay between proton decay and gravitational waves signal

It is interesting compare the information on  $M_1$  one can obtain both from proton decay and gravitational waves observation. We first have seen from Fig. 7.2 and Fig. 7.3 that the values of  $M_1$  compatible with proton decays observation can produce a signal that

could be detected by next generation gravitational waves experiments. Therefore using both Hyper-Kamiokande and gravitational waves experiments we could be able to exclude or verify experimentally many breaking chains of SO(10) completely. A particularly interesting fact is that we can already compare the information obtained from PTA experiments and determine if they are consistent with the current constraint on  $M_1$  for proton decay.

From the simulation that we used for Fig. 7.4 and Fig. 7.5 we can determine the range of  $G\mu$  which is consistent with the signal and then convert it in a range on  $M_1$ . Subsequently we can relate  $M_1$  to the grand unification scale  $M_U$  and therefore to proton decay lifetime as we have done earlier and determine if this range has already been tested. For this

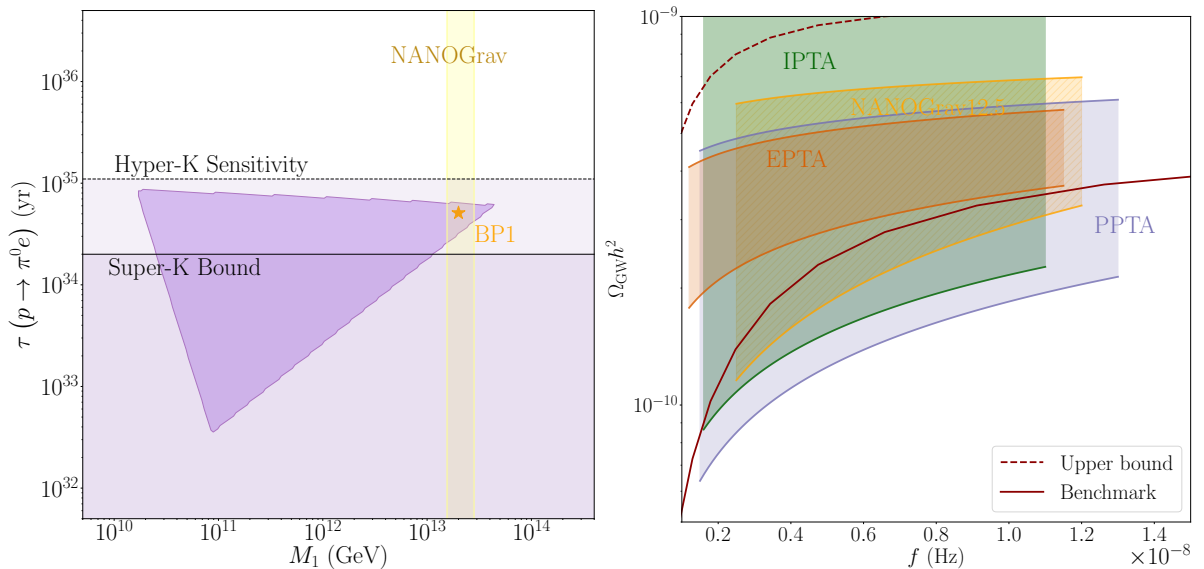


Figure 7.5: Left: Proton decay lifetime compared with the region of  $M_1$  consistent with NANOGrav12.5, we can see that there is a region of the parameter space which can be tested by Hyper-K, which is consistent with NANOGrav. The black star indicates BP1. Right: Blown-up image of the nHz region of the gravitational waves spectrum of the benchmark point and the upper bound. This is compared with the region of EPTA, IPTA, PPTA and NANOGrav consistent with the observation of an SGWB.

simulation we have used a slightly different NANOGrav signal with a fixed  $\gamma = \frac{13}{3}$ . The range on  $A$  is  $(1.37, 2.67) \times 10^{-15}$ . Comparing the simulation with such as signal we have found that the range allowed by NANOGrav on  $M_1$  is

$$M_1 = (1.55, 2.81) \times 10^{13} \text{ GeV}. \quad (7.35)$$

In Fig. 7.5 we can see our results. The main result is that the whole range consistent with the NANOGrav could be tested in the future by Hyper-Kamiokande.

There is the possibility of testing  $SO(10)$  simultaneously by proton decay experiments and PTA observations: if this last signal we considered will be confirmed together with a future observation of proton decay from Hyper-K we could have a first clear experimental proof of the validity of  $SO(10)$ .

## Scan results and NANOGrav signal

Finally we can take the results of our scan and determine if they are consistent with NANOGrav signal. The crucial values we need to take in account for all the points in the scan is  $M_{N_3}$ . From

$$M_{N_3} = Y_{\overline{126}} M_1 \quad (7.36)$$

and imposing  $Y_{\overline{126}} \leq M_1$  we obtain

$$M_{N_3} \leq M_1. \quad (7.37)$$

It is important to notice that in our model  $M_1$  and  $M_{N_3}$  are not in a one-to-one correspondence. Therefore every point in the scan is compatible with any value of  $M_1$  provided it is bigger than  $M_{N_3}$ . As we have said in the last section we can find a range of  $M_1$  consistent with NANOGrav signal. The two figures in Fig. ?? can be divided in three parts. The upper part, the one above the range of  $M_1$  allowed by NANOGrav is excluded because one would have  $M_{N_3} > M_1$ . The part below the range is

consistent with all  $M_1$  of the range. The points in the center part are still consistent with NANOGrav signal even if we need to point out that if some future observation will narrow down the range some of this region might be excluded and become part of the upper region.

The results show that most of the points of our scan are consistent with the signal of NANOGrav and some of this points predict also the correct amount of baryon asymmetry. Therefore we have showed that our model can predict successfully baryon asymmetry and being consistent with current proton decay and gravitational waves observations, especially the ones from PTA experiments.

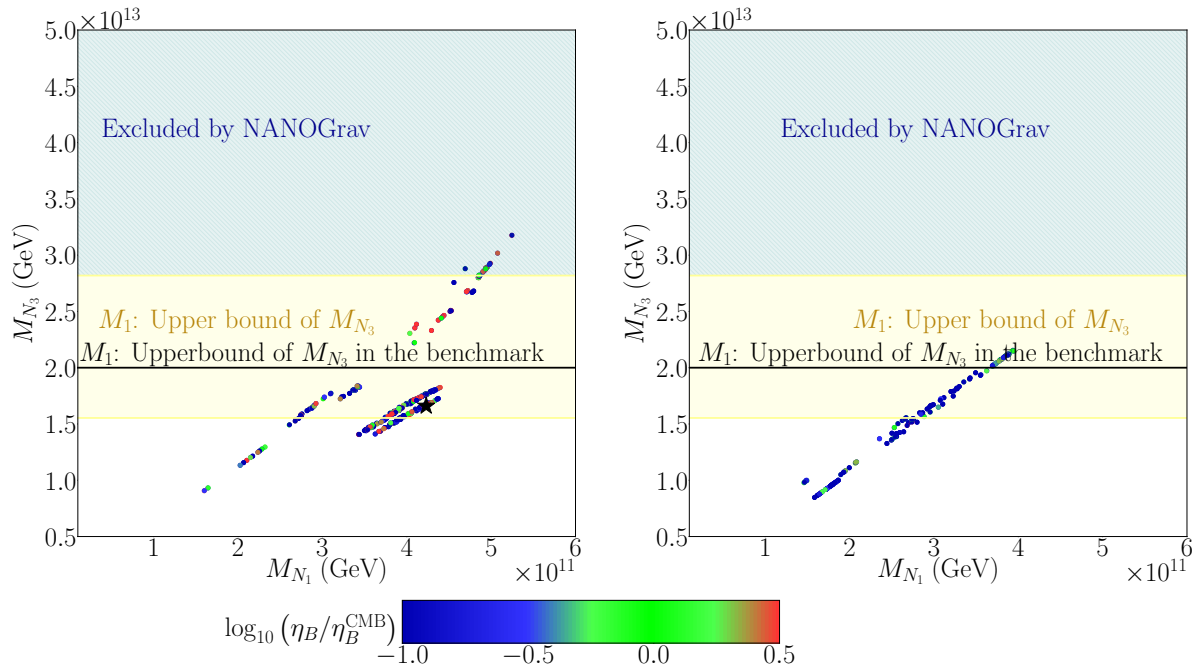


Figure 7.6: Comparison between the results of our scan and NANOGrav12.5 bound. The yellow shaded region includes all the values of  $M_1$  consistent with NANOGrav12.5. Being  $M_1$  an upper bound for  $M_{N_3}$  we can see how most of the points in our scan are consistent with NANOGrav12.5. In the left(right) we have the results of the first (second) octant.

# Conclusions

The Standard Model is an incomplete theory and it does not predict neutrino masses, baryogenesis, and dark matter. GUT theories are possible extensions of the Standard Model which predict gauge coupling unification. We have focused on the GUT model  $SO(10)$ , which predicts the existence of the right-handed neutrino explaining neutrino masses and baryon asymmetry. Moreover, differently than the Standard Model, it predicts fermion masses and mixing.

In this work we have studied a particular breaking chain of  $SO(10)$  with three intermediate spontaneous breakings respectively at the scale  $M_1, M_2$ , and  $M_3$ .

$$\begin{aligned}
 & SO(10) \\
 & \mathbf{54} \downarrow \text{broken at } M_U \\
 G_3^c & \equiv SU(4) \times SU(2)_L \times SU(2)_R \times Z_2^C \\
 & \mathbf{210} \downarrow \text{broken at } M_3 \\
 G_2^c & \equiv SU(3)_c \times SU(2)_L \times SU(2)_R \times U(1)_X \times Z_2^C \\
 & \mathbf{45} \downarrow \text{broken at } M_2 \\
 G_1 & \equiv SU(3)_c \times SU(2)_L \times SU(2)_R \times U(1)_X \\
 & \overline{\mathbf{126}} \downarrow \text{broken at } M_1 \\
 G_{SM} & \equiv SU(3)_c \times SU(2)_L \times U(1)_Y. \tag{8.1}
 \end{aligned}$$

The grand unification scale  $M_U$  can be related to the proton lifetime and therefore it can be constrained by proton decay experiments. We studied the running of the couplings and, imposing the unification of the couplings, one can relate  $M_1$  to  $M_U$ . We have then found a range of possible values of  $M_1$  compatible with proton decay experiments and that can be tested completely with Hyper-K. From Super-K results, we have found that the

upper bound on  $M_1$  is  $4.4 \times 10^{13}$  GeV. The scale  $M_1$  is particularly important because in this step  $U(1)_{B-L}$  is spontaneously broken. The  $U(1)$  breaking indeed generates a network of cosmic strings that produces a stochastic background of gravitational waves. The violation of  $B-L$  symmetry generates also the maionara masses of the right-handed neutrinos  $M_{N_1}$ ,  $M_{N_2}$ , and  $M_{N_3}$ , which are proportional to  $M_1$ .

We studied the parameter space of the Yukawa sector to predict fermion masses. We used as input of our scan the quark sector masses and mixing and then we fitted our predictions of the lepton sector with the current measured values.

We found regions of the parameter space with many points which fit correctly fermion masses with  $\chi^2 < 10$  and which satisfy the bound on heavy neutrino mass given by proton decay. One of the most important consequences of this scan is that right-handed neutrinos should be hierarchical and also that  $M_{N_3}$  is constrained to be around  $10^{13}$  GeV. Assuming a Yukawa coupling for  $N_3$  of order  $\mathcal{O}(1)$  this automatically translates into a constraint on  $M_1$ , expected to be of the same order of magnitude. The scale  $M_1$  therefore can be constrained both by proton decay, gravitational waves experiments, and fermion masses and mixing.

Subsequently, we examined the details of the theory of leptogenesis and how it can be embedded in  $SO(10)$ . We have found that most of the successful points of the parameter space which fit fermion masses also predict the correct amount of baryon asymmetry. We proved therefore that there is no need for a high fine tuning of the parameters to achieve it. Most of the points of the scan predict  $m_{\beta\beta}$  to be between 5 and 30 meV. Next-generation  $0\nu\beta\beta$  decay experiments such as Legend-1000 [111], nEXO [112], NEXT-HD [113], DARWIN[114], SNO+II [115], and CUPID-Mo [116] will push the current bound around 8 meV thus testing a significant fraction of the successful points of the scan.

We have seen that this model can be tested by detecting a SGWB produced by cosmic strings by next-generation experiments such as LISA , DECIGO , AEDGE , TianQuin, Tajii, MAGIC. We considered also the signal found by Pulsar Time Arrays experiments which can be seen as a hint for the detection of a SGWB: we found consistency between our prediction and such a signal, in particular, we have found that the range on  $M_1$  is compatible with NANOGrav observation. The range of the values of  $M_1$  allowed by NANOGrav has not yet been tested by Super-K but will be completely tested by Hyper-K. Such a region predicts the correct values for right-handed neutrino masses and it is consistent with the fermion masses and mixing predictions.

In summary, we studied a model which predicts fermion masses, baryon asymmetry and that is consistent with a possible detection of an SGWB by Pulsar Time Arrays and

that can furtherly be tested by a variety of next-generation experiments which covers different physical phenomena:  $0\nu\beta\beta$  decay, proton decay, and gravitational waves. This work can be extended by improving the scan. Indeed, it is still partial and it has been done in a restricted parameter space after we have made some approximations, the next step is to make a more general and efficient scan that can be applied to many GUT models. Then we could extend our discussion to other breaking chains of  $SO(10)$  to make the work more general and determine how well  $SO(10)$  models consistent with proton decay bound can predict baryogenesis and give a correct prediction of fermion masses and mixing. Another possible step is going beyond non-supersymmetric models of  $SO(10)$  and extend the work also to a super-symmetric model of  $SO(10)$ . In such a case there could be also the possibility of testing the super-symmetric scale using topological defects. It is worth also improving our comprehension of an SGWB by cosmic strings by considering back-reaction effects for example and studying some cosmological consequences of the existence of a cosmic string network which could furtherly test their existence.

# Bibliography

- [1] SUPER-KAMIOKANDE COLLABORATION collaboration, Evidence for oscillation of atmospheric neutrinos, *Phys. Rev. Lett.* **81** (1998) 1562.
- [2] SNO COLLABORATION collaboration, Direct evidence for neutrino flavor transformation from neutral-current interactions in the sudbury neutrino observatory, *Phys. Rev. Lett.* **89** (2002) 011301.
- [3] M. Fukugita and T. Yanagida, Baryogenesis Without Grand Unification, *Phys. Lett.* **B174** (1986) 45.
- [4] H. Georgi, H.R. Quinn and S. Weinberg, Hierarchy of interactions in unified gauge theories, *Phys. Rev. Lett.* **33** (1974) 451.
- [5] H. Georgi and S.L. Glashow, Unified weak and electromagnetic interactions without neutral currents, *Phys. Rev. Lett.* **28** (1972) 1494.
- [6] S.M. Barr, A New Symmetry Breaking Pattern for SO(10) and Proton Decay, *Phys. Lett.* **112B** (1982) 219.
- [7] J. Derendinger, J.E. Kim and D.V. Nanopoulos, Anti-SU(5), *Phys. Lett. B* **139** (1984) 170.
- [8] A. De Rujula, H. Georgi and S. Glashow, FLAVOR GONIOMETRY BY PROTON DECAY, *Phys. Rev. Lett.* **45** (1980) 413.
- [9] I. Antoniadis, J.R. Ellis, J. Hagelin and D.V. Nanopoulos, The Flipped SU(5) x U(1) String Model Revamped, *Phys. Lett. B* **231** (1989) 65.
- [10] J.C. Pati and A. Salam, Unified Lepton-Hadron Symmetry and a Gauge Theory of the Basic Interactions, *Phys. Rev. D* **8** (1973) 1240.
- [11] P. Minkowski,  $\mu \rightarrow e\gamma$  at a Rate of One Out of  $10^9$  Muon Decays?, *Phys. Lett. B* **67** (1977) 421.

- [12] T. Yanagida, Horizontal gauge symmetry and masses of neutrinos, Conf. Proc. C **7902131** (1979) 95.
- [13] M. Gell-Mann, P. Ramond and R. Slansky, Complex Spinors and Unified Theories, Conf. Proc. C **790927** (1979) 315 [1306.4669].
- [14] P. Di Bari and A. Riotto, Successful type I Leptogenesis with SO(10)-inspired mass relations, Phys. Lett. B **671** (2009) 462 [0809.2285].
- [15] P. Di Bari and A. Riotto, Testing SO(10)-inspired leptogenesis with low energy neutrino experiments, JCAP **04** (2011) 037 [1012.2343].
- [16] C.S. Fong, D. Meloni, A. Meroni and E. Nardi, Leptogenesis in SO(10), JHEP **01** (2015) 111 [1412.4776].
- [17] E. Nezri and J. Orloff, Neutrino oscillations versus leptogenesis in SO(10) models, JHEP **04** (2003) 020 [hep-ph/0004227].
- [18] A. Dueck and W. Rodejohann, Fits to SO(10) Grand Unified Models, JHEP **09** (2013) 024 [1306.4468].
- [19] SUPER-KAMIOKANDE collaboration, Search for proton decay via  $p \rightarrow e^+\pi^0$  and  $p \rightarrow \mu^+\pi^0$  with an enlarged fiducial volume in Super-Kamiokande I-IV, Phys. Rev. D **102** (2020) 112011 [2010.16098].
- [20] HYPER-KAMIOKANDE collaboration, Hyper-Kamiokande Design Report, 1805.04163.
- [21] W. Buchmuller, V. Domcke, H. Murayama and K. Schmitz, Probing the scale of grand unification with gravitational waves, Phys. Lett. B **809** (2020) 135764 [1912.03695].
- [22] J.A. Dror, T. Hiramatsu, K. Kohri, H. Murayama and G. White, Testing the Seesaw Mechanism and Leptogenesis with Gravitational Waves, Phys. Rev. Lett. **124** (2020) 041804 [1908.03227].
- [23] T.W.B. Kibble, Topology of cosmic domains and strings, Journal of Physics A: Mathematical and General **9** (1976) 1387.
- [24] S.F. King, S. Pascoli, J. Turner and Y.-L. Zhou, Gravitational Waves and Proton Decay: Complementary Windows into Grand Unified Theories, Phys. Rev. Lett. **126** (2021) 021802 [2005.13549].
- [25] S.F. King, S. Pascoli, J. Turner and Y.-L. Zhou, Confronting SO(10) GUTs with proton decay and gravitational waves, JHEP **10** (2021) 225 [2106.15634].

- [26] B. Fu, S.F. King, L. Marsili, S. Pascoli, J. Turner and Y.-L. Zhou, A predictive and testable unified theory of fermion masses, mixing and leptogenesis, 2022. 10.48550/ARXIV.2209.00021.
- [27] LISA collaboration, Laser Interferometer Space Antenna, 1702.00786.
- [28] NANOGrav collaboration, The NANOGrav 12.5-year Data Set: Search For An Isotropic Stochastic Gravitational-Wave Background, 2009.04496.
- [29] S. Chen et al., Common-red-signal analysis with 24-yr high-precision timing of the European Pulsar Timing Array: inferences in the stochastic gravitational-wave background search, *Mon. Not. Roy. Astron. Soc.* **508** (2021) 4970 [2110.13184].
- [30] J. Antoniadis et al., The International Pulsar Timing Array second data release: Search for an isotropic gravitational wave background, *Mon. Not. Roy. Astron. Soc.* **510** (2022) 4873 [2201.03980].
- [31] B. Goncharov et al., On the Evidence for a Common-spectrum Process in the Search for the Nanohertz Gravitational-wave Background with the Parkes Pulsar Timing Array, *Astrophys. J. Lett.* **917** (2021) L19 [2107.12112].
- [32] S. Weinberg, A model of leptons, *Phys. Rev. Lett.* **19** (1967) 1264.
- [33] F. Englert and R. Brout, Broken symmetry and the mass of gauge vector mesons, *Phys. Rev. Lett.* **13** (1964) 321.
- [34] P.W. Higgs, Broken symmetries and the masses of gauge bosons, *Phys. Rev. Lett.* **13** (1964) 508.
- [35] G.S. Guralnik, C.R. Hagen and T.W.B. Kibble, Global conservation laws and massless particles, *Phys. Rev. Lett.* **13** (1964) 585.
- [36] C. Burgess and G. Moore, *The Standard Model: A Primer*, Cambridge University Press (2006), 10.1017/CBO9780511819698.
- [37] M. Kobayashi and T. Maskawa, CP-Violation in the Renormalizable Theory of Weak Interaction, *Progress of Theoretical Physics* **49** (1973) 652.
- [38] C. Giunti and C.W. Kim, *Fundamentals of Neutrino Physics and Astrophysics*, Oxford University Press (03, 2007), 10.1093/acprof:oso/9780198508717.001.0001.
- [39] K. Abe, R. Abe, I. Adachi, B.S. Ahn, H. Aihara, M. Akatsu et al., Observation of large cp violation in the neutral b meson system, *Physical review letters* **87** (2001) 091802.

- [40] B. Aubert, D. Boutigny, J.-M. Gaillard, A. Hicheur, Y. Karyotakis, J. Lees et al., Observation of  $CP$  violation in the  $B^0$  meson system, *Physical review letters* **87** (2001) 091801.
- [41] Z. Maki, M. Nakagawa and S. Sakata, Remarks on the Unified Model of Elementary Particles, *Progress of Theoretical Physics* **28** (1962) 870 [<https://academic.oup.com/ptp/article-pdf/28/5/870/5258750/28-5-870.pdf>].
- [42] I. Esteban, M. Gonzalez-Garcia, M. Maltoni, T. Schwetz and A. Zhou, The fate of hints: updated global analysis of three-flavor neutrino oscillations, *Journal of High Energy Physics* **2020** (2020) .
- [43] SUPER-KAMIOKANDE COLLABORATION collaboration, Atmospheric neutrino oscillation analysis with external constraints in super-kamiokande i-iv, *Phys. Rev. D* **97** (2018) 072001.
- [44] SNO COLLABORATION collaboration, Combined analysis of all three phases of solar neutrino data from the sudbury neutrino observatory, *Phys. Rev. C* **88** (2013) 025501.
- [45] MINOS COLLABORATION collaboration, Measurement of neutrino and antineutrino oscillations using beam and atmospheric data in minos, *Phys. Rev. Lett.* **110** (2013) 251801.
- [46] and K. Abe, R. Akutsu, A. Ali, C. Alt, C. Andreopoulos, L. Anthony et al., Constraint on the matter–antimatter symmetry-violating phase in neutrino oscillations, *Nature* **580** (2020) 339.
- [47] KAMLAND COLLABORATION collaboration, Reactor on-off antineutrino measurement with kamland, *Phys. Rev. D* **88** (2013) 033001.
- [48] NOVA collaboration, Improved measurement of neutrino oscillation parameters by the NOvA experiment, *Phys. Rev. D* **106** (2022) 032004 [2108.08219].
- [49] M. Aker, D. Batzler, A. Beglarian, J. Behrens, A. Berlev, U. Besserer et al., Improved eV-scale sterile-neutrino constraints from the second KATRIN measurement campaign, *Physical Review D* **105** (2022) .
- [50] A. Loureiro, A. Cuceu, F.B. Abdalla, B. Moraes, L. Whiteway, M. McLeod et al., Upper bound of neutrino masses from combined cosmological observations and particle physics experiments, *Physical Review Letters* **123** (2019) .
- [51] S. Weinberg, Baryon- and lepton-nonconserving processes, *Phys. Rev. Lett.* **43** (1979) 1566.

- [52] M. Magg and C. Wetterich, Neutrino mass problem and gauge hierarchy, *Physics Letters B* **94** (1980) 61.
- [53] R.N. Mohapatra and G. Senjanović, Neutrino masses and mixings in gauge models with spontaneous parity violation, *Phys. Rev. D* **23** (1981) 165.
- [54] R.N. Mohapatra, *Unification and Supersymmetry*, Springer New York, NY (1986), <https://doi.org/10.1007/978-1-4757-1928-4>.
- [55] R.E. Marshak and R.N. Mohapatra, Quark - Lepton Symmetry and B-L as the U(1) Generator of the Electroweak Symmetry Group, *Phys. Lett. B* **91** (1980) 222.
- [56] A. Davidson,  $b - l$  as the fourth color within an  $SU(2)_L \times U(1)_R \times U(1)$  model, *Phys. Rev. D* **20** (1979) 776.
- [57] R.N. Mohapatra and G. Senjanović, Neutrino mass and spontaneous parity nonconservation, *Phys. Rev. Lett.* **44** (1980) 912.
- [58] D. Chang, R.N. Mohapatra and M.K. Parida, Decoupling of parity- and  $SU(2)_R$ -breaking scales: A new approach to left-right symmetric models, *Phys. Rev. Lett.* **52** (1984) 1072.
- [59] F. Buccella, L. Cocco, A. Sciarrino and T. Tuzi, The price of unification signatures in a  $so(10)$  model with left-right symmetry broken at the highest scale, *Nuclear Physics B* **274** (1986) 559.
- [60] K.S. Babu and E. Ma, Symmetry breaking in  $so(10)$ : Higgs-boson structure, *Phys. Rev. D* **31** (1985) 2316.
- [61] R. Slansky, Group theory for unified model building, *Physics Reports* **79** (1981) 1.
- [62] R.N. Mohapatra and B. Sakita,  $SO(2n)$  grand unification in an  $SU(n)$  basis, *Phys. Rev. D* **21** (1980) 1062.
- [63] W.J. Marciano and G. Senjanović, Predictions of supersymmetric grand unified theories, *Phys. Rev. D* **25** (1982) 3092.
- [64] U. Amaldi, W. de Boer and H. Fürstenau, Comparison of grand unified theories with electroweak and strong coupling constants measured at lep, *Physics Letters B* **260** (1991) 447.
- [65] T.W.B. Kibble, G. Lazarides and Q. Shafi, Walls bounded by strings, *Phys. Rev. D* **26** (1982) 435.

- [66] F. Buccella, L. Cocco and C. Wetterich, An  $so(10)$  model with  $54 + 126 + 10$  higgs, Nuclear Physics B **243** (1984) 273.
- [67] L.-F. Li, Group theory of the spontaneously broken gauge symmetries, Phys. Rev. D **9** (1974) 1723.
- [68] D. Chang and A. Kumar, Symmetry breaking of  $so(10)$  by the 210-dimensional higgs boson and michel's conjecture, Phys. Rev. D **33** (1986) 2695.
- [69] M. Abud, F. Buccella, L. Rosa and A. Sciarrino, A  $so(10)$  model with majorana masses for the  $\nu$ 's around 1011 gev, Zeitschrift für Physik C Particles and Fields **44** (1989) 589.
- [70] M.D. Schwartz, Quantum Field Theory and the Standard Model, Cambridge University Press (2013), 10.1017/9781139540940.
- [71] S. Bertolini, L. Di Luzio and M. Malinsky, Intermediate mass scales in the non-supersymmetric  $SO(10)$  grand unification: A Reappraisal, Phys. Rev. D **80** (2009) 015013 [0903.4049].
- [72] L. Abbott, The background field method beyond one loop, Nuclear Physics B **185** (1981) 189.
- [73] M.E. Machacek and M.T. Vaughn, Two Loop Renormalization Group Equations in a General Quantum Field Theory. 1. Wave Function Renormalization, Nucl. Phys. B **222** (1983) 83.
- [74] S. Weinberg, Effective Gauge Theories, Phys. Lett. B **91** (1980) 51.
- [75] Z. zhong Xing, H. Zhang and S. Zhou, Impacts of the higgs mass on vacuum stability, running fermion masses, and two-body higgs decays, Physical Review D **86** (2012) .
- [76] R.N. Mohapatra and M.K. Parida, Threshold effects on the mass-scale predictions in  $SO(10)$  models and solar-neutrino puzzle, Physical Review D **47** (1993) 264.
- [77] S. Weinberg, Baryon and Lepton Nonconserving Processes, Phys. Rev. Lett. **43** (1979) 1566.
- [78] Y. Aoki, T. Izubuchi, E. Shintani and A. Soni, Improved lattice computation of proton decay matrix elements, Physical Review D **96** (2017) .
- [79] K.S. Babu and R.N. Mohapatra, Predictive neutrino spectrum in minimal  $SO(10)$  grand unification, Physical Review Letters **70** (1993) 2845.

- [80] B. Bajc, A. Melfo, G. Senjanović and F. Vissani, Yukawa sector in nonsupersymmetric renormalizable SO(10), *Physical Review D* **73** (2006) .
- [81] B. Bajc and G. Senjanović , Radiative seesaw mechanism and degenerate neutrinos, *Physical Review Letters* **95** (2005) .
- [82] A.S. Joshipura and K.M. Patel, Fermion masses in *so*(10) models, *Phys. Rev. D* **83** (2011) 095002.
- [83] B. Dutta, Y. Mimura and R. Mohapatra, Neutrino masses and mixings in a predictive *so*(10) model with CKM CP violation, *Physics Letters B* **603** (2004) 35.
- [84] G. Altarelli and G. Blankenburg, Different SO(10) paths to fermion masses and mixings, *Journal of High Energy Physics* **2011** (2011) .
- [85] Z.-z. Xing, H. Zhang and S. Zhou, Updated values of running quark and lepton masses, *Phys. Rev. D* **77** (2008) 113016.
- [86] and P. A. R. Ade, N. Aghanim, M. Arnaud, M. Ashdown, J. Aumont, C. Baccigalupi et al., iplanck/i2015 results, *Astronomy & Astrophysics* **594** (2016) A13.
- [87] A.D. Sakharov, Violation of CP Invariance, C asymmetry, and baryon asymmetry of the universe, *Pisma Zh. Eksp. Teor. Fiz.* **5** (1967) 32.
- [88] L. Covi, E. Roulet and F. Vissani, CP violating decays in leptogenesis scenarios, *Physics Letters B* **384** (1996) 169.
- [89] M.S.T. Edward W. Kolb, *The Early Universe* (1990), <https://doi.org/10.1201/9780429492860>.
- [90] W. Buchmüller, R. Peccei and T. Yanagida, LEPTOGENESIS AS THE ORIGIN OF MATTER, *Annual Review of Nuclear and Particle Science* **55** (2005) 311.
- [91] W. Buchmüller, P.D. Bari and M. Plümacher, Leptogenesis for pedestrians, *Annals of Physics* **315** (2005) 305.
- [92] W. Buchmüller, P. Di Bari and M. Plümacher, Cosmic microwave background, matter–antimatter asymmetry and neutrino masses, *Nuclear Physics B* **643** (2002) 367.
- [93] V. Kuzmin, V. Rubakov and M. Shaposhnikov, On anomalous electroweak baryon-number non-conservation in the early universe, *Physics Letters B* **155** (1985) 36.

- [94] V. Mukhanov, *Physical Foundations of Cosmology*, Cambridge University Press (2005), 10.1017/CBO9780511790553.
- [95] A.D. Simone and A. Riotto, Quantum boltzmann equations and leptogenesis, *Journal of Cosmology and Astroparticle Physics* **2007** (2007) 002.
- [96] M. Beneke, B. Garbrecht, M. Herranen and P. Schwaller, Finite number density corrections to leptogenesis, *Nuclear Physics B* **838** (2010) 1.
- [97] S. Blanchet, P.D. Bari and G.G. Raffelt, Quantum zeno effect and the impact of flavour in leptogenesis, *Journal of Cosmology and Astroparticle Physics* **2007** (2007) 012.
- [98] M. Beneke, B. Garbrecht, C. Fidler, M. Herranen and P. Schwaller, Flavoured leptogenesis in the CTP formalism, *Nuclear Physics B* **843** (2011) 177.
- [99] K. Moffat, S. Pascoli, S. Petcov, H. Schulz and J. Turner, Three-flavored nonresonant leptogenesis at intermediate scales, *Physical Review D* **98** (2018) .
- [100] A. Abada, S. Davidson, F.-X. Josse-Michaux, M. Losada and A. Riotto, Flavour issues in leptogenesis, *Journal of Cosmology and Astroparticle Physics* **2006** (2006) 004.
- [101] A. Abada, S. Davidson, A. Ibarra, F.X. Josse-Michaux, M. Losada and A. Riotto, Flavour Matters in Leptogenesis, *JHEP* **09** (2006) 010 [[hep-ph/0605281](#)].
- [102] E. Nardi, Y. Nir, E. Roulet and J. Racker, The importance of flavor in leptogenesis, *Journal of High Energy Physics* **2006** (2006) 164.
- [103] P.D. Bari, See-saw geometry and leptogenesis, *Nuclear Physics B* **727** (2005) 318.
- [104] C.S. Fong, E. Nardi and A. Riotto, Leptogenesis in the universe, *Advances in High Energy Physics* **2012** (2012) 1.
- [105] S. Blanchet, D.A. Jones, P. Di Bari and L. Marzola, Leptogenesis with heavy neutrino flavours: from density matrix to boltzmann equations, 2011. 10.48550/ARXIV.1112.4528.
- [106] R.N. Mohapatra and M. Severson, Leptonic CP violation and proton decay in SUSY SO(10), *Journal of High Energy Physics* **2018** (2018) .
- [107] W. Grimus and H. Kühböck, A renormalizable SO(10) GUT scenario with spontaneous CP violation, *The European Physical Journal C* **51** (2007) 721.
- [108] PLANCK collaboration, Planck 2015 results. XIII. Cosmological parameters, *Astron. Astrophys.* **594** (2016) A13 [[1502.01589](#)].

- [109] A. Granelli, K. Moffat, Y.F. Perez-Gonzalez, H. Schulz and J. Turner, ULYSSES: Universal LeptogeneSiS Equation Solver, *Comput. Phys. Commun.* **262** (2021) 107813 [2007.09150].
- [110] M. Beneke, B. Garbrecht, M. Herranen and P. Schwaller, Finite Number Density Corrections to Leptogenesis, *Nucl. Phys. B* **838** (2010) 1 [1002.1326].
- [111] LEGEND Collaboration, N. Abgrall, I. Abt, M. Agostini, A. Alexander, C. Andreoiu et al., Legend-1000 preconceptual design report, 2021. 10.48550/ARXIV.2107.11462.
- [112] G. Adhikari, S.A. Kharusi, E. Angelico, G. Anton, I.J. Arnquist, I. Badhrees et al., nexo: neutrinoless double beta decay search beyond  $10^{28}$  year half-life sensitivity, *Journal of Physics G: Nuclear and Particle Physics* **49** (2021) 015104.
- [113] J.J. Gomez-Cadenas, Status and prospects of the next experiment for neutrinoless double beta decay searches, 2019. 10.48550/ARXIV.1906.01743.
- [114] F. Agostini, S.E.M.A. Maouloud, L. Althueser, F. Amaro, B. Antunovic, E. Aprile et al., Sensitivity of the darwin observatory to the neutrinoless double beta decay of  $^{136}\text{Xe}$ , .
- [115] S. Andringa, E. Arushanova, S. Asahi, M. Askins, D.J. Auty, A.R. Back et al., Current status and future prospects of the SNO+ experiment, *Advances in High Energy Physics* **2016** (2016) 1.
- [116] E. Armengaud, C. Augier, A.S. Barabash, F. Bellini, G. Benato, A. Benoît et al., The CUPID-mo experiment for neutrinoless double-beta decay: performance and prospects, *The European Physical Journal C* **80** (2020) .
- [117] A. Vilenkin and E.P.S. Shellard, *Cosmic Strings and Other Topological Defects*, Cambridge University Press (7, 2000).
- [118] N. Turok and P. Bhattacharjee, Stretching cosmic strings, *Phys. Rev. D* **29** (1984) 1557.
- [119] D. Garfinkle and T. Vachaspati, Fields due to kinky, cusplless, cosmic loops, *Phys. Rev. D* **37** (1988) 257.
- [120] A.E. Everett, Cosmic strings in unified gauge theories, *Phys. Rev. D* **24** (1981) 858.
- [121] C.J.A.P. Martins and E.P.S. Shellard, Quantitative string evolution, *Physical Review D* **54** (1996) 2535.

- [122] C.J.A.P. Martins and E.P.S. Shellard, Extending the velocity-dependent one-scale string evolution model, *Physical Review D* **65** (2002) .
- [123] S.R. Coleman and E.J. Weinberg, Radiative Corrections as the Origin of Spontaneous Symmetry Breaking, *Phys. Rev. D* **7** (1973) 1888.
- [124] L. Sousa and P.P. Avelino, Stochastic gravitational wave background generated by cosmic string networks: Velocity-dependent one-scale model versus scale-invariant evolution, *Physical Review D* **88** (2013) .
- [125] P. Auclair, J.J. Blanco-Pillado, D.G. Figueroa, A.C. Jenkins, M. Lewicki, M. Sakellariadou et al., Probing the gravitational wave background from cosmic strings with LISA, *Journal of Cosmology and Astroparticle Physics* **2020** (2020) 034.
- [126] J.J. Blanco-Pillado and K.D. Olum, Stochastic gravitational wave background from smoothed cosmic string loops, *Physical Review D* **96** (2017) .
- [127] S.A. Sanidas, R.A. Battye and B.W. Stappers, Constraints on cosmic string tension imposed by the limit on the stochastic gravitational wave background from the european pulsar timing array, *Physical Review D* **85** (2012) .
- [128] J.J. Blanco-Pillado, K.D. Olum and B. Shlaer, Large parallel cosmic string simulations: New results on loop production, *Physical Review D* **83** (2011) .
- [129] J.J. Blanco-Pillado, K.D. Olum and B. Shlaer, The number of cosmic string loops, *Phys. Rev. D* **89** (2014) 023512 [1309.6637].
- [130] J.J. Blanco-Pillado and K.D. Olum, Stochastic gravitational wave background from smoothed cosmic string loops, *Phys. Rev. D* **96** (2017) 104046 [1709.02693].
- [131] B. Abbott, R. Abbott, T. Abbott, M. Abernathy, F. Acernese, K. Ackley et al., Observation of gravitational waves from a binary black hole merger, *Physical Review Letters* **116** (2016) .
- [132] A.I. Renzini, B. Goncharov, A.C. Jenkins and P.M. Meyers, Stochastic gravitational-wave backgrounds: Current detection efforts and future prospects, 2022. 10.48550/ARXIV.2202.00178.
- [133] N. Christensen, Stochastic gravitational wave backgrounds, *Reports on Progress in Physics* **82** (2018) 016903.
- [134] Y. Cui, M. Lewicki, D.E. Morrissey and J.D. Wells, Probing the pre-BBN universe with gravitational waves from cosmic strings, *Journal of High Energy Physics* **2019** (2019) .

- [135] M.B. Hindmarsh and T.W.B. Kibble, Cosmic strings, Reports on Progress in Physics **58** (1995) 477.
- [136] W.-H. Ruan, Z.-K. Guo, R.-G. Cai and Y.-Z. Zhang, Taiji Program: Gravitational-Wave Sources, 1807.09495.
- [137] TIANQIN collaboration, TianQin: a space-borne gravitational wave detector, Class. Quant. Grav. **33** (2016) 035010 [1512.02076].
- [138] V. Corbin and N.J. Cornish, Detecting the cosmic gravitational wave background with the big bang observer, Class. Quant. Grav. **23** (2006) 2435 [gr-qc/0512039].
- [139] N. Seto, S. Kawamura and T. Nakamura, Possibility of direct measurement of the acceleration of the universe using 0.1-Hz band laser interferometer gravitational wave antenna in space, Phys. Rev. Lett. **87** (2001) 221103 [astro-ph/0108011].
- [140] MAGIS collaboration, Mid-band gravitational wave detection with precision atomic sensors, 1711.02225.
- [141] AEDGE collaboration, AEDGE: Atomic Experiment for Dark Matter and Gravity Exploration in Space, EPJ Quant. Technol. **7** (2020) 6 [1908.00802].
- [142] L. Badurina et al., AION: An Atom Interferometer Observatory and Network, JCAP **05** (2020) 011 [1911.11755].
- [143] B. Sathyaprakash et al., Scientific Objectives of Einstein Telescope, Class. Quant. Grav. **29** (2012) 124013 [1206.0331].
- [144] LIGO SCIENTIFIC collaboration, Exploring the Sensitivity of Next Generation Gravitational Wave Detectors, Class. Quant. Grav. **34** (2017) 044001 [1607.08697].
- [145] L. Lentati et al., European Pulsar Timing Array Limits On An Isotropic Stochastic Gravitational-Wave Background, Mon. Not. Roy. Astron. Soc. **453** (2015) 2576 [1504.03692].
- [146] NANOGrAV collaboration, The NANOGrav 11-year Data Set: Pulsar-timing Constraints On The Stochastic Gravitational-wave Background, Astrophys. J. **859** (2018) 47 [1801.02617].
- [147] G. Janssen et al., Gravitational wave astronomy with the SKA, PoS **AASKA14** (2015) 037 [1501.00127].
- [148] GAIA collaboration, Gaia Data Release 2, Astron. Astrophys. **616** (2018) A1 [1804.09365].

- [149] THEIA collaboration, Theia: Faint objects in motion or the new astrometry frontier, 1707.01348.
- [150] J. Ellis and M. Lewicki, Cosmic String Interpretation of NANOGrav Pulsar Timing Data, Phys. Rev. Lett. **126** (2021) 041304 [2009.06555].

# A brief introduction to cosmology

The Universe is expanding according to the Hubble law:

$$v = Hl \tag{A.1}$$

where  $l$  is the distance between two comoving points and  $H$  is the Hubble constant. The distance between two points may be expressed as:

$$d = a(t)l \tag{A.2}$$

where  $l$  is the comoving distance between the points. We can express the Hubble constant as:  $H = \frac{\dot{a}(t)}{a(t)}$  The metric which describes an expanding universe is the Friedmann-Robertson-Walker (FRW) metric:

$$ds^2 = dt^2 - a^2(t)dl^2, \tag{A.3}$$

it can be rewritten in spherical coordinates:

$$dl^2 = \frac{dr^2}{1 - Kr^2} + r^2 (d\theta^2 + \sin^2 \theta d\phi^2) \tag{A.4}$$

where  $K$  is the curvature constant and describes the topology of the Universe.

- $K > 0$  means that the Universe is closed and the topology is the one of  $S^3$
- $K = 0$  means a flat Universe
- $K < 0$  means a open Universe, with the topology of  $H^3$

It is convenient to introduce the comoving time  $d\tau = \frac{t}{a(t)}$  so that we can write the metric as:

$$ds^2 = a^2(\tau) [d\tau^2 - dl^2] \tag{A.5}$$

For the energy momentum tensor of the Universe we use the one of a perfect fluid with energy density  $\rho$  and pressure  $p$ . By plugging the metric in the Einstein equation we obtain the Friedmann equations:

$$\dot{\rho} + 3\frac{\dot{a}}{a}(\rho + p) \quad (\text{A.6})$$

$$\left(\frac{\dot{a}}{a}\right)^2 + \frac{K}{a^2} = \frac{8\pi G}{a^2} \quad (\text{A.7})$$

It is useful to define the redshift parameter

$$1 + z \equiv \frac{a(t)}{a(t_0)} \quad (\text{A.8})$$

which is a more convenient parameter for describing the evolution of a system in cosmological time scales. For each species of the Universe with energy density  $\rho_i$  such as baryon matter, dark matter, neutrino and so on we can define an adimensional parameter  $\Omega = \rho/\rho_c$  where  $\rho_c = \frac{3}{32\pi G t^2}$  is the energy for which the Universe would be flat and it is called critical energy. The evolution of the Planck constant is given by:

$$H(z) = H_0 (\Omega_R(1+z)^4 + \Omega_M(1+z)^3 + \Omega_k(1+z)^2 + \Omega_\Lambda)^{1/2} \quad (\text{A.9})$$

where

- $\Omega_R$  is the fraction of energy of the total radiation in the Universe
- $\Omega_M$  is the fraction of energy of all the types of matter in the Universe
- $\Omega_\Lambda$  is the fraction of energy of the cosmological constants which explain the accelerated expansion of the Universe.

Depending on which quantity has the biggest energy fraction we call the cosmological era as radiation dominated era, matter dominated era, dark-energy dominated era. The early universe was in a radiation-dominated era and then in transitioned to a matter-dominated era. Now we are in a dark-energy dominated era. The Hubble time is defined to be  $1/H(z)$  and we define  $\chi_H$  as the Hubble length: the distance travelled by light during an Hubble time.